Spring 2008

The evaluation of the instrumentation of an acoustic measurement buoy designed to monitor the underwater acoustic environment during pile driving activity

David P. Moceri

University of New Hampshire, Durham

Follow this and additional works at: https://scholars.unh.edu/thesis

THE EVALUATION OF THE INSTRUMENTATION OF AN ACOUSTIC

MEASUREMENT BUOY DESIGNED TO MONITOR THE

UNDERWATER ACOUSTIC ENVIRONMENT DURING PILE DRIVING

ACTIVITY

BY

DAVID P. MOCERI

THESIS

Submitted to the University of New Hampshire
In Partial Fulfillment of
The Requirements for the Degree of

Master of Science

in

Ocean Engineering

May 2008

UMI Number: 1455009

INFORMATION TO USERS

The quality of this reproduction is dependent upon the quality of the copy
submitted. Broken or indistinct print, colored or poor quality illustrations and
photographs, print bleed-through, substandard margins, and improper
alignment can adversely affect reproduction.

In the unlikely event that the author did not send a complete manuscript
and there are missing pages, these will be noted. Also, if unauthorized
copyright material had to be removed, a note will indicate the deletion.
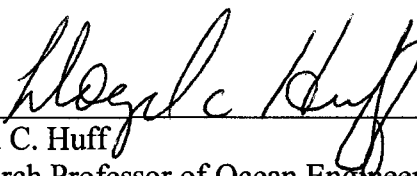
UMI®

UMI Microform 1455009
Copyright 2008 by ProQuest LLC.
All rights reserved. This microform edition is protected against
unauthorized copying under Title 17, United States Code.
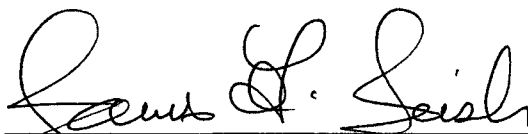
This thesis has been examined and approved.

Thesis Director, Kenneth C. Baldwin
Professor of Mechanical and Ocean
Engineering

Lloyd C. Huff
Research Professor of Ocean Engineering

James D. Irish
Research Professor of Ocean Engineering

23 April 2009
Date

DEDICATION

To my family, friends, and co-workers for their support, patience and

encouragement. My parents would have been proud that I had the ambition and drive to

complete this thesis, especially to my father, who valued education, and spent his life at

sea to support his family

ACKOWLEDGEMENTS

TABLE OF CONTENTS

LIST OF TABLES

LIST OF FIGURES

LIST OF EQUATIONS

xvii

ABSTRACT

THE EVALUATION OF THE INSTRUMENTATION OF AN ACOUSTIC MEASUREMENT BUOY DESIGNED TO MONITOR THE UNDERWATER ACOUSTIC ENVIRONMENT DURING PILE DRIVING ACTIVITY

by

David P. Moceri

University of New Hampshire, May, 2008

Driving large support piles in brackish estuaries results in permanent damage, and possibly death to marine mammals and fragile infant fish spawned in these areas. The damage is a result of excessive acoustic intensities produced by the pile driving activity. To monitor this 'noise', students in the Undergraduate Ocean Research Projects: TECH 797 2005-2006 (Risso et al. 2006), working with Dr. Ken Baldwin as their advisor, proposed the concept of using an 'Acoustic Measurement Buoy'. Their project was funded by the National Sea Grant College Program, NOAA, and Department of Commerce.

Their problem statement was "To develop a portable, robust, and inexpensive system for measurement of waterborne noise associated with construction in coastal and estuarine regions" (Risso et al. 2006). Based upon extensive testing and experimentation, this thesis evaluates the feasibility of their design, the problems encountered, some solutions and recommendations for improvements in putting the 'Acoustic Measurement

Buoy' to practical use. The individual components were analyzed to compare their requirements, specifications and performance.

Evaluations were performed on a test bench, in the tank in the Jere Chase Ocean Engineering Lab, on the R/V Gulf Challenger and at a floating dock in a coastal marine environment. The data were collected using National Instruments LabVIEW™ software, data acquisition hardware, and post processed using Matlab™ software. Standard techniques in failure and root cause analysis, such as cause and effect diagrams, fishbone diagrams, flow diagrams and process maps will be used in the data and component analysis.

CHAPTER 1

INTRODUCTION

1.1 **Background**

Noise in the ocean is caused by many sources. A major source of underwater

noise is construction, in and around near coastal areas, such as when driving piles for

bridges. Based upon previous pile driving studies, estimates indicate source levels (*SL*)

up to 265 dB re 1μPa at 1m at a depth of 10m (Nedwell et al. 2003). During the activity

of pile driving, mechanical energy is transferred into acoustic energy and ultimately

propagates throughout the water column. The underwater acoustic sound pressures, and

particle motion emanating from a pile during the 'hammering' process have produced

adverse affects to fish and marine life in the adjacent environment. Acoustic sound

pressure levels (*SPL*) greater than 180 dB re 1μPa are known to cause cell damage and

can affect marine fish and their natural processes, such as spawning and habitation.

(http://mapping.orr.noaa.gov/website/portal/pies/Pile_Driving_Refs.pdf)

An initial project was focused on designing an acoustic measurement system to

record the *SPL* during pile driving activity. The design criteria were based upon acoustic

pressures greater than 240 dB re 1μPa. Expected frequencies are from 200Hz to 4kHz,

depending on the length of the pile with a drive pulse duration of 50 to 100 ms (Risso et

al. 2006). The major concerns in the recording system were the source levels and

frequencies generated. The design and fabrication of a prototype acoustic measurement

system to enable in-situ sound collection was undertaken by Risso et al. (2006). Source

levels and local sound pressure levels could then be measured and calculated. The existing reports on this situation were available in the 'gray literature' of consultant reports. It became apparent that there was a need to develop a measurement system capable of recording these acoustic events at multiple depths and locations.

It was anticipated that monitoring of the 'noise' or sound pressure levels and data collection would take place at three locations and three depths (Risso et al. 2006). Location one was an area where the *SPL* would be greater than 220 dB dB re 1μPa. Location two was where the expected *SPL* would be greater then 180 dB re 1μPa but less than 220 dB re 1uPa. Location three was where the expected *SPL* would be less than 180 dB re 1uPa. The three locations are shown schematically in Figure 1. The buoy and mooring were designed to be readily monitored and moved to the required locations in order to calculate the *SPL* at range. The mooring-buoy description and analysis were performed in Risso et al. (2006).
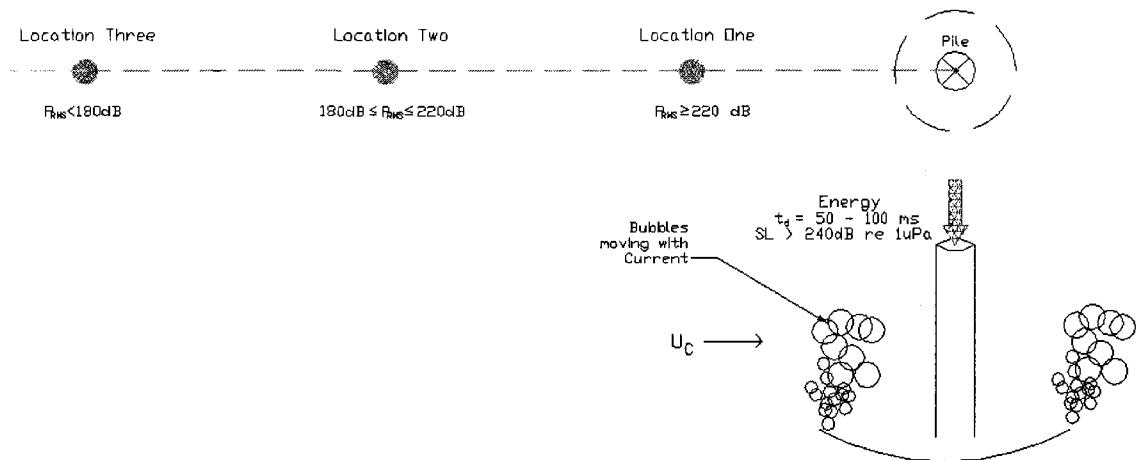
Figure 1: Three physical locations and expected *SPL*s of concern. The air bubbles that are shown in the diagram will be explained.

The hydrophones on each mooring were to be deployed at three different depths. One of the hydrophones near the water surface, one in the mid-water column and one

near the sea floor, as shown in Figure 2. Each hydrophone would have a temperature

sensor co-located.
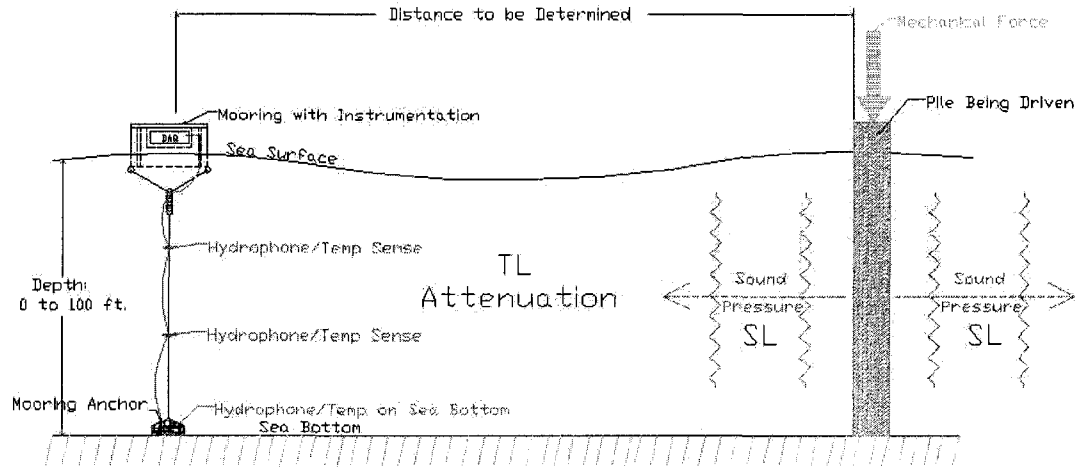
Figure 2: Concept schematic of mooring, hydrophone and buoy layout.

Methods have been proposed and used to attenuate pile driving source levels in

water using air as an attenuation medium in the form of 'bubble curtains'. These are

typically composed of concentric cylinders (Laughlin 2006) or closed rectangles made

from neoprene or similar materials placed vertically around the pile. Air is pumped from

compressors into a perforated 'ring' creating a 'shell' of bubbly water around the

construction zone. This can be considered the insertion loss (*InL*), due to the impedance

mismatch between the two mediums (seawater and air). Any transmission loss (*TL*) from

the source to the hydrophones must be taken into account.

1.2   Data Acquisition System Description

The prototype monitoring system was designed to have multiple (three)

hydrophone elements and a data acquisition system (DAQ). The mooring-buoy was

designed to be self-contained with the 'instrument package' inserted inside a watertight

cylinder (Risso et al. 2006). The DAQ was necessary to acquire and store the raw data and was controlled with a PC running under the Microsoft Windows™ operating system. An integral component was a National Instruments 4 channel, 16 bit analog to digital converter (A/D) capable of a sampling rate of 100,000 samples per second per channel. The A/D is connected via a USB port to the host PC. The LabVIEW™ graphical language was used to record and display the real-time data. The raw data files, formatted to be post-processed and analyzed using Matlab™, were stored on the hard drive for retrieval through a USB port. As designed, a wireless connection would be used for DAQ control and data retrieval, using a remote PC.

Wired connections run from the DAQ system to the three omni-directional hydrophone assemblies. Inside the individual hydrophone assemblies are a hydrophone and a preamplifier. Analog filtering circuits were not specified or purchased in the original proposal between the A/D and the hydrophone assemblies. The system was implicitly designed for signals at frequencies less than 10kHz. Analog high pass filtering circuits were found to be required on each channel. They were designed as a DC block, as the output signals from the hydrophones sit at a DC level. The DC level has the potential of reducing the dynamic range of the hydrophones. The AC input signal from the hydrophones ride on this DC level, ($\frac{1}{2}$ V_{supply}). This initial prototype design was presented in Risso et al. (2006), but it was not subjected to a rigorous engineering evaluation. The overall goal of this thesis was to provide an engineering evaluation of the 'Acoustic Measurement Buoy', using an approach shown graphically in Figure 3. This approach was designed to evaluate each system component, the interaction of the components, and the compatibility of the components.
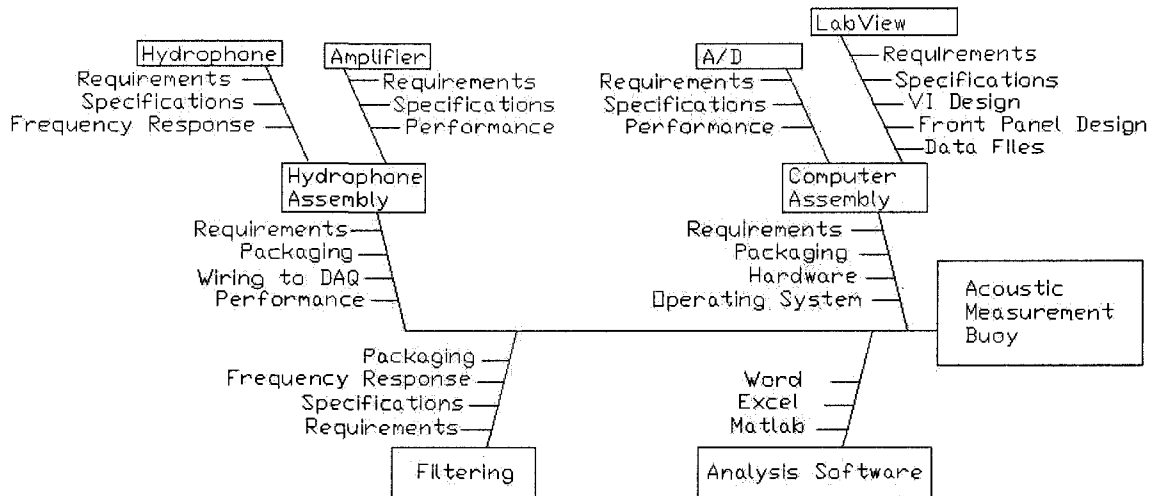
Figure 3: Fishbone diagram of the components of the Acoustic Measurement Buoy.

1.3 Goals and Objectives

The specific goals of this research were intended to perform a rigorous evaluation of the existing prototype system and make recommendations for improvements. The specific goals were:

1) Complete the build, as generally designed, making changes as necessary.

2) Perform an in-depth electrical, acoustical and mechanical evaluation of the individual components and system performance.

3) Based upon this evaluation, perform redesigns and modifications, as required to the original components.

4) Analyze the reliability of this acoustic measuring system for acquiring local sound pressure data from the activity of pile driving in an accurate and consistent manner at the locations prescribed.

The feasibility study began by completing the build of the DAQ package and hydrophone assemblies. The operation of the hydrophones, data acquisition module and computer were verified. A calibration of the hydrophones was performed using the substitution method, along with a calibrated source, separate measuring system and independent Reson hydrophones. Tank testing was accomplished at higher frequencies, and finally field data were obtained at a floating dock on the Annisquam River in Gloucester Massachusetts, to test low frequencies that are impractical in a tank.

The original data acquisition system and hydrophone design went through many changes and iterations. The experiments, data analysis, problems incurred, solutions, and recommendations are presented in subsequent chapters. Many problems were encountered and some solutions were implemented, while others were proposed to make the system more robust and reliable. As the testing and data collection proceeded, ongoing analysis was performed and redesigns were implemented. With the collected data, a careful failure analysis was performed on the system using such tools as root cause analysis, and cause–effect diagrams (fishbone diagrams). Figure 4 describes the process map of the analysis approach taken to evaluate the feasibility of the Acoustic Measurement Buoy as designed and built. This thesis focuses on the evaluation of the canister instrumentation and hydrophones.

```
                    ┌─────────────────┐
                    │ Recognize  Need │
                    └─────────────────┘
                             │
                    ┌─────────────────┐
                    │ Define  Problem │
                    └─────────────────┘
                             │
                    ┌─────────────────┐
                    │ Design  Concept │
                    └─────────────────┘
                             │
          ┌──────────────┌───────┐ ─ ─ ─ ─ ─ ─ ─ ┐
          │              │ Build │                │
          │              └───────┘                │
          │                  │                    │
   ┌────────────┐  ┌──────────────────┐  ┌────────────────┐
   │ Acoustics  │  │ Data Acquisition │  │ Buoy-Mooring   │
   └────────────┘  └──────────────────┘  └────────────────┘
          │                  │                    └── Risso et al. 2006
          │         ┌─────────────────────────────┐
          └────────▶│ Component and System Test   │
                    └─────────────────────────────┘
                             │
                    ┌─────────────────────┐
                    │ Analysis  -  Changes│
                    └─────────────────────┘
                             │
                    ┌─────────────────────┐
                    │ System Evaluation   │
                    └─────────────────────┘
                             │
                    ┌─────────────┐
                    │ Conclusion  │
                    └─────────────┘
                             │
                    ┌───────────────┐
                    │ Presentation  │
                    └───────────────┘
```
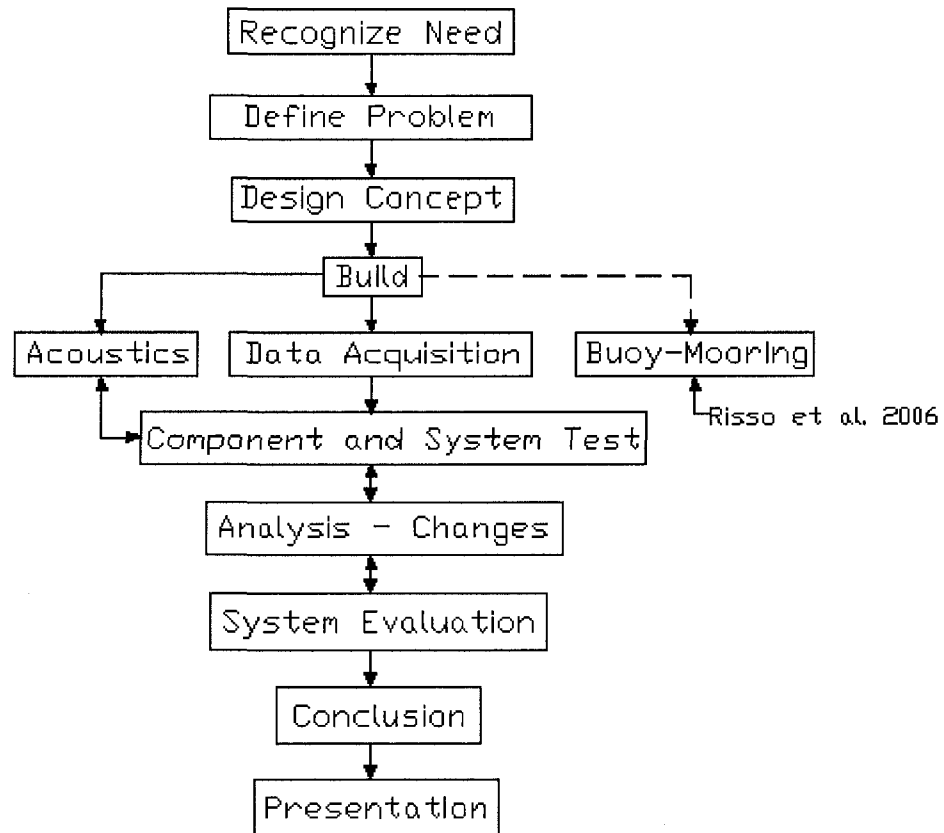
Figure 4: Process map of total design, build and evaluation of the Acoustic
Measurement Buoy. The buoy-mooring build and evaluation were
completed by Risso et al. (2006).

CHAPTER 2

MEASUREMENT SYSTEM DESIGN

2.1   Introduction

The objective of the initial student project was "to provide a portable and robust tool for measurement of underwater sound profiles at multiple locations near marine construction sites" (Risso et al. 2006). The preferred means of deployment of the Acoustics Measurement Buoy was to use vessels of opportunity. The project design was meant to be compact, easily transported, easily deployed, and waterproof. This chapter describes their original design, with exceptions noted. The evaluation was begun with furnished components from the TECH 797 class of 2005/2006.

The design approach was comprised of three categories, acoustics, data acquisition, and instrument buoy. These three topics were addressed in Risso et al. (2006). At the end of that project, hardware and some software were available for all three aspects of the project. The goal of this thesis was to test and evaluate the prototype acoustic and data acquisition issues and set criteria for future system fabrication. The instrument buoy components consisted of the buoy float, which contained the instrument canister, and mooring lines. Self-contained Onset H080 temperature loggers with programmable sampling frequency and internal data storage were purchased for each of the hydrophones to measure effects of temperature on sound propagation and are described in Risso et al. 2006. However, in this thesis, temperature effects were not considered and the temperature sensors not used. Disregarding the temperature loggers,

8

the basic initial system configuration is schematically shown as a block diagram in Figure
5.
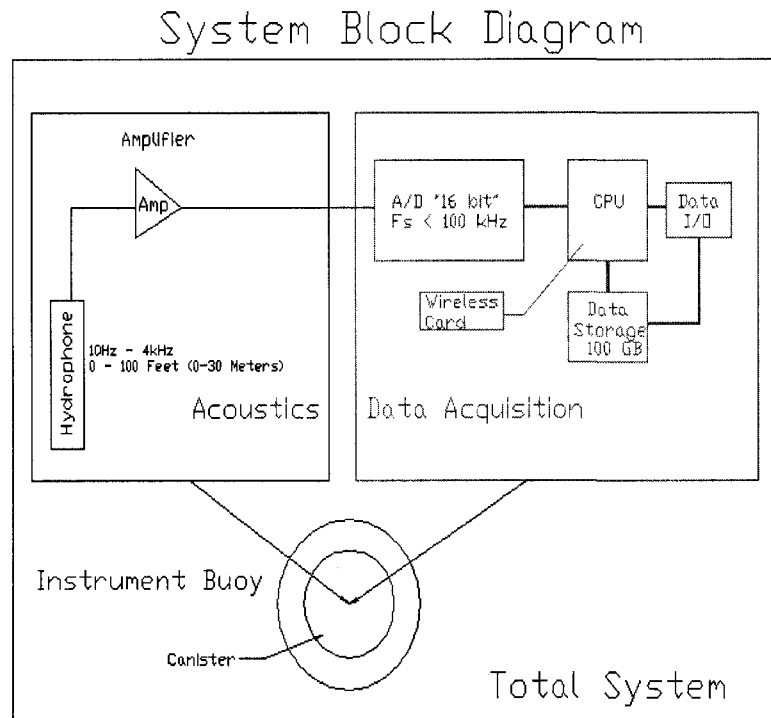
Figure 5: Block diagram of the components of the acoustic measurement buoy
with the categories of the project specified.

The acoustics components were the hydrophones with preamplifiers, and signal

wiring. The data acquisition components were the motherboard with CPU, memory, hard

drive for data storage, wireless network card, power supply card, analog to digital

converter, and rechargeable battery. Microsoft Windows™ XP was selected as the

operating system using National Instruments LabVIEW™ and DAQmx™ software to

control the data acquisition hardware and software. The hardware was assembled and

contained in a sealed pressure vessel housed within the main buoy. The Acoustic

Measurement Buoy components are summarized below:

- VIA EPIA MII10000, 512M RAM, and 100 GB Hard Drive, running under the Windows™ XP Operating System. An external CD-ROM drive was required.

- National Instruments NI-USB-9125A Data Acquisition Module 4 Channel A/D controlled by LabVIEW™ Version 7.1 and DAQmx™ software with data sampling up to 100,000 samples per second per channel.

- Linksys™ WPC54G wireless networking card with PCMCIA compatibility with the mainboard and 802.11b/g for wireless connection capability.

- Benthos AQ-2000 onmi-directional hydrophones (x3), AQ-201 single ended preamplifiers (x3).

- Onset H080 Self contained Temperature Loggers (x3) (Max depth = 100 ft).

- Concorde PVX-1234T AGM Lead Acid 34 amp-hour 12V rechargeable battery.

An alternative graphical representation of the system and the relationship between components are shown in Figure 6. This presentation was the road map for the system analysis and evaluation documented in this thesis.
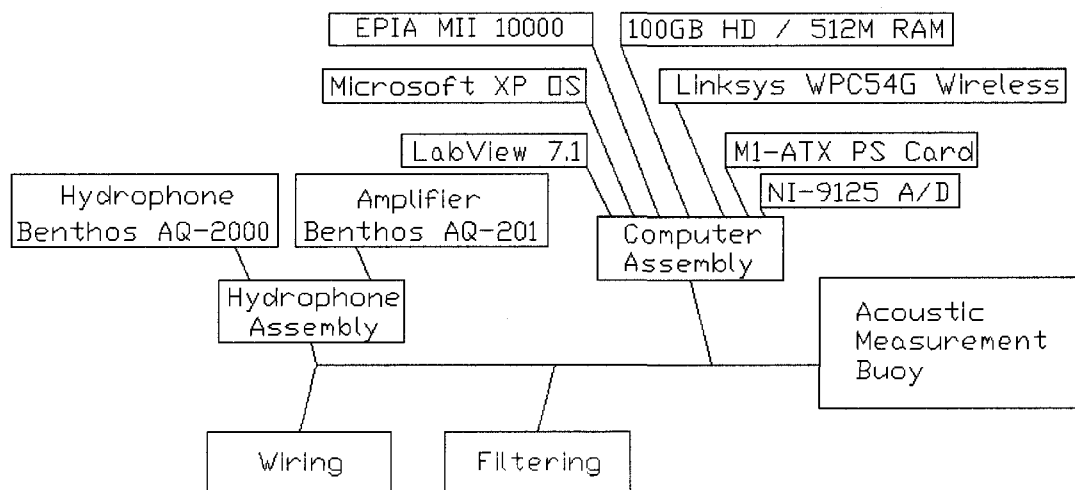
Figure 6: Fishbone diagram of the components of the Acoustic Measurement Buoy.

2.2   DAQ Package

The DAQ was designed and built around an EPIA MII-Series Mini-ITX Mainboard, with a Nehemiah 1GHz core microprocessor. The mainboard had 512 MB of RAM installed and I/O ports for a monitor, keyboard, mouse, and USB-compatible accessories. The DAQ was self-contained and ran under the Microsoft Windows™ XP operating system. A 100GB Hitachi Travelstar™ 5K100 laptop hard drive was selected for data storage. The hard drive was plugged into the IDE connector via an 8" ribbon cable. A portable flash memory device was used to transfer data from the measurement computer via USB port. A Linksys™ WPC54G wireless networking card with PCMCIA compatibility with the mainboard and 802.11b/g for wireless connection capability was also installed.

The NI-USB-9215A A/D module was selected for data acquisition and provides plug-and-play connectivity via a USB port for faster setup and measurements. This module was capable of accepting up to four data input channels simultaneously, providing sampling with 16-bit accuracy, and a sampling frequency up to 100,000 samples/sec/channel. The module provides 250 V_{RMS} channel-to-earth ground isolation for safety, noise immunity and high common-mode voltage range. The operating range of the A/D input channels are from –10.5 to +10.5 volts. The signals from the three channels of hydrophone data were hard wired to the input channels of the A/D as presented in Figure 7. Anti-aliasing filtering was not provided because of the low expected frequencies. The hardware was assembled in a compact configuration, using a custom-built frame of aluminum L-section bar stock, stainless and nylon hardware. Figure 8 shows the motherboard computer and peripheral devices after assembly.

11
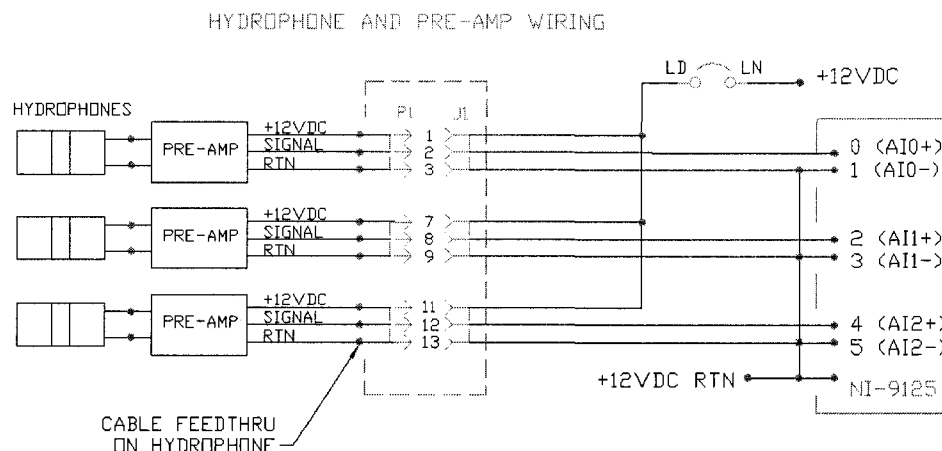
Figure 7: Schematic diagram of hydrophone and A/D electrical configuration.
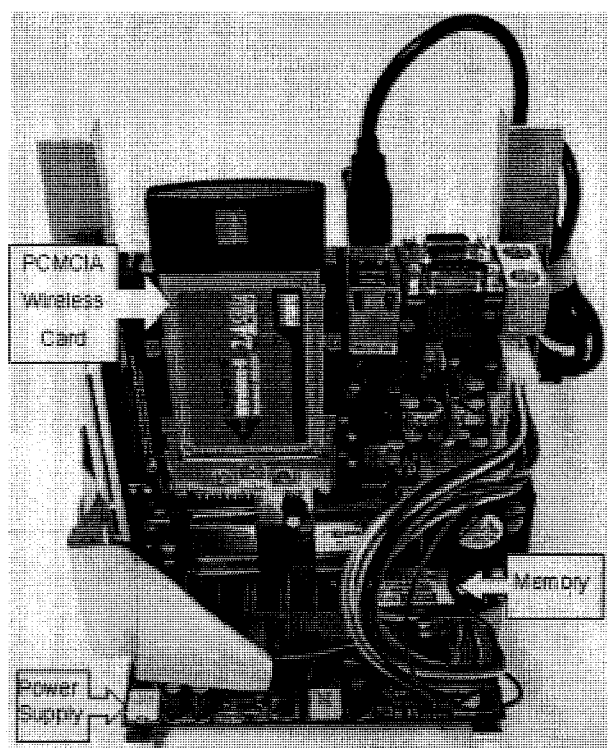
Figure 8: Layout of DAQ computer and peripheral devices. (Risso et al. 2006)

The total power consumption for the CPU, ADC, HD, RAM, and wireless adapter was estimated at 100W and required a 12VDC voltage source. The original source was a borrowed battery with a 34 amp-hour capacity. This battery was ultimately replaced with an inexpensive, lawn motor battery because of failure to hold a charge. The system

power was distributed and controlled by a model M1-ATX power supply card, with a 90W output power capacity, 12VDC compatibility, and soft-shutdown feature. Appendix A of this thesis contains a complete description, and manufacturer specifications for the components of the DAQ system.

2.3   Software Description

Applications used to record and display the data real time from the A/D were designed with the LabVIEW^{TM} Version 7.1 graphical interface software. Specific operations can easily be programmed. Virtual instruments (VI), capable of data capture and storage were written, acquiring data at selectable sampling frequencies from 20,000 to 40,000 samples/second/channel. The functionality and complexity of the virtual instruments were kept as simple as possible. As the graphical script or VI becomes more complicated, the speed at which they 'ran' conflicted with the amount of computing power available to the user. The more tasks performed, the slower the host computer ran. The NI-USB-9125A module was run under the NI DAQmx^{TM} high-performance multithreaded driver software. Appendix B describes the LabVIEW^{TM} virtual instruments used during the evaluation.

The data was displayed and stored onto the hard drive as ASCII text files with an LVM or TXT extension as LabVIEW^{TM} Version 7.1 does not allow writing binary files. Saving data files as ASCII was cumbersome due to the file size. This problem was overcome by converting the acquired data to binary files using Matlab^{TM}. A representation of the Matlab^{TM} code is contained in Appendix C of this thesis.

2.4   Hydrophone Assemblies

The *SPL* of concern was greater than 180 dB re 1μPa. Most construction-related waterborne noise occurs at frequencies less than 4kHz (Rizzo et al. 2006). The task was to specify low-frequency hydrophones capable of recording *SPL*s between 180 dB re 1μPa and 260 dB re 1μPa. Risso et al. (2006) selected Benthos AQ-2000 hydrophones with AQ-201 preamplifiers. These hydrophones were typically used in low frequency towed arrays. It was their low frequency operation, which lead to their selection. Manufacturer specifications and an analysis of the hydrophone components are presented in Appendix D of this thesis. Construction of the hydrophone assemblies had problems of its own. A non-corrosive container was required to protect the electronics from water intrusion but still allow the hydrophones to be sensitive enough for low level signal capture. The original hydrophone assembly was made up of reinforced braided vinyl tubing with an inner diameter of ¾", and the data cable exiting one end for connection to the data acquisition system as shown in Figure 9. This was selected for the housing material due to low cost, abrasion resistance, and ease of construction. Housing ends were fabricated out of PVC. The ¾" diameter, 1 ½" long barbed PVC plugs were filled with marine epoxy putty, inserted into each end of the vinyl housing and secured with stainless steel pipe clamps. A fluid was required to fill the container for transmission of the acoustic signal from the container wall to the element that was non-electrically conductive. Mineral oil was selected as a suitable filler fluid for hydrophone construction, based on it being nearly incompressible, environmentally-benign, and its acoustic impedance matching properties. Brass bleed tubes with stainless steel screws, rubber seals, and brass washers were incorporated into each hydrophone end to allow

14

filling with mineral oil. The bleed tubes also allowed the evacuation of air from the hydrophone assembly. Initial testing proved the original design to be inadequate, as the vinyl tubing attenuated the incoming signals, assumed to be due to mechanical loading of the elements and the stiffness of the tubing.
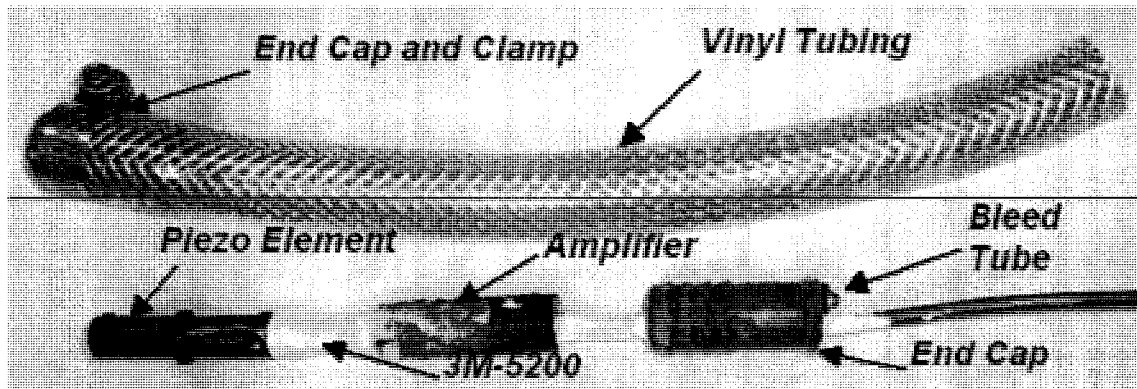
Figure 9: Pictorial original hydrophone design showing piezo-element and amplifier inserted into vinyl tubing filled with mineral oil.

2.5   Instrument Canister Description

The instrument canister was made from PVC pipe, approximately 10" in diameter and 22" in length. The bottom, made of PVC was rigidly sealed, while the cover was removable, and made watertight using neoprene rings and Neilsen clamps. A 14" diameter PVC flange was attached to the top end of the canister. This allowed the canister to rest in-place within the buoy. The hydrophone wiring was fed through the cover using watertight compression fittings. Internal connectors and a wiring harness were installed to provide easy removal of individual components.

CHAPTER 3

ACOUSTICAL CONSIDERATIONS

3.1   Introduction

To better understand the concept and limitations of the Acoustic Measurement

Buoy some theoretical considerations of underwater acoustics, were needed. Basic

definitions of pertinent sonar parameters were required to evaluate transducer

performance and propagation issues. These were coupled with fundamental data

acquisition concepts to complete the measurement system parameterization. A basic

SONAR model was used to evaluate the problem.

3.2   The SONAR Equation

The SONAR equation defines the relationship between source level, sound

pressure level, transmission loss and other physical attributes. There are different forms

of the SONAR equation, which depend on whether the sonar is passive or active. In the

passive case, hydrophones are used to detect independent acoustic signals. This is

characterized by equation 3.1.

$$SL - TL = NL - DI + DT \ \text{ units of dB re 1 uPa} \quad \text{(Urick 1983)} \quad (3.1)$$

Where SL is the source level of the signal, TL is the transmission loss, DI is the receiver

directivity index, NL is the noise level and DT is the detection threshold. For this

application and analysis, a more specific form of the equation was used. From a SONAR

perspective,

16

$$SPL = SL - TL - InL \quad units\ of\ dB\ re\ 1\ \mu Pa \qquad (3.2)$$

The insertion loss (*InL*) is calculated as the algebraic difference in the calculated value of the sound pressure level, taking the source level and transmission loss into account. In this context, the insertion loss is signal loss due to any attenuating materials or physical properties such as air bubbles. The *SPL* is measured directly in a hardware perspective from the hydrophones using equation 3.3.

$$SPL = -OCVR - Gain + 20log_{10}(V_{RCVD}) \quad units\ of\ dB\ re\ 1\ \mu Pa \qquad (3.3)$$

OCVR is the open circuit response of the hydrophone. This is also referred to as the *FFVS* (free field voltage sensitivity) or the sensitivity (M_x). *Gain* is any amplification applied to the signal from the hydrophone and V_{RCVD} is the output voltage of the hydrophone. Figure 10 is a representation of the components of the SONAR equation and dependencies as related to the passive model.
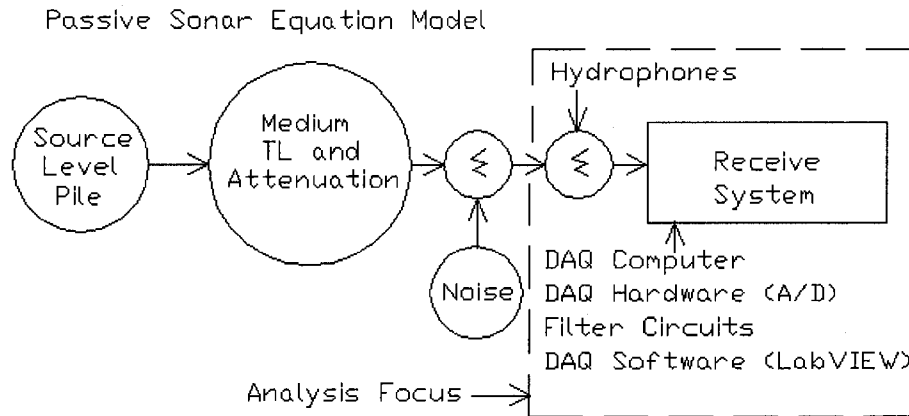
Figure 10: Block diagram of the passive sonar model. The analysis focussed on the data acquisition system and hydrophones.

3.3   Sound Intensity and Sound Pressure Relationship

Acoustic intensity is the fundamental measure of sound and is a measure of power per unit area. It is not always useful in a practical sense. The standard measurable

parameter is the acoustic or sound pressure (Kinsler et al. 2000). In a small amplitude

plane wave, instantaneous intensity is related to the instantaneous acoustic pressure

(Urick 1983). The SI units for pressure are the Pascal or Pa (Newtons/meter^2). The

relationship between the acoustic intensity (I), sound pressure (P) and sound speed (c) are

related through the expression:

$$I = P^2 / \rho_0 c \quad units\ of\ watts/meter^2 \quad \text{(Urick 1983)} \quad (3.4)$$

Where, ρ_0 is the specific density of the medium. The term $\rho_0 c$ is the acoustic impedance

(z), measured in Rayles. (1 Rayle = 1 kgm^{-2}s^{-1}). For seawater this term can be

approximated as:

$$z = \rho c = 1027 x 1500 = 1.54 x 10^6 Rayles \quad (3.5)$$

(ρ_0 = 1027 kg/meter^2, c = 1500 meter/second) (Kinsler et al. 2000)

The acoustic impedance is an important parameter as it controls the magnitude

and nature of reflection from an interface between two different z's. The acoustic

intensity (I) of a sound wave is the average rate of flow of energy through a unit area

normal to the direction of wave propagation. Normally the pressure (P) is taken to

represent the average of the squared pressure over an interval of time in order to give an

average intensity (I) for that interval.

$$E = \int_0^\infty I\ dt = \frac{1}{\rho c} \int_0^\infty P^2\ dt \quad \text{(Urick 1983)} \quad (3.6)$$

This equation is valid for transient signals, where signal distortion is prevalent. It

is described as the energy flux density (Urick 1983). Acoustic intensity and pressure can

vary over a wide range. The traditional method to describe these quantities has been to

use the decibel (dB). This has many advantages as we are often only interested in ratios

of pressure (or intensity) and not absolute values. Large changes in pressures can be easily represented. The intensity level (*IL*) with intensity (*I*), is defined as:

$$IL = 10 \log(I_{Im}/I_0) \quad units\ of\ dB\ re\ 1uPa \quad (3.7)$$

I_{Im} is the measured acoustic intensity (watts/meter^2) defined at 1 meter and I_0 is the reference acoustic intensity of 0.667 x 10^{-18} watts/meter^2.

$$IL = 10 \log(I / I_o) \ and\ IL/10 = \log(I / I_o) \quad (3.8)$$

Taking the inverse log is equivalent to raising 10 to the power of both sides of the equation:

$$10^{IL/10} = (I / I_o) \quad (3.9)$$

$$I = I_o \, 10^{IL/10} \quad (3.10)$$

Because a hydrophone is a transducer that converts sound pressure to voltage, sound pressure changes are easily detected and recorded. The sound pressure level (*SPL*) is defined as:

$$SPL = 20 \log 10(P/P_{ref}) \quad units\ of\ dB\ re\ P_{ref} \quad (3.11)$$

For seawater, the reference acoustic pressure $P_{ref} = 1\ \mu$Pa. The *SPL* at any location is a ratio of the local sound pressure to P_{ref}.

3.4   Transmission Loss

Transmission loss (*TL*) is defined as the "weakening" of an acoustic signal between any point 1m from the source to a receiver at some distance or range. Given two Intensities (I_0 1m from the source and I_1 the intensity at range), the *TL* can be calculated as:

$$TL = 10 \log(I_0/I_1) = 20 \log(P_0/P_1) \quad (3.12)$$

Where I_0 is the reference intensity (at 1 meter), P_0 is the reference pressure (1 μPa), I_1 is the intensity and P_1 is the pressure at some range. The *TL* is the loss of acoustic energy per unit area and is composed of two components, spreading (Geometry) and absorption (Losses).

$$TL = TL \ (Geometry) + TL \ (Losses) \qquad (3.13)$$

Spreading refers to the "weakening" of sound as it travels away from a source. The sound energy expands as it moves outward from the source, as it does, the total energy is spread over a greater area. The spreading of the sound can be either spherical or cylindrical. How the signal spreads is based on the boundaries of the environment. In an unbounded medium, the acoustic energy radiates from a source in all directions as a sphere. This occurs in deep water (within surface / bottom boundaries) and is known as spherical spreading. By definition, power equals intensity times area:

$$P = 4\pi r_1^2 I_1 = 4\pi r_2^2 I_2) \quad \text{(Urick 1983)} \qquad (3.14)$$

If r_1 equals 1m, the TL at range r_2 becomes:

$$TL_{Spherical} = 10log(I_0/I_1) = 10log(r_2^2) = 20log(r_2) \qquad (3.15)$$

Applying the geometrical and loss terms, the complete solution becomes:

$$TL = 20 \ log \ (r_2) + \alpha R \ \ units \ of \ dB \ re \ 1m \qquad (3.16)$$

The absorption (α) depends on temperature, salinity, pressure, and pH of the water and are losses due to the "conversion of acoustic energy into heat". (Au 1993) Absorption is expressed as dB per kilometer. For our analysis, where the receiver was typically 1 meter from the source, this term is not significant, as absorption is irrelevant when dealing with the frequencies and ranges we are analyzing. The maximum range of data collection was 10 meters.

In a bounded medium such as in shallow water, the surface and bottom

boundaries affect the acoustic energy. At this point *cylindrical spreading* occurs.

$$P = 2\pi L r_1 I_1 = 2\pi (L r_2 I_2) \tag{3.17}$$

If r_1 equals 1m, and the Length (L) remains constant, the TL at range r_2 becomes:

$$TL_{Cylindrical} = 10 \log (r_2) + \alpha R \quad units \ of \ dB \ re \ 1m \tag{3.18}$$

Figure 11 displays the transmission loss (*dB re 1 μPa*) for spherical and

cylindrical spreading versus the range in meters.
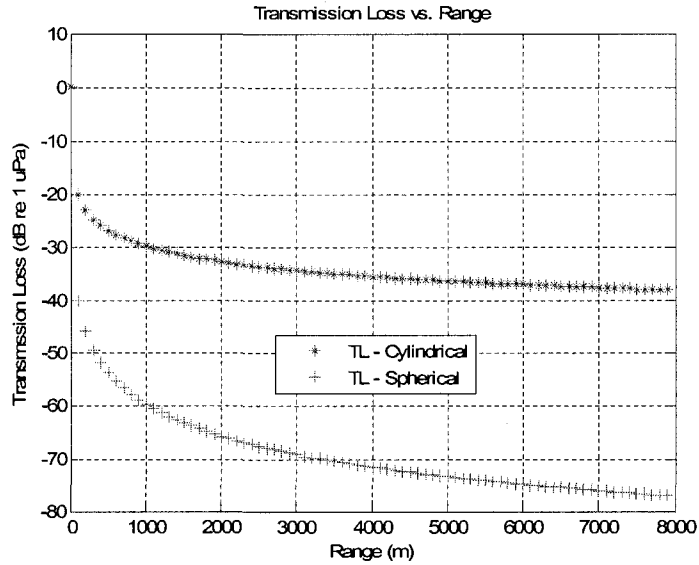
Figure 11: Representation of TL for spherical and cylindrical spreading.

3.5   Frequency and Wavelength Spatial and Temporal Relationships

The wavelength (λ) of a propagating acoustic signal is dependant on the frequency

(f) and the sound speed (c). The wavelengths versus the frequencies of interest for our

analysis are plotted in Figure 12. Lower frequencies have longer wavelengths which

compromise high fidelity data collection in an enclosed volume of water because of

interactions between the sound and the boundaries.

21
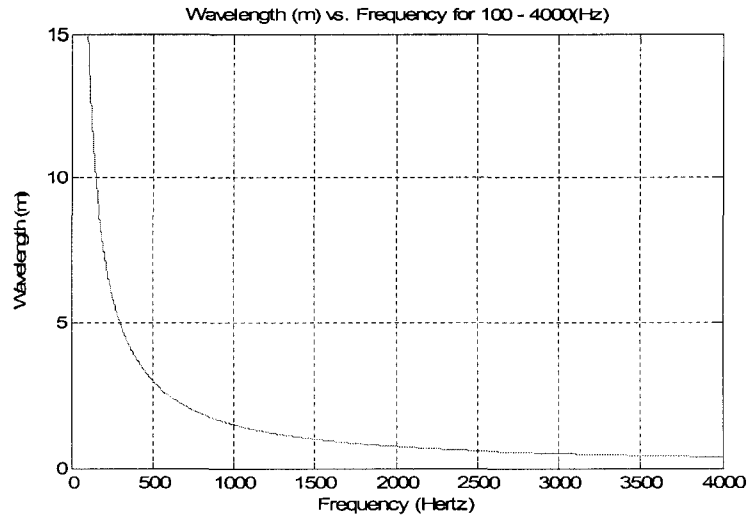
Figure 12: Plot of wavelength plotted versus frequencies of interest.

Frequency (f) (Hertz – cycles / second)	Wavelength(λ) (meters)	Period$_{stimulus}$ (T) (milliseconds) T = 1 / f
250	6	4
500	3	2
1000	1.5	1
2000	0.75	0.5
4000	0.375	0.25
8000	.1875	.125

Table 1: Frequency and wavelength relationship.
Assuming c = 1500 meter per second.

$$\lambda = c / f \qquad\qquad (3.19)$$

Table 1 compares how the frequency of a signal affects the wavelength and the period

length (in time). The wavelength is the major constraint in analyzing a transmitted

signal, especially in an enclosed volume. Spatially, you must have enough distance in the

water for the transmit signal to fit without interacting with the boundaries. Accurate data

collection becomes impractical in test tanks at low frequencies. The limiting factor is the

size of the tank and physical properties of the transmit frequencies. In the Jere Chase

Ocean Engineering Laboratory, the tank dimensions are 18.3 meters (60 feet) long, 12.2 meters (40 feet) wide and 6.1 meters (20 feet) deep. Using an omni-directional source, signals in the tank propagate in all directions, bounce off the walls and set up interference patterns and reverberation which will corrupt the received signal. Because of size limitations of the Jere Chase Ocean Engineering Laboratory tank, evaluation of frequencies below 10kHz in that tank tend to be imprecise.

CHAPTER 4

EVALUATION, TESTING AND RESULTS

4.1 <u>Introduction</u>

The initial prototype design of the Acoustic Measurement Buoy was not subjected to rigorous engineering evaluation as presented in Risso et al. (2006). This chapter presents the evaluation, testing and results of the feasibility study of the measurement instrumentation of the Acoustics Measurement Buoy prototype and subsequent modifications. The evaluation was systematically performed in a series of steps beginning with preliminary testing and calibration of the individual components and conducted using various experimental methods. From the onset of the project, the evaluation and testing of the prototype and the relationship between the hardware and the software was tenuous.

During the summer of 2006, the DAQ system was assembled, and tested to optimize the robustness of the system. This included adding DC wiring and a circuit breaker with bracket to the DAQ computer. Hydrophone wiring to the A/D through the canister cover was completed, requiring terminal strips and internal connectors to be designed and constructed. Shielding was provided from the hydrophones to the input terminal block. Control of the measurement system is based upon the software. LabVIEW™ 7.1 and required DAQmx™ drivers for the A/D were installed onto the DAQ computer. This allowed the acoustic data from the hydrophones to be converted into digital data through the NI-USB-9125A A/D. Multiple virtual instruments were

written and evaluated. Some of the designs included filtering in software while others simply acquired and saved data. Ultimately a very simple, but functional, virtual instrument was selected. The hydrophones were redesigned, repackaged and repaired during the summer.

Into the fall of 2006, initial testing began in the tanks of the Jere Chase Ocean Engineering Laboratory. The hydrophones required an analog filtering interface to be designed. A DC block (high pass filter) and wiring interface was built and implemented. Matlab^{TM} algorithms were written and verified for data analysis.

The main focus of the evaluation began in the spring term of 2007. The hydrophones and DAQ system were calibrated using the substitution method and more in-depth experimentation and tank testing was performed. An attenuating wrap placed around the source to evaluate the dynamic range of the system, and possible usage in recording low-level acoustic signals. Results included analysis comparison using an independent acoustic measurement system with Reson hydrophones.

In the Fall of 2007, in situ data collection was performed at a floating dock, using a Lubell source, (reference Appendix E) with an SL >180 dB re 1μPa at frequencies from 500Hz to 8000Hz. These frequencies were too low to have been accurately analyzed in the tank in the Jere Chase Ocean Engineering Laboratory. The stability of the Benthos hydrophone assemblies were evaluated. The packaging and design of the filter networks were replaced by a modular design and the original DAQ computer was replaced with a more powerful Innovation Station mini-computer, requiring a packaging re-design. This self contained computer was borrowed from the TECH 797 class of 2006/2007 and was able to be operated from the 12 VDC power system installed into the instrument canister.

4.2 Hydrophones

The hydrophones were the most fundamental component of the measurement system. Early analysis of the prototype hydrophones revealed design flaws. They lacked repeatable sensitivity, were susceptible to noise, and did not meet manufacturer's *OCVR* (Open Circuit Voltage Response), also known as the *FFVS*, (Free Field Voltage Sensitivy) or sensitivity (M_x) specifications, due to packaging. Figure 13 displays a fishbone diagram of the aforementioned problems. The major topics are blocked titles with the dependencies shown on each 'bone'. The categories are co-dependant and affect each other. The hydrophones were assembled from the Benthos AQ-2000 piezo elements and AQ-201 preamplifiers.
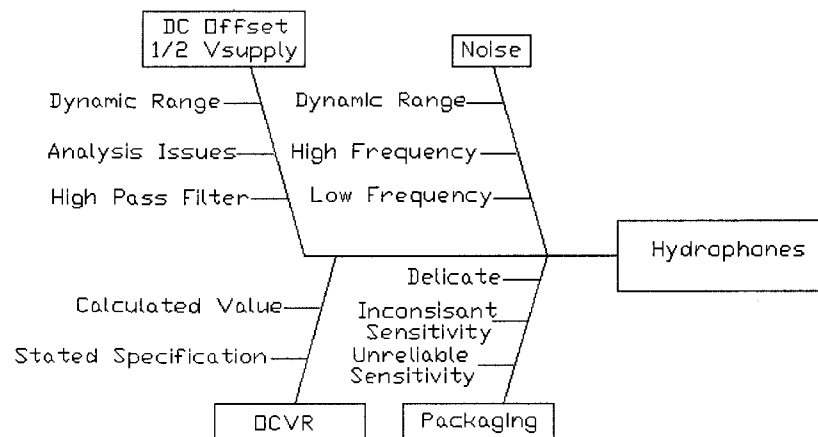
Figure 13: Fishbone diagram of error components of Benthos hydrophones.

The hydrophone and preamplifier packaging was the first problem addressed, as greater sensitivity was required for signal recording. Repackaging of the hydrophone assembly was performed, allowing the piezo-element to be in direct contact with the water. The heat shrink tubing placed around the element reduced the sensitivity of the hydrophone by modifying the axial response. A pictorial of the final design is shown in Figure 14.

26
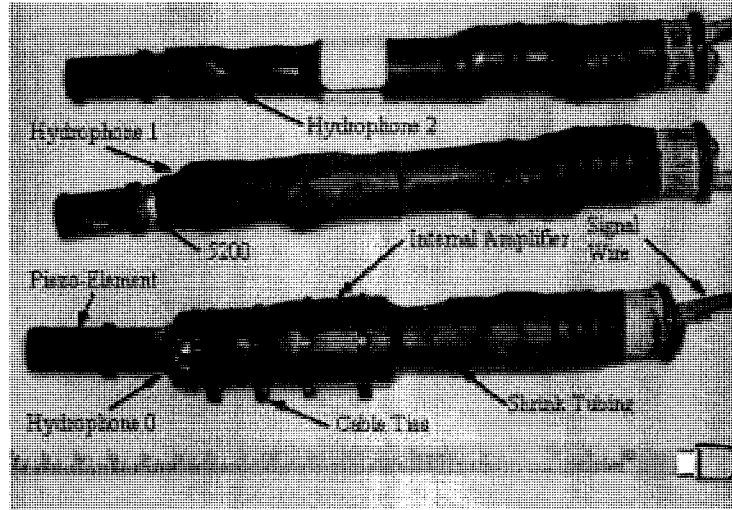
Figure 14: Final design of Benthos hydrophones.

The hydrophone evaluation began with the premise that acoustic signals could be

acquired and recorded at the expected sound pressure levels and frequencies. The Lubell

source and hydrophone assemblies were submerged into the deep tank in the Jere Chase

Ocean Engineering Laboratory. The analysis was primarily a qualitative analysis where

signals of expected frequencies and different acoustic source levels were transmitted into

the water. The acoustic signals were received using the Benthos hydrophones,

preamplifiers and DAQ system. To accurately measure sound pressure levels, the *OCVR*

or sensitivity of the hydrophones must be known. A more precise data collection process

began with the calibration of the Benthos AQ-2000 hydrophones and AQ-201

preamplifiers with reference hydrophones, Reson TC4014 (designated as #1 and #2).

The specifications of the Reson hydrophones are contained in Appendix F of this thesis.

The substitution method was used to evaluate the magnitude of the sensitivity of the

Benthos hydrophones. This was accomplished by transmitting a known source level with

a calibrated source, ITC-1042 serial number: 1337, at 10kHz into the water and receiving

the signal with multiple hydrophones. The specifications of the source are contained in

Appendix G of this thesis. Using Matlab™ scripts, the data was analyzed and the

sensitivity was established. Knowing the *SL* and the *TL* at range, the *SPL* is calculated

using equation 4.1.

$$SPL = SL - TL \quad units \ of \ dB \ re \ 1\mu Pa \qquad (4.1)$$

The *SL* was calculated and validated using the independent Reson reference hydrophones,

knowing the calibrated *TVR* (Transmit Voltage Response in dB re 1μPa /V) and the input

voltage (V_{RMS}) of the source. The *TVR* is a function of frequency and is so noted. The

SL is calculated using the following relationship.

$$SL = TVR(f) + 20log10(V_{RMS}) \quad units \ of \ dB \ re \ 1\mu Pa \qquad (4.2)$$
$$(Kuntsel \ et \ al. \ 1992)$$

The *SPL* at range is found using equation 3.3. Rearrange terms and solving for the

OCVR:

$$OCVR = -SPL - Gain + 20log(V_{in}) \quad units \ of \ dB \ re \ 1\mu Pa \qquad (4.3)$$

All measurements were made in the far field which begins at a range described by

equation 4.4.

$$far \ field \ distance \ \geq \ Area \ of \ transducer/\lambda \qquad (4.4)$$

Measurements made in the near field can be very difficult to interpret. Accurate

measurements must be made in the far field as diagrammed in Figure 15.
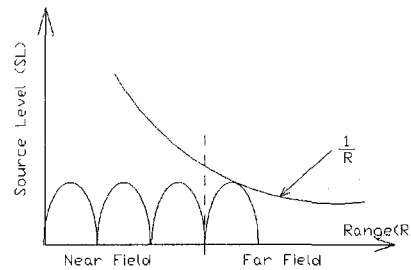
Figure 15: Near field / Far field representation. (Adapted from Lurton, 2002)

A calibration, using a gated pulse, with a known *SL* at 10kHz was performed as follows. The Benthos and Reson hydrophones were secured in a custom designed rigid frame. The frame formed an arc at a range of 1.5 meters from the source as depicted in Figure 16. The separation and physical layout are shown in Figure 17. The ITC-1042 source, along with the Benthos and Reson hydrophones were installed in the tank at a depth of 10 feet (3.3 meters) with a separation distance of 1.5 meters. Foam and neoprene rubber were used to isolate any vibrations between the hydrophones and the frame.
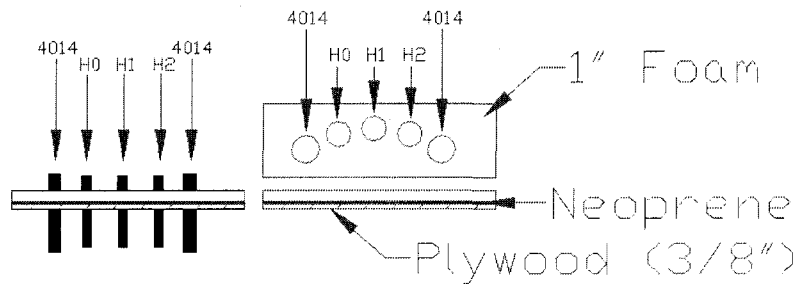
Figure 16: Geometric layout of hydrophones installed in frame for calibration.
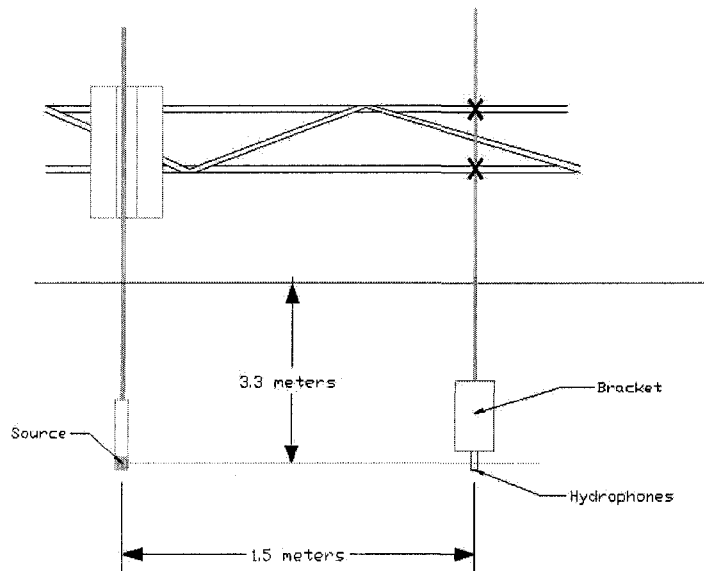
Figure 17: Schematic of hydrophone calibration setup.

Three different drive voltages were used to check linearity. The *SPL* at the Reson

hydrophones were calculated and the *OCVR* of the Benthos hydrophones were adjusted

accordingly as to bring all the values to a common intersection. Multiple measurements

were conducted, varying the number of cycles for each data file. This procedure allowed

the *SPL* and *OCVR* calculations to be validated multiple times. To keep the data

collection uncoupled, the Reson hydrophone data were captured using an independent

system made up of the OE Sony notebook PC with National Instruments Virtual Scope™

V2.0 and NI-5102 USB data acquisition module. The setup of the calibration is

schematically shown in Figure 18.
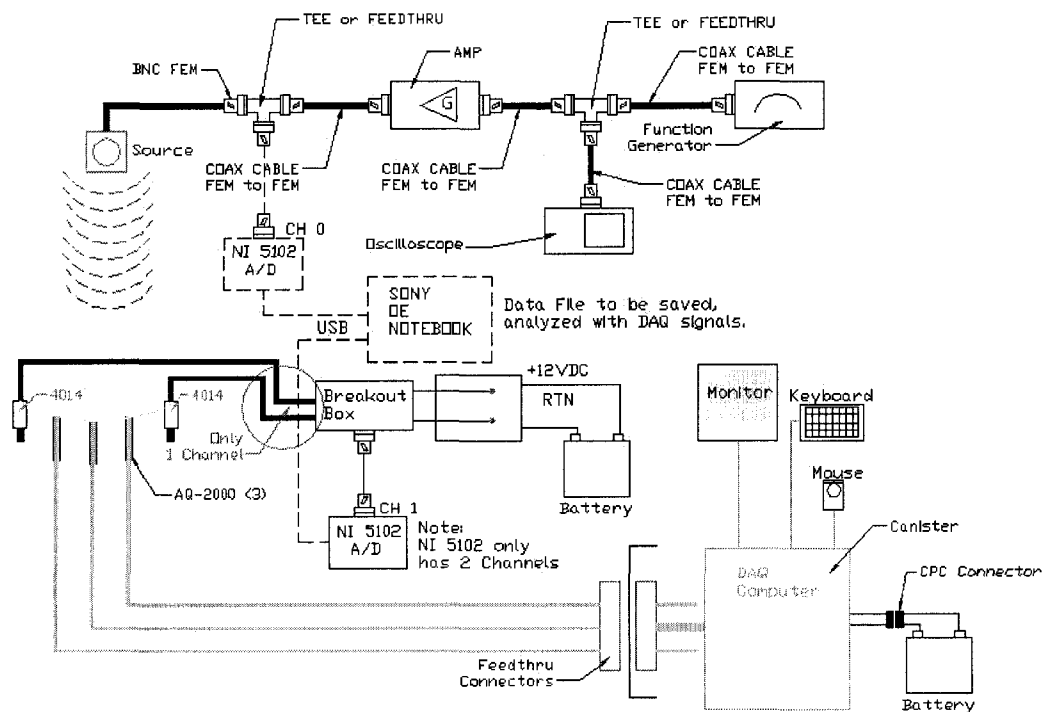
Figure 18: Schematic diagram of electrical test equipment used in the
hydrophone calibration.

The vendor specification for the *OCVR/FFVS* of the Benthos AQ-2000

hydrophones were stated as -201 dB re 1Vrms / μPa ± 1.5 dB. The hydrophone

calibration produced values less than specified, which was attributed to the packaging of

the hydrophones. The calibrated *OCVR* for each hydrophone from Feb 2007 is presented

in Table 2. The center column values are for the hydrophone without the preamplifier.

The *OCVR* of the hydrophones, at the terminal ends, with internal AQ-201 preamplifiers

with a fixed gain of 26 dB are shown in the far right column. As the magnitude of the

OCVR increases, the sensitivity decreases.

Hydrophone	OCVR (dB re 1Vrms / µPa ± 1.5 dB) Hydrophone Only	OCVR (dB re 1Vrms / µPa ± 1.5 dB) Hydrophone with Internal Amp
Hydrophone 0	-209	-183
Hydrophone 1	-209	-183
Hydrophone 2	-203	-179

Table 2: Calibrated *OCVR* – Feb 2007.

4.3 **Filtering**

The initial design, as proposed by Risso et al. (2006), included 'signal filtering' as

a generalization. Data collection and analysis was begun with this original configuration.

The output signals from the three channels of hydrophone data were hard wired to the

input channels of the A/D, as seen in Figure 7. During the evaluation, analog high pass

filters were designed and implemented. The frequency response is plotted in Figure 19

and a complete analysis of this high pass filter is contained in Appendix D of this thesis.
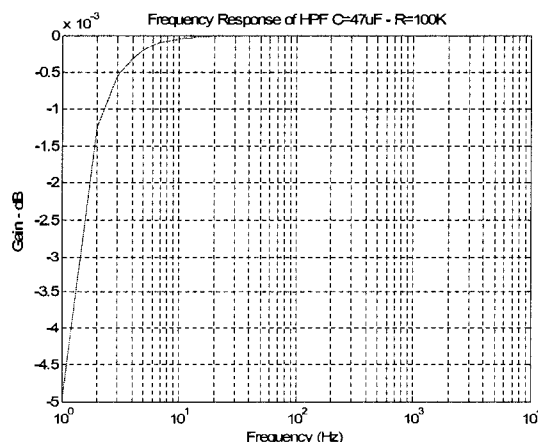
Figure 19: Preamplifier de-coupling circuit frequency response.

A DC offset equal to ½ the supply voltage was present on the input signals as can

be seen in Figure 20. During preliminary analysis, this DC offset corrupted calculations

and needed to be eliminated to perform accurate data analysis and to increase the

dynamic range of the measurements. A solution was to design and build single pole high

pass filtering networks, which acted as a DC blocking circuit. Each channel requires its

own network.
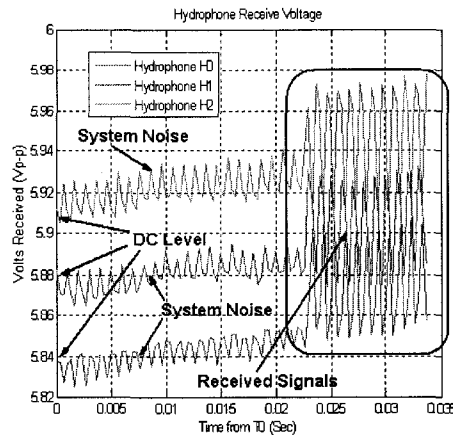
Figure 20: Plotted data from Benthos hydrophones showing DC offsets and
system noise. The three channels sit at different DC levels.

The high pass filters were inserted between the wiring from the hydrophones to

the input channels of the A/D as shown schematically in Figure 21. Different values of

the electrical components values were analyzed, while effectively removing the DC

component of the signals. These component values of these single pole filters were

chosen to optimize capture of low frequency signals. Figure 22 schematically diagrams

the original filter component assembly and wiring. This design was improved upon and

packaged as a modular unit as shown in Figures 23 and 24. The final design package was

configured for use in future experiments. Electrically, the wiring is equivalent between

the high pass filter packages, with the addition of an added DC power connector, On/Off

switch and 1 amp fuse in the modular package.
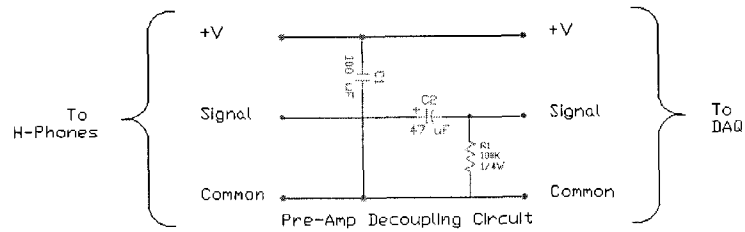
Figure 21: Schematic diagram of high pass filter for hydrophone signals.
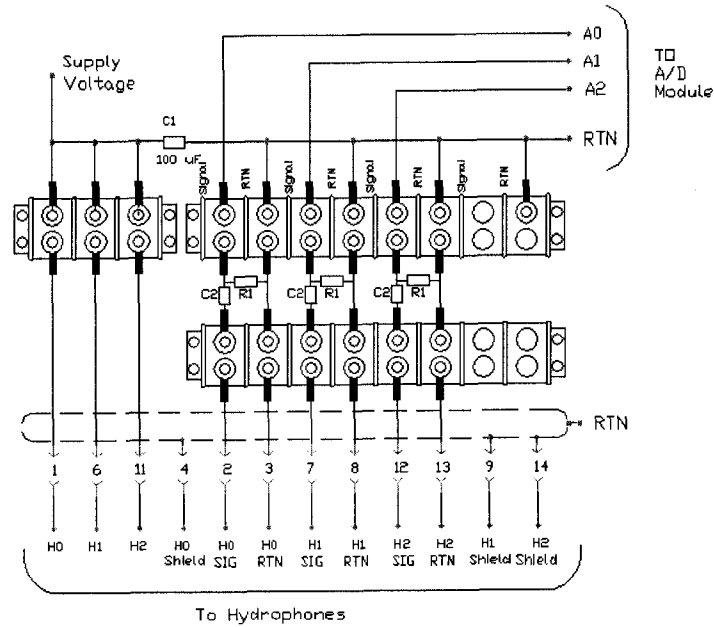
Figure 22: Assembly diagram of the components of the high pass filter. For simplicity, hydrophone 0 is denoted as H0, hydrophone 1 is denoted as H1, hydrophone 2 is denoted as H2.
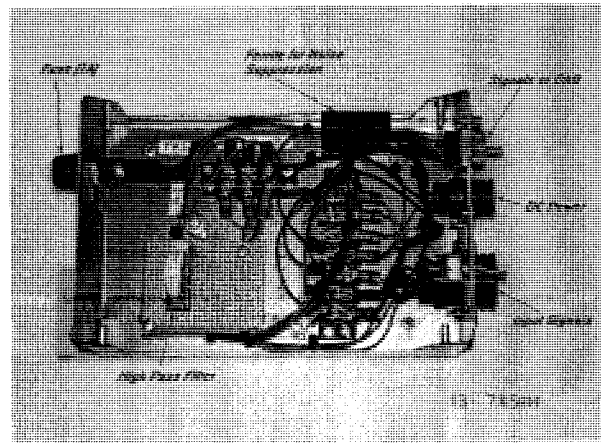
Figure 23: Overhead view of single pole high pass filtering circuits. The packaging of the components are put together in a modular fashion.

33
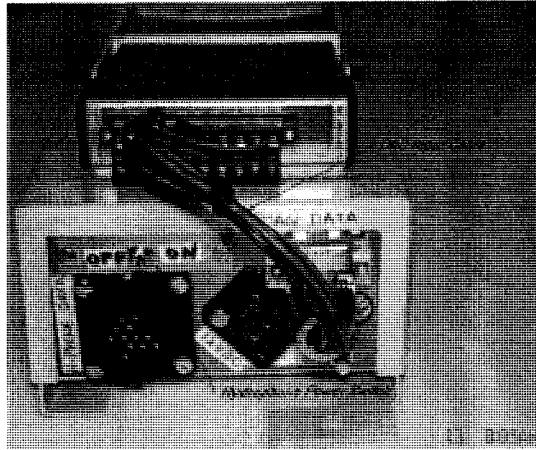
Figure 24: End view of modular filter package and NI-USB-9125A A/D.

4.4   DAQ Computer Assembly

The DAQ computer was meant to be low cost, and compact. The design included a wireless card potentially allowing a remote wireless connection. During this evaluation the wireless card and original computer proved to be unreliable. The use of the wireless card were abandoned. The components are shown as a fishbone diagram in Figure 25.
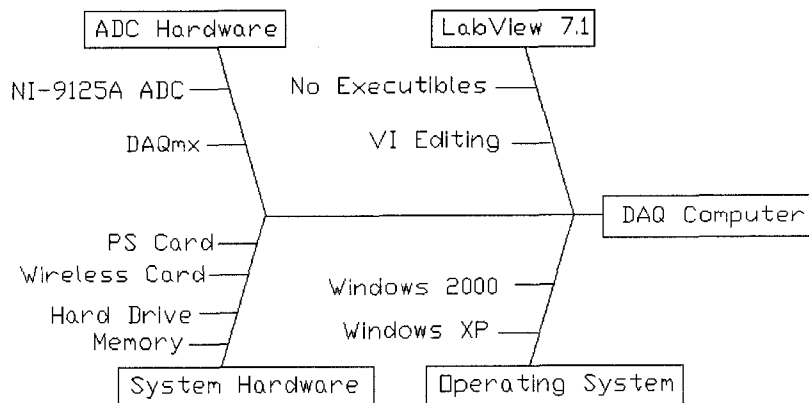
Figure 25: Fishbone diagram of the DAQ computer.

The original schematic diagrams are displayed in Figures 26 and 27. Changes were required to the DAQ computer design and wiring. A system return was required

34

from the hydrophone supply voltage return to the A/D return. A simple LabVIEW™

virtual instrument, capable of data capture and data storage was written and used to test

the functionality of the data acquisition system. For evaluation, the functionality and

complexity were kept as simple as possible.
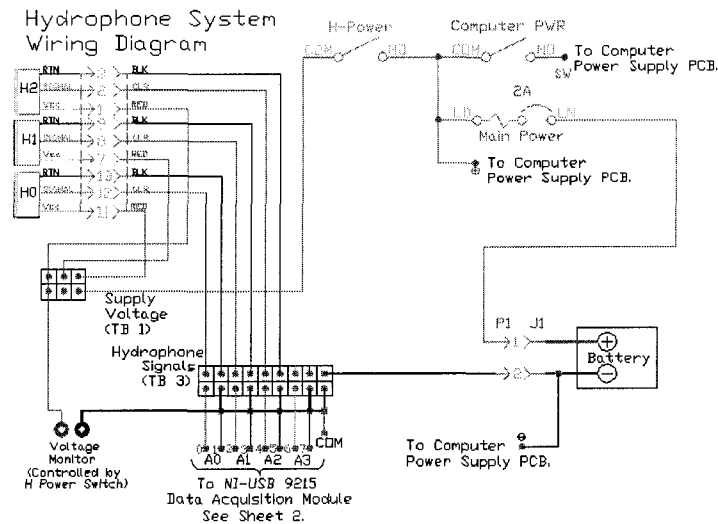
Figure 26: Schematic diagram of original hydrophone assembly and system power.
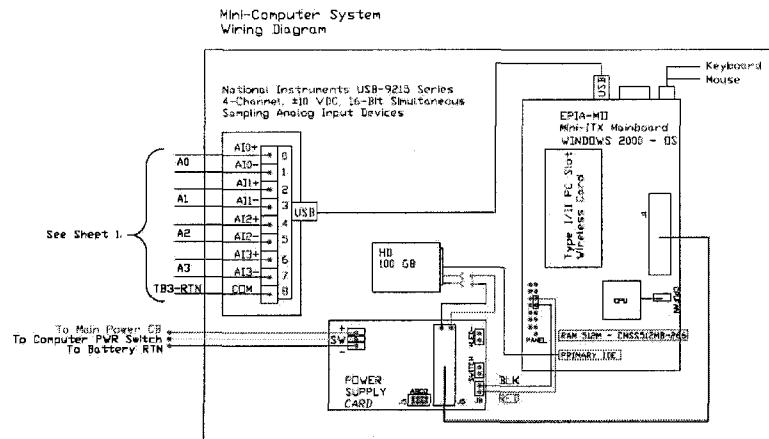
Figure 27: Schematic diagram of the DAQ computer system and A/D electrical
configuration.

The wiring from the hydrophone assemblies to the A/D were modified to incorporate the

analog high pass filters as shown schematically in Figure 28 and is depicted in Figure 29.
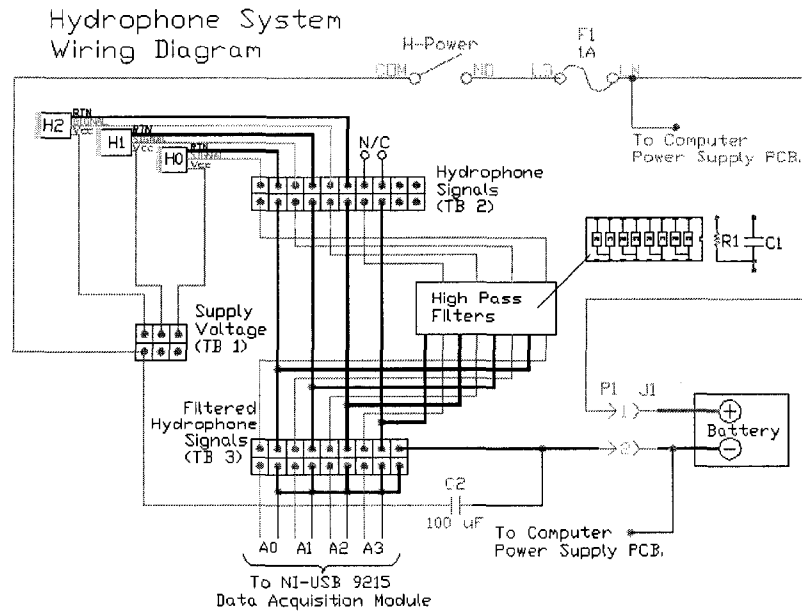
Figure 28: Schematic diagram of redesigned hydrophone assembly and system power.
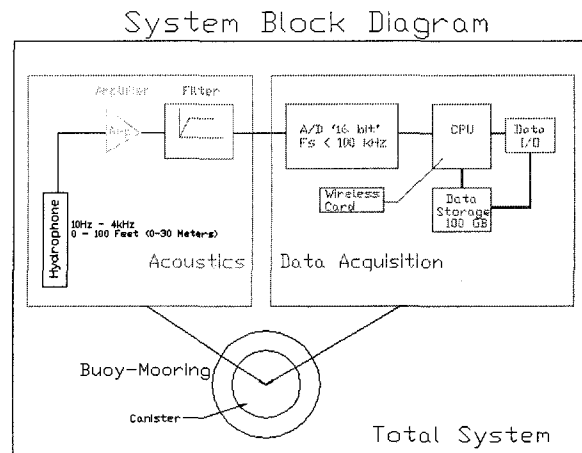
Figure 29: Block diagram of the components of the acoustic measurement buoy with
the high pass filters added.

During the evaluation, the DAQ computer encountered system problems, such as
not booting, locking up, inability to run or edit LabVIEW™, and an unreliable wireless
connection. After making many changes, the DAQ computer would still encounter
numerous blue screens (system hardware errors). This rendered the system unusable and

unreliable for data collection. The operating system of the prototype DAQ computer was Windows™ XP, was replaced with Windows™ 2000 in an effort to improve system reliability. Problems encountered are summarized in Table 3.

- Would not start up – only error code beeps.
- Blue Screen: IRQL_NOT_LESS_OR_EQUAL.
- Blue Screen on Computer. Would not start up – Error Codes.
- Blue screen. Video error.
- Computer would not start up. Could not establish wireless connection.
- The wireless connection dropped in and out.
- Blue Screen. Could not establish wireless connection.
- Could not find wireless card drivers.
- Locked up after 5 minutes. Could not establish wireless connection.
- Locked up (Labview™ not responding). No response from hydrophones
- Cannot edit in LabVIEW™. System locks up.
- Computer ran REAL SLOW. LabVIEW™ locked up.
- Cannot edit in LabVIEW™. Would lockup. Takes 4 starts to run LabVIEW™.
- Tried running system in deep tank. Too much noise on the signal to acquire any data.

Table 3: Summary of DAQ Computer problems.

The NI-USB-9125A A/D worked satisfactorily, with the DAQmx™ hardware drivers. These drivers limited the complexity of the virtual instruments that could be written. A source of the problem may have been the amount of random access memory installed, 512MB. The hard drive became greatly fragmented. The motherboard, by not having a true Pentium™ class CPU, lacked computing power to run the operating system and the LabVIEW™ data collection software.

4.5   LabVIEW™ Operation and Matlab™ Analysis Software

The analog data from the hydrophones was captured using the NI-USB-9125A A/D. The rate at which an analog signal is sampled (Fs) has a profound effect on accurately reproducing the signal in the digital world. To preserve the frequency of an analog signal, the signal must be sampled at least 2 times the highest signal frequency.

37

This is known as the *Nyquist Criteria*.

$$Fs \quad \geq 2*F_{highest} \qquad (4.5)$$

The higher the sampling rate or frequency, the more accurate the waveform or signal can

be represented. Aliasing will occur when the analog signal is not sampled at a frequency

equal to or higher than the Nyquist criteria.

For analysis of the data file, the header was removed and saved for reference.

The header contains the pertinent metadata such as the date, time and sample frequency.

A sample header is contained in Table 4. The data were saved in three columns as shown

in the sample data in Table 5. Each column contains the raw data for the separate

hydrophones.

```
LabVIEW Measurement
Writer_Version  0.92
Reader_Version  1
Separator       Tab
Multi_Headings  No
X_Columns       No
Time_Pref       Absolute
Operatorunh
Date     2007/02/19
Time     15:11:09.366267
***End_of_Header***
Channels        3
Samples 1100    1100    1100
Date    2007/02/19      2007/02/19      2007/02/19
Time    15:11:09.824999   15:11:09.824999   15:11:09.824999
Y_Unit_Label    Volts   Volts   Volts
X_Dimension     Time    Time    Time
X0       0.00000000E+0   0.000000000E+0 0.00000000E+0
Delta_X 2.500000E-5      2.500000E-5     2.500000E-5
***End_of_Header***
X_Value Hydro 0 (Trigger)  Hydro 1 (Trigger)  Hydro 2 (Trigger)
```

Table 4: Sample data file header.

0.024288	0.048775	0.035727
0.011216	0.038345	0.026808
0.023012	0.045615	0.034134
0.044374	0.063631	0.048787

Table 5: Sample data file.

The data files were tagged with the date, start time, and file number in the collection interval. The data were saved in discrete time intervals with file names as follows:

Data_DD_MM_YY_hhmm_ff

where DD is the day, MM is the month, YY is the year, hhmm is the hour and minutes and ff is the incremental file number in the acquisition interval. The data were then loaded into Matlab™ and converted into a binary file with a ".mat" extension. Raw data from a typical file: *Data_1556_003.m,* were plotted in Figure 30. These data were sampled at 40,000 samples/sec/channel and contain plots for the three hydrophone channels.
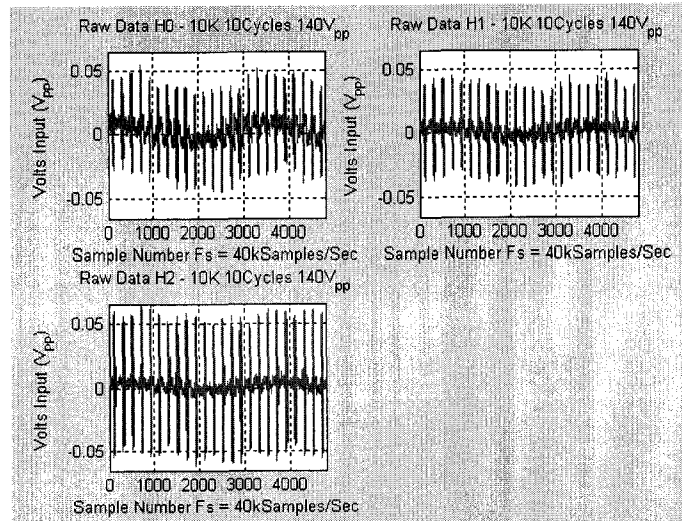
Figure 30: File: *Data_1556_003.m* raw data plot of all hydrophones.

Figure 31 plots an instance where two pulses were detected using the one shot triggerred virtual instrument (*2-1_Save_Data_40K_1min.vi*). One pulse from the hydrophone and a smaller earlier pulse from cross talk in the hydrophone wiring (File: *Data_07_02_01_1528_003*). In this application, noise from false triggering became prevalent which rendered this particular virtual instrument unstable and was abandoned. The constant capture virtual instrument (*1 minute Files Save All Data Sept 18.vi*), while more reliable, increased the size of the data file.
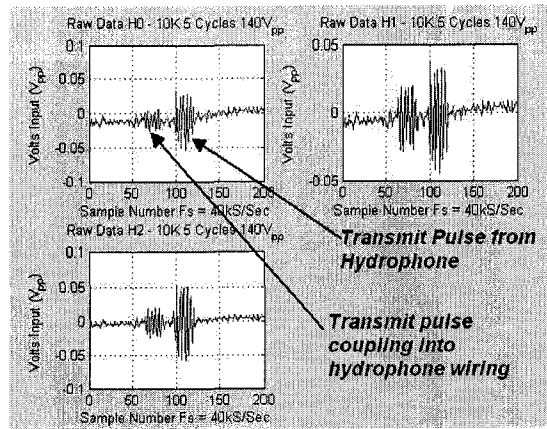
Figure 31: Plotted raw data of triggered signal, file: *Data_07_02_01_1528_003*.

As can be seen from the plotted data in Figure 32 (file: *Data_1600_001*), low frequency noise is present on the received signals. Frequencies around 60Hz dominate. The voltage inputs from the hydrophones are not consistent in any steady state level. The data were collected with an acoustic frequency of 10kHz and a source level of 151.9 dB re 1μPa at 1m. The virtual instrument captured data in one-minute time intervals. Twelve (12) pulses are visible in this data collection interval. The physical separation between the source and the receivers was 1.5m.
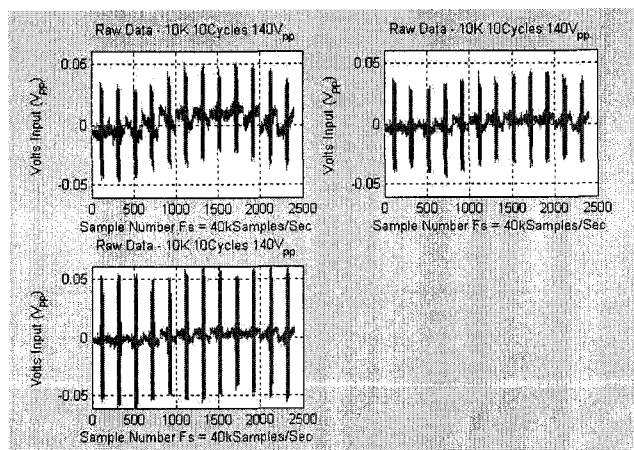
Figure 32: Raw data plot of Matlab™ file: *Data_1600_001*.

Figure 33 plots the filtered data. Figure 34 plots a 'Zoom' window of an individual pulse,

allowing calculation of the SPL_{RMS}.
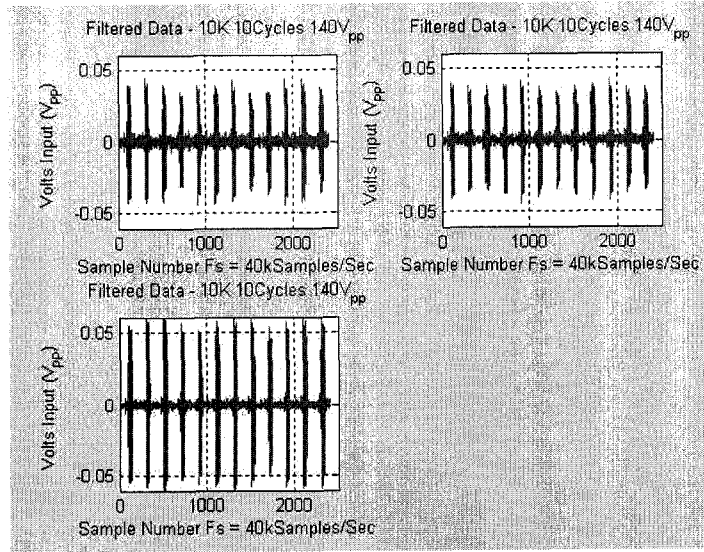
Figure 33: Filtered data plot of Matlab™ file: *Data_1600_001*. The plotted data was filtered in Matlab™ using an FIR Chebyshev type 2 bandpass filter, centered on 10kHz with a bandwidth of 8kHz.
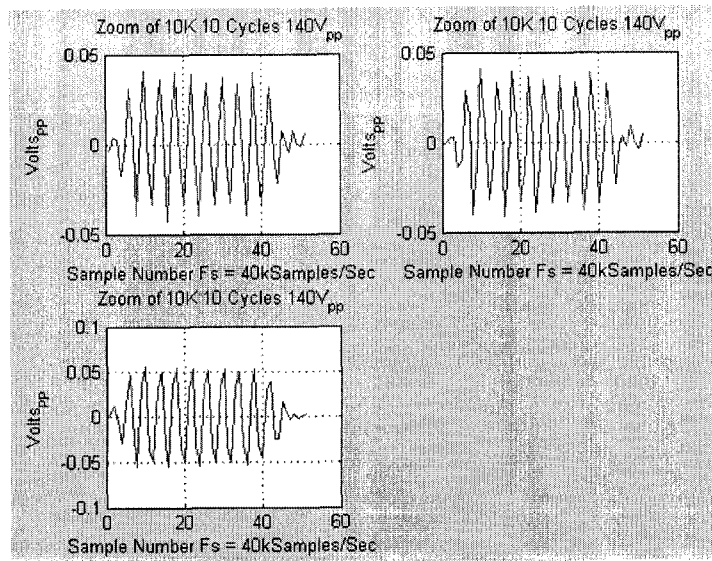
Figure 34: 'Zoom' of one pulse of filtered data plot of Matlab™ file: *Data_1600_001*, allowing analysis and calculation of SPL_{RMS}. The SPL is calculated to 150.5 +/- 0.5 dB re 1μPa for the three hydrophones.

The sampling frequency was verified using an Excel spreadsheet of the above

data for channel A0 (hydrophone 0). This was done to analyze the data for the possibility

of aliasing of the signal. The data is displayed in Figure 35. It can be seen there are 40

(4 points per cycle) data points, while the signal frequency is 10kHz as shown by the FFT

analysis in Figure 36. The sampling frequency was verified at 40,000 samples/sec.
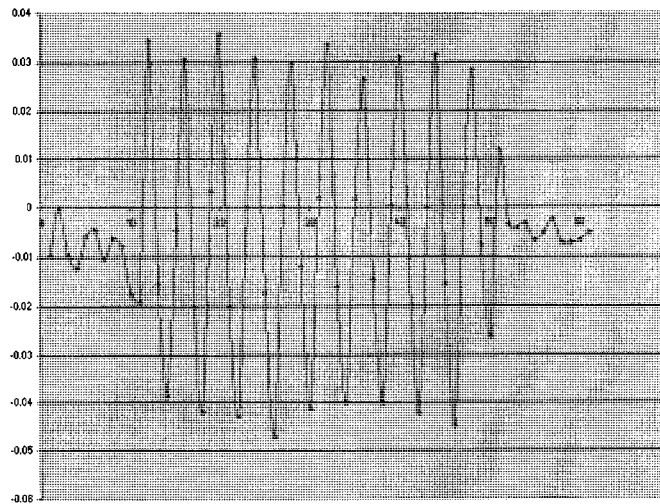
Figure 35: Excel plot of 'Zoom' of one pulse of filtered data file: *Data_1600_001*.
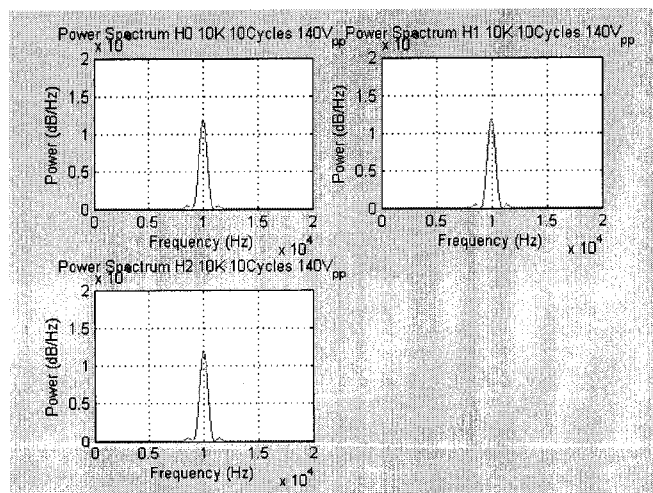
Figure 36: FFT analysis of one pulse of filtered data file: *Data_1600_001*.

4.6   Deep Tank – Wrap Testing Experiment

Sound can be absorbed or reflected by different bottom substrates or materials such as air bubbles, or air trapped in materials in the water. This can be regarded as insertion loss (*InL*). Insertion loss is similar to transmission loss, in that the source level of the signal has a reduction in sound pressure. An experiment was conducted in the Jere Chase Ocean Engineering Laboratory to evaluate the effectiveness of the prototype DAQ system for use in insertion loss measurements. This is diagrammed in figure 37. Insertion Loss is described by equation 3.2. At the measurement of the *SPL*, the *SL* is decreased by the *TL* and any *InL*.
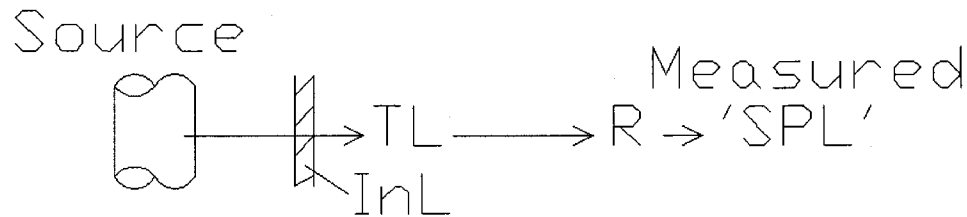
Figure 37:   Concept of *InL* (Insertion Loss), *TL* (Transmission Loss), *R* (Range), and *SPL* (Sound Pressure Level).

In SI units the acoustic impedance (ρc) of air = 415 Pa s/m @ 20°C and for seawater = 1.54×10^6 Pa s/m @ 13°C) (Kinsler et al. 2000). The difference in impedance between the two mediums is approximately 1.45×10^6 Pa s/m. When sound energy travels from one medium to another and encounters a discontinuity, part of the energy is transferred across the boundary and part is reflected or scattered back into the original medium. The greater the difference in acoustic impedance, the greater will be the percentage of reflected or scattered energy. Consequently, a significant decrease in the *SPL* outside of the "bubble curtain" would occur assuming a free bubble curtain surrounded a pile. Other methods of developing an insertion loss fixture for a pile may

employ air trapped in materials. This could be an insulating expanding foam, wrapped by neoprene rubber or can be as simple as plastic balls of different sizes, filled with air, wrapped around the pile. To evaluate the dynamic range of the prototype system, a Lubell source was confined by a cylindrical frame. An attenuating wrap composed of insulating foam neoprene rubber was placed around source and as shown in Figure 38. The source was secured midway in the tank. A SL >170 dB re 1μPa at 10kHz was transmitted and the effectiveness of the wrap was evaluated. The Reson hydrophones were once again used as an independent measuring system using the OE Sony notebook PC with National Instruments Virtual Scope^{TM} V2.0 and NI-5102 USB data acquisition module. Signals were acquired with the control Reson hydrophone acoustic system and the prototype system with Benthos hydrophones.
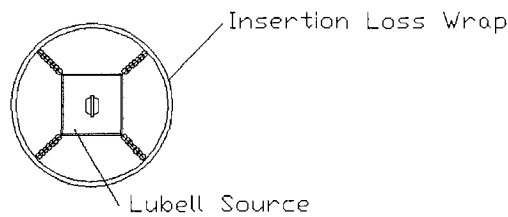
Figure 38: Concept drawing of the Lubell source installed inside the insertion loss wrap.

The attenuation wrap reduced the source level by as much as 40 dB as was verified by the Reson 4014 hydrophones. The effective source level was less than 140 dB re 1μPa. This low-level acoustic signal was unable to be captured by the prototype DAQ system as can be seen in Figure 39 from file: *Data_1322_001_C_Sampled.* The prototype design was to work within the following range: 180 dB re 1μPa < SPL < 240 dB re 1μPa. Any insertion loss evaluation was not included in the original design criteria as presented by Risso et al. (2006)
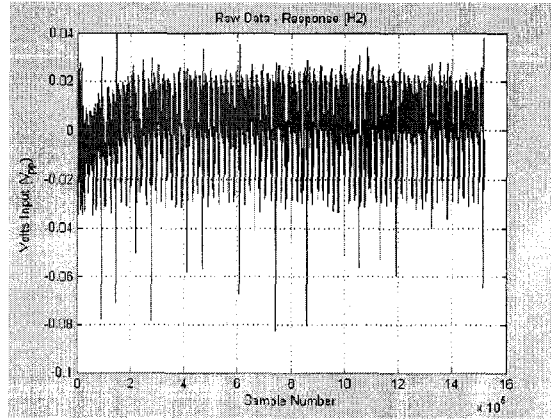
Figure 39: Plotted data of file: *Data_1322_001_C_Sampled* during insertion loss.

The sensitivities of the hydrophone along with a fixed maximum gain of 26 dB, did not allow signal capture with the attenuation wrap. This was a problem, as the *SL* signals were calculated from the Reson data to be 173.9 dB re $1\mu Pa$ at 10kHz while the *SPL* was calculated to be 135.6 dB re $1\mu Pa$, using the insertion loss wrap. (File: *Data_10kg20n15filter1h1c1*). The Reson 4014 hydrophones have an *OCVR* of –186 dB re 1Vrms / µPa, with a variable gain up to 50 dB. At a gain of 20 dB this can be thought to have an equivalent sensitivity of -166 dB re 1Vrms / µPa. The Benthos hydrophones with a fixed preamplifier gain of 26 dB have sensitivities around –180 dB re 1Vrms / µPa. The difference in sensitivities is approximately 24 dB.

4.7 Dock Experiment

At a floating dock on the Annisquam River in Gloucester Massachusetts on October 6, 2007, an experiment was setup. The Lubell source was used to transmit signals from 500Hz to 8000Hz at > 170 dB re $1\mu Pa$ and hydrophone data were collected at a range of 10 meters from the transmitter. The stability of the source becomes unstable at 250Hz. Since the dimensions of the source in wavelengths was less than 18.75 cm at the highest

45

frequency. It is reasonable to state that the 10 meter separation between the transmitter and

receiving hydrophones was sufficient for the measurement to be characterized as "far

field". See Figure 40 for a pictorial of the experiment setup. Table 6 describes the

environmental parameters during the data collection process.
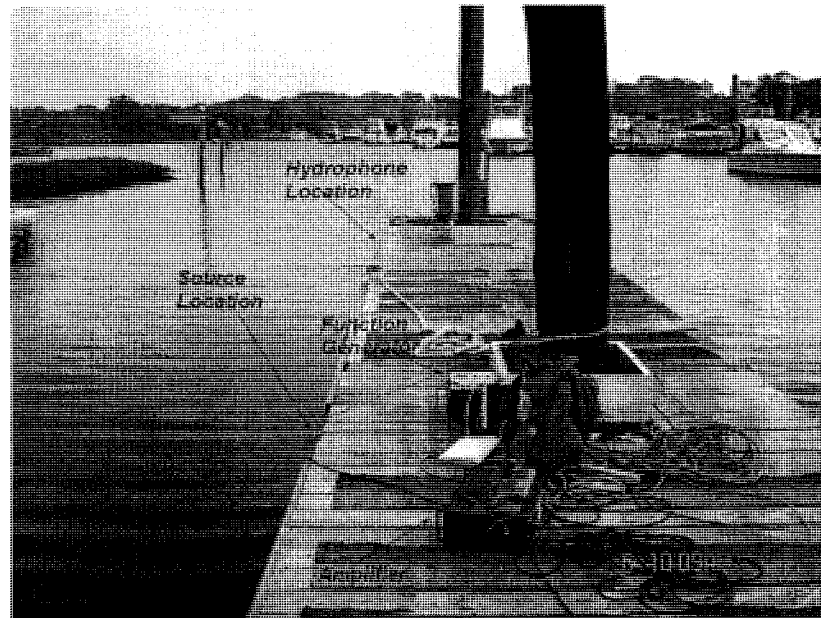
Figure 40: View of dock experiment location and equipment setup.

Date:	October 6, 2007
Location: Yankee Fleet Dock	42° 36.82 N 070° 40.90 W
Air Temp:	approximately 70 degrees F
Water Temp at at 5 feet below surface:	approximately 59 degrees F
Water Depth:	17 to 20 feet at hydrophones 11 to 14 feet at source
Hydrophone Depth:	9.9 ft (3m))
Source Depth:	6.6 ft (2m)
Data Collection Time:	0900 to 1045 EDT
Time of High Tide:	0827 EDT

Table 6: Environmental parameters of the dock experiment and subsequent analysis.

The experiment was conducted in a precise and deliberate manner and was intended

to prove the feasibility of the DAQ system to collect acoustic baseline *SPL* data with low

frequency signals in shallow water. Table 7 references the approximate time of

transmission for the particular frequencies, allowing data files to be correlated to the

frequencies and the water depth, which varied with the tide. The data acquisition system was started, a virtual instrument was run, and acoustic data were collected continuously in one-minute time intervals at a sampling frequency of 20,000 samples/second/channel.

Frequency	Time of Transmission
500	0929 to 0936, 1006, and 1008 to 1012
1000	0940 to 0943
2000	0944 to 0946 and 1007
3000	0947 to 0948
4000	0949 to 0953
5000	0954 to 0956
6000	0957 to 1001
7000	1001 to 1004
8000	1005
Random Boat Passing	0913 / 0927 / 1000

Table 7: Approximate time of different frequency transmissions.

To validate the *OCVR* of the hydrophones, a known *SL*, at 500Hz from the Lubell source was transmitted. The *SPL* calculations were performed on the initial data. The analysis showed that the *OCVR* values from the earlier calibration had shifted on hydrophones 0 and 1. A field calibration was performed using the substitution method with hydrophone 2 as the reference. File *Data_07_10_06_0936_48* was used to back calculate the *OCVR* of hydrophones 0 and 1. An independent measurement system and reference hydrophones were not available for this analysis. See Table 8 for the calculated *OCVR* values on Oct 7, 2007. The magnitude of the sensitivity of hydrophone 0 had increased by 6 dB, while the magnitude of hydrophone 1 had decreased by 14 dB from the calibration in Feb 2007. Hydrophone 0 was rebuilt after suffering catastrophic failure and a difference was expected. The shift in hydrophone 1 may be attributed to the expansion and contraction and water absorption within the 3M-5200^{TM}, changing the internal position of the piezo-element. In future data collection, this would have a

profound affect on the accuracy of calculated *SPLs*, producing unreliable results. See

Table 9 for the *OCVR* differences from Feb 2007 and Oct 2007.

Hydrophone	OCVR (dB re 1Vrms / μPa) Hydrophone Only	OCVR (dB re 1Vrms / μPa) Hydrophone with Internal Amp
Hydrophone 0	-203	-177
Hydrophone 1	-217	-191
Hydrophone 2	-203	-177

Table 8: Hydrophone *OCVR* values for the dock experiment – Oct 7, 2007.

Hydrophone	OCVR (dB re 1Vrms / μPa) Hydrophone with Internal Amp October 2007	OCVR (dB re 1Vrms / μPa) Hydrophone with Internal Amp Feb 2007	Delta
Hydrophone 0	-177	-183	+6
Hydrophone 1	-191	-183	-8
Hydrophone 2	-177	-179	+2

Table 9: Calculated delta and hydrophone *OCVR* values for Oct 2007 and Feb 2007.

File *Data_07_10_06_0936_48* was one of the first data files. The data is plotted in Figure

41. At the beginning of data collection, usable hydrophone data was possible from all

three hydrophones. For correlation, an FFT was performed on the data and is plotted in

Figure 42.
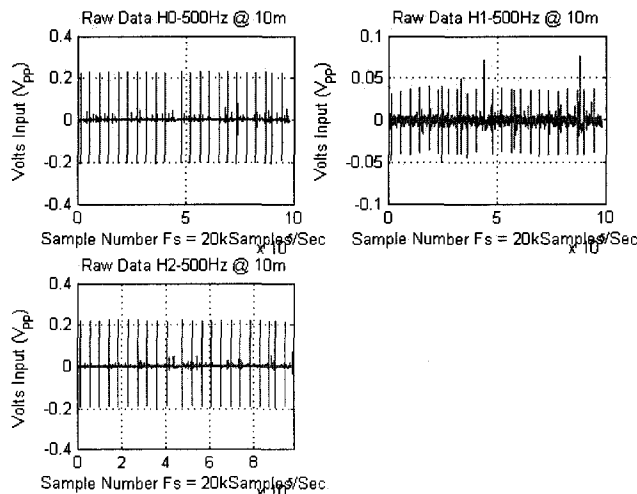
Figure 41: File: *Data_07_10_06_0936_48* raw data plot at 500 Hz at a range of 10m
where the TL=20dB. This file contains multiple pulses
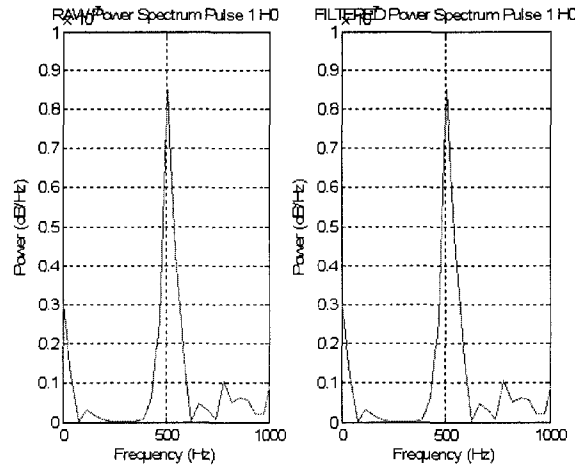
Figure 42: FFT analysis of a single pulse of file: *Data_07_10_06_0936_48* displays the transmitted signal frequency of 500Hz.

For signal verifications, The *SL* was calculated from the published data of the Lubell source and equation 4.2. The *TVR* at 500Hz = 136.22, Vin = 49.97 and the *SL* at 500Hz = 170.2 dB re 1μPa at 1m. The difference from the *SPL* received from at hydrophones was less than 1.2 dB for file *Data_07_10_06_0936_48*. The calculation was performed using spherical spreading *TL*, equal to 20 dB re 10m. This was deemed valid, as the calculated *SL* was 170.2 dB re 1μPa at 1m and the *SPL* was calculated to be approximately equal to 151 dB re 1μPa. The data are summarized in Table 10, with source level equal to 170.2 dB re 1μPa at 1m.

Hydrophone	OCVR (dB re 1Vrms / μPa)	SPL dB re 1μPa	Calculated SL dB re 1μPa @ 1m	Actual SL dB re 1μPa @ 1m	Delta (dB)
Hydrophone 0	-177	151.4	171.4	170.2	1.2
Hydrophone 1	-191	150.9	170.9	170.2	0.7
Hydrophone 2	-177	151.3	171.3	170.2	1.1

Table 10: *OCVR* of hydrophones and back calculation of source levels.

During the time of data collection, the data from hydrophone 2 became unreliable, while the low *OCVR* of hydrophone 1 rendered this *SPL* data suspect, as can be seen in Figure

49

43 from file: *Data_07_10_06_1009_81*. During the next data set, hydrophone 2 suffered

a catastrophic failure as shown in the in Figure 44 from file: *Data_07_10_06_1010_82*.

This incurs other implications as this hydrophone was used as the baseline and for the

field calibration of hydrophones 0 and 1. It is evident from Table 9 and Figure 40,

hydrophones 0 and 2 worked on the onset of this experiment. From the plotted data it can

be seen that the hydrophones and wiring are unreliable for accurate repeatable data

collection, were unstable and changed over time and seasons. Any data collected is

suspect. Data collection has proved that an alternative package for the hydrophone

elements is required for consistent and repeatable sensitivity.
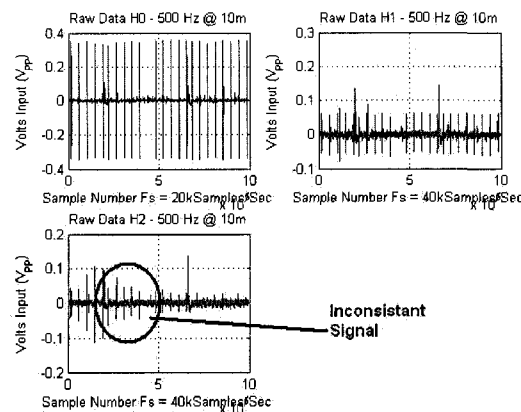
Figure 43: Plotted data from file: *Data_07_10_06_1009_81*.
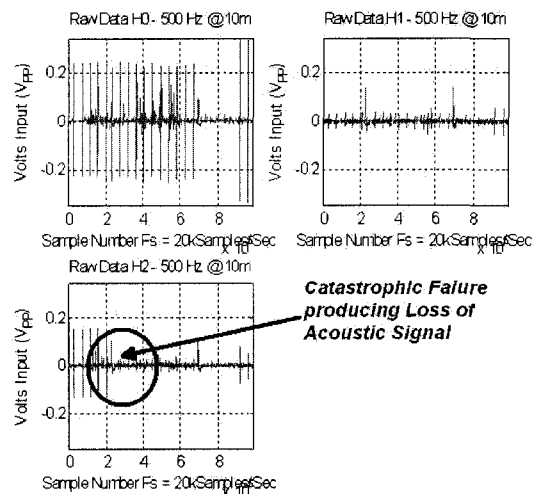
Figure 44: Plotted data from file: *Data_07_10_06_1010_82*.

CHAPTER 5

SUMMARY AND RECOMENDATIONS

5.1 <u>Introduction</u>

This closing chapter summarizes the evaluation performed on the measurement

instrumentation of the prototype Acoustic Measurement Buoy. Recommendations are

made to improve the performance of the DAQ system. Experiments and data were

presented in previous chapters of this thesis. The components were evaluated for

required specifications, actual performance based upon evaluation and future expansion

possibilities. The components of the data acquisition system, hydrophones, DAQ

computer, A/D hardware and filtering circuits are discussed separately.

5.2 <u>Hydrophones</u>

During the evaluation, the hydrophones incurred many problems and issues. The

original hydrophones were pre-assembled in a watertight package when the evaluation

began as was seen in Figure 9. Preliminary experimentation proved the hydrophones

weren't sensitive to low-level acoustic signals, which was attributed to mechanical

loading of the elements. The hydrophones were re-packaged during this evaluation to

allow the piezo elements to be in direct contact with the water. Figure 45 is a pictorial

with components and stress locations noted.
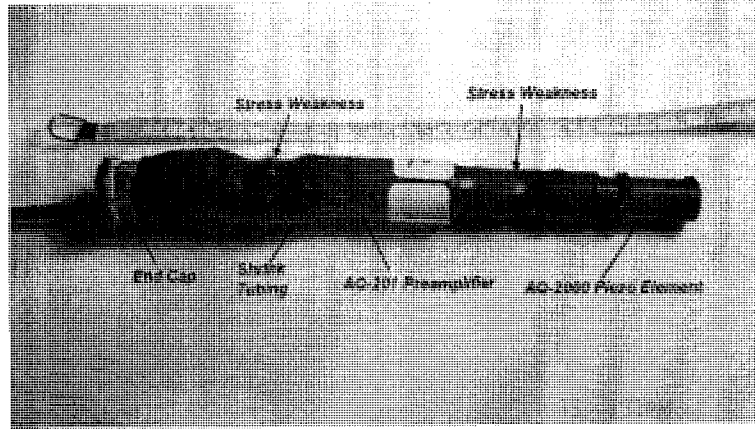
Figure 45: Repackaged hydrophone with stress weakness locations at interfaces noted.

While increasing the sensitivity, the hydrophones became susceptible to handling and environmental damage. The hydrophone packaging, which was not rigid, allowed movement between the internal preamplifier and the 3M-5200™ marine sealant. This allowed salt water to permeate the shrink tubing and the 3M-5200™ filler and absorb moisture within the material, promoting corrosion of the wiring and soldered connections. The shrink tubing also applied pressure onto the hydrophone case. This affected the operating modes of the hydrophones as the elements were not allowed to vibrate freely. This affected the repeatability and reduced the sensitivity of the hydrophones. The magnitude of the sensitivities of the hydrophones were not equal or consistent over time as seen in Table 9 of this thesis. Although the sensitivities were increased, low-level acoustic signals (SPL<140 dB re 1μPa) still could not be captured due to noise on the signals with a fixed gain of 26 dB. This would cause data collection problems if used for any insertion loss or noise suppression analysis as was described in the insertion loss experiment. Having suffered catastrophic failure of signal acquisition, two of the hydrophones were rebuilt after initial repackaging. A failure analysis of the

components revealed broken wiring inside the hydrophone assembly. The 'new' design was not robust enough to allow consistent data collection in the dock experiment. Based upon the evaluation performed, it was concluded that the hydrophones need to be repackaged in such a way that will allow as much sensitivity as possible but still rugged enough to protect the piezo element. The package should be built to allow non-destructive disassembly of the individual pieces. An easier but more costly solution and drastic measure would be to replace the entire hydrophone assemblies with fabricated factory calibrated hydrophones specified to optimize the required range of expected *SPL*. This would probably require designing another interface to the A/D.

Another problem to be addressed is the range of *SPL* that can be accurately recorded. Based upon performance specifications, the hydrophones are limited in their ability to capture *SPL* over a wide dynamic range. After analysis and discussion with the supplier (Benthos) the maximum *SPL* for standard AQ-2000 hydrophones with AQ-201 preamplifiers is approximately 192 dB re 1μPa. This value is explained as follows:

- The AQ-201 preamplifiers use clamping diodes on the input for protection. The signal input needs to be below about 0.3 volts to prevent the diodes from clipping the signal. This directly relates to the maximum *SPL*.

- This is a signal level from the hydrophone of -10 dBV as can be seen in equation 5.1.

$$dBV = 20log10(.3) = -10\ dBV \qquad (5.1)$$

- The stated *OCVR* (sensitivity) of the hydrophone is -201 dB re $1v/\mu$Pa. The maximum sound pressure level needs to be less than the difference, see equation 5.2:

$$(dBV - OCVR) = SPL_{Maximum} \qquad (5.2)$$

$$(-10\ dBV - (-202\ dB\ re\ 1v/\mu Pa)) = 192\ dB\ re\ 1\mu Pa \qquad (5.3)$$

The design criteria from Risso et al. (2006) was based upon three areas of concern: (1) Where the *SPL* is greater than 220 dB re 1μPa. (2) Where the *SPL* is greater than 180 dB re 1μPa but less than 220 dB re 1μPa and (3) where the *SPL* is less than 180 dB re 1μPa. Based upon calculations, the AQ-2000 when used in this application with the AQ-201 preamplifier would not allow SPL measurements above 192 dB. The selected hydrophones used with the selected preamplifiers do not meet the design criteria. The *SPL* operating range of the AQ-2000 hydrophone with AQ-201 preamplifiers can be characterized as:

150 dB re 1 μPa < *SPL Measurement Range* < 192 dB re 1 μPa

While the required *SPL* range from Risso et al. (2006) was:

180 dB re 1 μPa < *SPL Measurement Range* < 220 dB re 1 μPa

Analyzing *SPLs* less than 150 dB re 1 μPa was not proposed in Risso et al. (2006), but became an experiment in the evaluation of an insertion loss wrap. The useful range of measurement is based on amplification, A/D voltage range and system noise. A 16 bit A/D has potentially 96 dB of dynamic range assuming the maximum voltage equals the maximum A/D voltage and the system noise level is more than 96 dB down from the maximum. This calculated from equation 5.4.

$$16 \text{ bit A/D Dynamic Range} = 20log(2^\# \text{ A/D bits}) \qquad (5.4)$$

$$Dynamic\ Range = 20log(2^{16}) \qquad (5.5)$$

$$Dynamic\ Range = 20log(65536) = 96\ dB \qquad (5.6)$$

A possibility would be to have three hydrophones, each would have the sensitivity and gain set to be usable in a particular location for analysis. The preamplifiers would need to be optimized for the chosen locations. For example, one hydrophone could be setup to

acquire signals with an *SPL* > 220 dB re 1 μPa. Another hydrophone may have its sensitivity and gain optimized for 220 dB re 1 μPa < *SPL* < 180 dB re 1 μPa. The last hydrophone would be optimized for 140 dB re 1 μPa < *SPL* < 180 dB re 1 μPa. More research would be required to evaluate the operation limits of these and other hydrophones. Different hydrophones and preamplifiers would be required. Another possibility is to allow programmable variable gain amplifiers to be set up for specific areas of concern between the hydrophone assemblies and the A/D. This would require the parameters to be set before and during data collection. It would be labor and data analysis intensive. Throughout the analysis, when using the Reson control hydrophones, external gains of up to 50 dB (Reson VT-2000 module) were available, and could be controlled real time during data capture. The packaging of the circuits and hardware would be limited by the amount of available real estate in the canister. Because of the complexity and cost of using three channels, as well as the wide required dynamic range and with a 16 bit A/D, the DAQ system may operate better using only one midwater hydrophone.

Another issue, which may affect the long-term operation of the hydrophones, was damage occurred to the hydrophone cabling when it was run over mistakenly by the zodiac during an experiment on the R/V Gulf Challenger. The hydrophone cabling was repaired. Overtime, if the splices are not secure and waterproof, salt water could seep into the splice and cause corrosion.

5.3 DAQ System

In an effort to keep the prototype costs down, the original DAQ computer as designed lacked the necessary computing power to run Windows™ XP and LabVIEW™ efficiently. The original DAQ computer design was outfitted with a wireless connection, however it proved to be very unreliable and was not used. This would have made issues such as controlling the DAQ software easier and retrieving data for analysis as the acoustic data must to be retrieved using a USB port for post processing with Matlab™. The DAQ computer was replaced with an Innovation Solution mini-computer with a 1.6GHz Celeron processor, with 1 GB memory. This mini-computer and total DAQ system was able to be powered with a 12V lawn mower battery installed into the prototype instrument canister. Windows™ 2000 was the O/S, with LabVIEW™ Version 8.2 was installed, allowing executable files to be created. This increase in computing power greatly simplified the acoustic data collection. Fortunately, the virtual instruments written for the original DAQ computer were portable to the DAQ computer replacement. The original and replacement DAQ computer required 115VAC to run a monitor in order to edit any virtual instruments or data retrieval. This could be a problem in the field and introduced noise into the system.

Another possibility for the replacement DAQ computer was a notebook computer that would physically fit inside the canister. This would eliminate the need for external AC voltage, as a monitor would not be required, and editing of the VI would be possible real time. For a wireless connection, the notebook would require Windows™ XP or greater as the O/S. This allows ad hoc wireless connections between computers, allowing greater flexibility in data acquisition and analysis. However based again on cost

consideration it was decided not to go with a notebook computer and accept dealing with the external monitor.

5.4 A/D Module

The NI-USB-9125A A/D module worked satisfactorily, but low-level signals were too noisy to reliability capture data. Throughout the evaluation, noise was a major problem. The resolution of the A/D channel can be increased, but the plotted noise magnitude also increases. Figure 46 is a view of the DAQ channel setup. The signal input range within LabVIEW™, sets the expected values. The narrower the range, the greater the voltage resolution per bit, but the noise issue is more prevalent. If noise could be reduced, a VI triggered by a threshold set point could be used. The size of the data files would be reduced and data analysis would be more efficient.
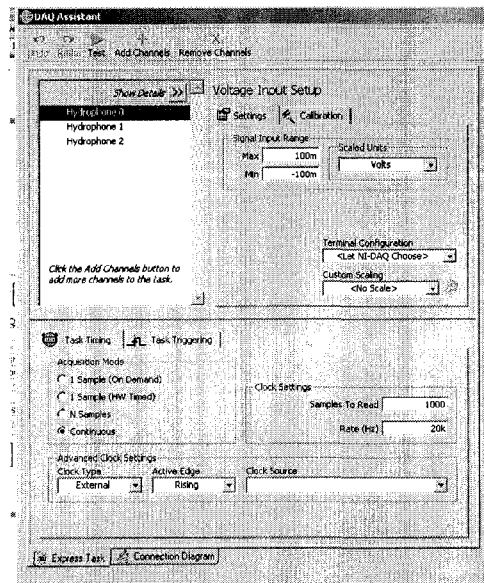
Figure 46: LabVIEW™ voltage setup screen.

The single ended wiring of the Benthos AQ-201 preamplifiers forced the wiring to the NI-USB-9125A A/D module to be wired single ended, eliminating the differential inputs

and common mode noise rejection. The A/D and hydrophone preamplifiers were not selected to work together in an efficient manner. Figure 47 proposes alternate wiring using a differential preamplifier such as the Benthos AQ-300 with a differential input anti-aliasing low-pass filter. Additional power supply circuitry would be required to convert the present DC supply voltage to usable levels. Appendix D of this thesis contains the specifications for the Benthos AQ-300 preamplifier. Other designs are possible, but the limiting factor is the cost of implementation.
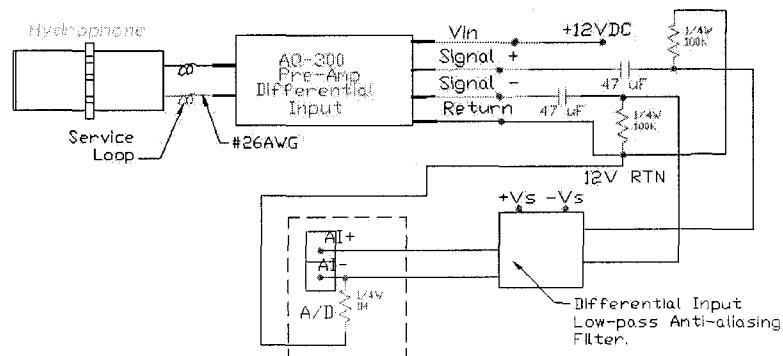
Figure 47: Schematic diagram of Benthos AQ-300 differential input preamplifier and low-pass anti-aliasing filter.

5.5   Filtering

In future design configurations, band-pass filters should be used on the input signals to eliminate the possibility of aliasing. Another possibility is using low-pass filters along with the present high pass filters. Band pass and low pass filters are available from a number suppliers in small form factors and could be packaged and installed into the modular filter assembly. If the present high-pass filters are retained, it would be desirable to improve the performance as these are single order pole filters. A major issue to be addressed is the need for +/- supply voltages for active filters.

Reference Appendix H for data sheets of possible filters that could be used. The

prototype instrument canister has only +12 VDC available. Any other voltages would

need additional power circuits. Typical operating voltages for external amplifiers are

from + 5 to + 15 VDC. Using the present Benthos AQ-201 preamplifier, an alternate

schematic is proposed using an anti-aliasing filter in Figure 48 and cost effective 9 volt

batteries. Another possibility for dual supply voltages is using an integrated circuit that

would produce +/- voltages from a single voltage input. This would involve more circuit

design and circuit board fabrication.
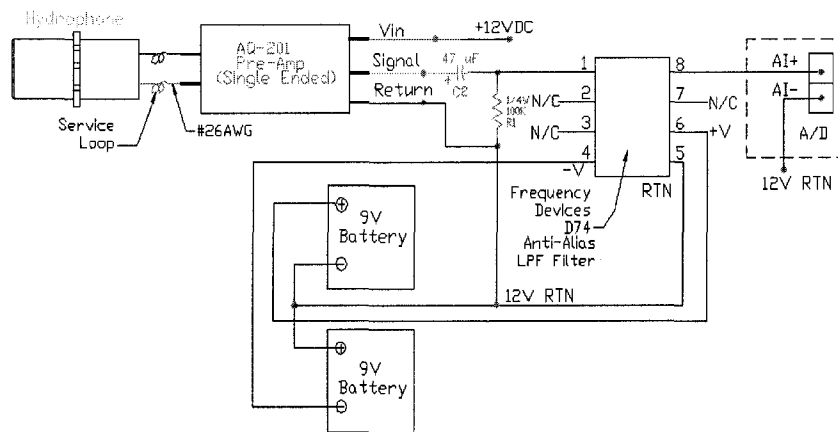
Figure 48: Alternate schematic diagram using present Benthos AQ-201
preamplifiers in series with the high-pass filter and the addition of
low-pass anti-aliasing filters.

5.6   Conclusion

The evaluation of the measurement instrumentation of the prototype of the

Acoustic Measurement Buoy posed some interesting challenges, electrically,

mechanically and acoustically. The major constraint was the cost. In an effort to keep

the system as low cost as possible several sources of errors were consequently

introduced. To answer the question, "Was it possible to design and build a low cost,

easily transported 'Acoustic Measurement Buoy' system capable of providing accurate and repeatable measurement of sound pressure data due to pile-driving activity in a near-coastal environment?" The short answer is, the lower the cost the greater the difficulty. As with many problems, there were multiple solutions and it is difficult to see how subtle problems associated with the low cost would combine to produce larger problems.

Expanding on any lessons learned from the prototype initial design, the problems and difficulties can be broken down into specific areas: (1) Acoustical problems (hydrophone performance and reliability), (2) electrical problems (noise in the data, and the need for analog filtering), (3) computer hardware (original DAQ computer, its replacement and the A/D module) and (4) computer software (LabVIEW™ and DAQmx™ A/D drivers). Each component or layer of the system is important. During the evaluation, multiple problems occurred. These problems were fixed, only to have problems reappear in another form later. The major frustration was the lack of repeatability of the individual pieces of the DAQ system.

For a quick answer to the question posed above, the answer is that the prototype as designed is inadequate to fulfill its design criteria. It should be possible with redesigns and with hardware changes to the system to make it more versatile. As part of the design validation it would take more experimentation and an evolving system analysis performed concurrently with the redesign of the data acquisition package. To make an acoustic measuring system workable over a wide range of *SPL* data one must make careful component selection, starting with the sensor (hydrophone) the band pass filtering, the additional gain stages and the A/D characteristics.

REFERENCES

Au, Whitlow (1993). '"The Sonar of Dolphins" W.L Au Springer, Verlag New York

Fergusen, Glen, Teledyne Benthos, 49 Edgerton Drive, North Falmouth, MA 02556 USA 'AQ-2000 Hydrophone and AQ-202 Preamplifier Specifications'

Kinsler, Lawrence E, Frey, Austin R., Coppens, Allen B. Sanders, James V. (2000). 'Fundamentals of Acoustics' 4th Edition: John Wiley and Sons Hoboken NJ

Kuntsel, Ender, Bunker, William A. (1992). 'Guidelines for Specifying Underwater Electroacoustic Transducers', ITC, International Transducer Corporation, Santa Barbara, CA

Laughlin, Jim (2006). "Effects of Pile Driving on Fish and Wildlife", Washington State Dept of Transportation, PO Box 330310, NB82-138, 15700 Dayton Ave. N, Seattle WA 98133

Lurton, Zavier (2002). "An Introduction to Underwater Acoustics – Principles and Applications" Praxis Publishing Ltd, Chichester, UK

Dr Jeremy Nedwell, Dr Andrew Tumpenny, Mr John Langworthy and Mr Bryan Edwards (2003). "Measurement of Underwater Noise during piling at the Red Funnel Terminal, Southhampton, and Observations of its Effect on Caged Fish" Subacoustics Lab, Chase Mill, Winchester Road, Bishop's Waltham

Pierce, Alan D. (1989). "Acoustics An Introduction to Its Physical Principles and Applications", Acoustical Society of America, Melvine NY

Risso, Ashley, Jerram, Kevin, Gaudet, Laurel (2006). "Acoustic Measurement Buoy", Undergraduate Ocean Research Projects TECH 797 Report, University of New Hampshire, Durham, NH

Urick, Robert J. (1983). 'Principles of Underwater Sound' 3rd Edition, McGraw-Hill Book Company New York NY

Waite, A.D. (2002). 'SONAR For Practicing Engineers' 3rd Edition. John Wiley and Sons Ltd., Chichester, West Sussex, England

APPENDICES

APPENDIX A

DATA ACQUISITION SYSTEM

A.1   <u>Data Acquisition Package</u>

The prototype DAQ system was a self-contained PC clone motherboard, (EPIA

MII-Series Mini-ITX Mainboard, with VIA C3/ VIA Eden EBGA processor), and 512

MB of RAM was installed. A 100 GB Hard Drive was plugged into the IDE connector

via an 8" ribbon cable. Two USB ports are available, one for data retrieval and the other

for connection to the National Instrument NI-USB-9125A A/D. A Keyboard, mouse and

monitor are used for initialization of the system. The DAQ computer requires a DC

power source, supplied by an M1-ATX Intelligent 90 Watts Automotive ATX Power

Supply card capable of the required output voltages, and operating with an input voltage

from 6 to 24VDC. This allowed the use of a borrowed 34 amp-hour 12VDC battery.

Figure A.1 is a detail of the A/D, hard drive, and underside of the motherboard of the data

acquisition assembly (Risso et al. 2006). The specifications of the DAQ computer

system are summarized in Table A.1.

The MI-ATX power supply card supplied the power required for the computer

and peripheral operation, the suppliers data sheet is displayed in Figure A.2. A potential

source of system noise is probably the MI-ATX power supply card. The A/D uses plug-

and-play connectivity via a USB port for faster setup and measurements. The A/D

module was capable of accepting up to four channels of data simultaneously. The data

can be sampled up to 100,000 samples/sec/channel with 16-bit accuracy. These modules

include 250 V_{RMS} channel-to-earth ground isolation for safety, noise immunity and high common-mode voltage range. The operating range of the A/D inputs allows signals from −10.5 to +10.5 volts. The suppliers data sheet for the NI-USB-9125A is displayed in Figure A.3. Figure A.4 is the wiring diagram for the NI-USB-9125A used for differential signal inputs. Figure A.5 are the terminal assignments for the NI-USB-9125A. Figure A.6 is a pictorial of the NI-USB 9125A.
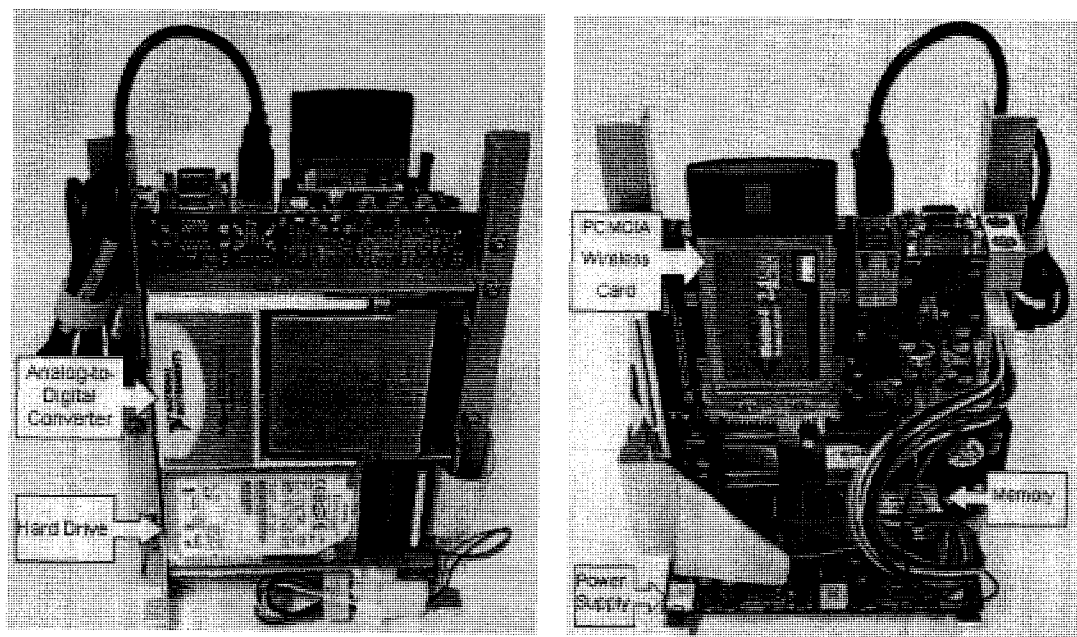
Figure A.1: Detail of A/D, hard drive, and underside of motherboard of data acquisition assembly. (Risso et al. 2006)

Processor	· VIA C3™/ VIA Eden™ EBGA processor
Chipset	· VIA CLE266 North Bridge · VIA VT8235 South Bridge
System Memory	· 1 DDR266 DIMM socket - Up to 1GB memory size
VGA	· Integrated VIA Unichrome AGP graphics w/MPEG-2 Accelerator
Expansion Slots	· 1 PCI
Onboard IDE	· 2 X UltraDMA 133/100/66 Connector
Onboard Floppy	· 1 x FDD Connector
Onboard LAN	· VIA VT6103 10/100 Base-T Ethernet PHY
Onboard Audio	· VIA VT1616 6 channel AC'97 Codec
Onboard TV Out	· VIA VT1622A TV Out
Onboard IEEE 1394	· VIA VT6307S IEEE 1394 (Optional)
Onboard CardBus / CompactFlash	· CardBus Type I & Type II · Ricoh R5C476 II / R5C485 CardBus Corntroller
Back Panel I/O	· 1 CardBus Type I and Type II slot +1 CompactFlash Slot · 1 CompactFlash slot · 1 RJ-45 LAN port · 1 PS2 mouse port · 1 PS2 keyboard port · 1 Serial port · 2 USB 2.0 ports · 1 VGA port · 1 RCA port (SPDIF or TV-Out) · 1 S-Video port · 1 1394 port · 3 Audio jacks: line-out, line-in and mic-in (Smart 5.1 Support)
Onboard I/O Connectors	· 1 USB connector for 2 additional USB 2.0 ports · 1 Front-panel audio connectors (mic-in and line-out) · 1 CD Audio-in connector · 1 Buzzer · 1 FIR connector · 1 CIR connector (Switchable for KB/MS) · 1 Wake-on-LAN connector · 1 LPT port header · CPU/Sys FAN/Fan 3 · 1 Connector for LVDS module (Optional) · 1 Serial port connector for second COM port · ATX Power Connector
BIOS	· Award BIOS · 2/4Mbit flash memory
System Monitoring & Management	· CPU voltage monitoring · Wake-on-LAN, Keyboard Power-on, Timer Power-on · System power management · AC power failure recovery
Operating Temperature	· 0~50°C
Operating Humidity	· 0% ~ 93% (relative humidity; non-condensing)
Form Factor	· Mini-ITX (6 layer) · 17 cm x 17 cm

Table A.1: Summary of DAQ motherboard specifications.

65

MI-ATX
Intelligent 90 Watts
Automotive ATX Power Supply

Intelligent Automotive Power Supply

Designed to provide power and to control the ON/OFF switch of a motherboard (based on ignition status), MI-ATX is a 6-24V input ATX PSU capable of surviving tough engine cranks (down to 5.7V) as well as transient over-voltage situations.

Multiple Shutdown Schemes

MI-ATX has 8 user selectable microcontroller driven timing modes, allowing you to choose up to 8 ignition/shutdown timing schemes. By removing all user-selectable jumpers, MI-ATX becomes a traditional PSU with no ignition control and it can be used in non-car applications.

Even if your computer is totally OFF, a PC will still consume few hundered milliwatts, needed to monitor PC ON/OFF status. When the computer is in the suspend/sleep mode, it will consume even more power, because the RAM needs to be powered at all times. The power consumption in the suspend mode is few watts. No matter how big your battery is, it will eventually drain your battery in a matter of days.

Deep Sleep Mode

While in deep sleep mode, MI-ATX constantly monitors your car battery voltage levels, preventing deep discharge situations by automatically shutting down until battery levels reach safe levels again.

No more dead batteries, no more computer resets during engine cranks, along with multiple timing schemes, small formfactor and competitive price makes the MI-ATX the premier solution for ATX vehicle power supply solutions.

Mechanical Characteristics

-Board measurements: 1.77"x6.31"
-Height: < 1", 1U formfactor compatible
-Formfactor compatible with mini-ITX Casetronics enclosures
-Designed for the mini-box Vehicle PC extruded enclosure

CPU and Board Support

-VIA X86 CPUs, PII, PIII and low power P4/AMD*
-Supports all VIA mini-ITX motherboards
*NOTE: Check the total 12V rail power consumption

Wire harness

MI-ATX comes equipped with ATX, HDD and Floppy cable harness, jumpers, faston connectors and 2 pin cables for motherboard ON/OFF switch. Just connect it to your car / boat / RV battery and power up your PC.

OEM Integration

Other timing schemes / designs are possible. OEM integration is welcome. Please send en email to mi-atx@mini-box.com with your custom requirements.

Minimum input Operating voltage	5.7V
Maximum input Operating voltage	30V
Min startup voltage	6V
Deep-Discharge shutdown threshold	11V
Input current limit (fuse protected)	10A
Max Output Power	90 Watts
Operating temperature	-20 to +85 degrees Celsius
Storage temperature	-40 to +125 degrees Celsius
MTBF	192,000 hrs @ 55C, 96,000 hrs @65C
Efficiency (input 7-24V)	>90% on 3.3,5,5VSB ~80% on 12V
PCB size	160x45mm
Input connectors	Faston 0.25" terminal
Input fuse	Mini-Blade fuse, 10A
Output Connector	ATX Power 20 pin (Molex P/N 39-01-2200)
J2, J4, J8, J6	Polarized Header 2x1, 0.1"

Maximum Power Characteristics

Output Rail	Current (Max)	Current Peak (<60 seconds)	Ripple (V p-p)	Regulation
5V	10A	15A	50mV	1.5%
3.3V	10A	15A	50mV	1.5%
5VSB	1.5A	2A	50mV	1.5%
-12V	0.15A	0.2A	150mV	10%
12V	2A	2.5A	100mV	1.5%

Corporate address: 43230 Christy St, Fremont, CA 94538
http://www.mini-box.com, email: sales@mini-box.com

Figure A.2: PS CARD specifications. (http://www.mini-box.com)

Portable USB-Based DAQ with Simultaneous Sampling

NI USB-9215A, NI USB-9215 *NEW!*

- Small, portable devices (12.1 by 8.6 by 2.5 cm)
- 4 channels of 16-bit simultaneously sampled analog input
- Built-in, removable connectors for easier and more cost-effective connectivity
- 250 V_{rms} channel-to-earth ground isolation
- Plug-and-play connectivity via USB
- Bus-powered

Operating Systems
- Windows 2000/XP
- Mac OS X
- Linux

Recommended Software
- LabVIEW
- LabWindows/CVI
- Measurement Studio

Measurement Services Software (included)[1]
- NI-DAQmx driver software
- VI Logger Lite data-logging software

[1] Mac OS X and Linux users must download NI-DAQmx Base driver.
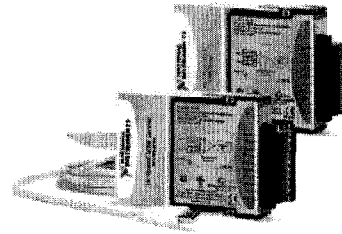
Product	Signal Type	Channels (DI)	Input Resolution (bits)	Sampling Rate (kS/s/ch)	Input Range (V)	Connector	Operating System	Driver Software[1]
USB-9215A	Voltage	4	16	100	±10	Screw Terminal, BNC	Windows	NI-DAQmx
USB-9215	Voltage	4	16	20 aggregate	±10	Screw Terminal	Mac OS X and Linux	NI-DAQmx Base

For up-to-date information on Mac OS X, visit ni.com/supporting/versions.htm

Table 1. Portable USB DAQ for Simultaneous Sampling Selection Guide

Hardware Description

National Instruments USB-9215A and USB-9215 are data acquisition modules with integrated signal conditioning that provide plug-and-play connectivity via USB for faster setup and measurements. They offer four channels of simultaneously sampled voltage inputs with 16-bit accuracy to provide minimal phase delay when scanning multiple channels. In addition, these modules include 250 V_{rms} channel-to-earth ground isolation for safety, noise immunity and high common-mode voltage range.

Software Description

The NI USB-9215A uses NI-DAQmx high-performance, multithreaded driver software for interactive configuration and data acquisition on Windows OSs. All NI data acquisition devices shipped with NI-DAQmx also include VI Logger Lite configuration-based data-logging software. The NI USB-9215 for Mac OS X and Linux uses NI-DAQmx Base, a multiplatform driver with a limited NI-DAQmx programming interface. You can use NI-DAQmx Base to develop customized data acquisition applications with National Instruments LabVIEW or C-based development environments. NI-DAQmx Base includes a ready-to-run data logger application that acquires and logs up to four channels of analog data.

Recommended Accessories

The USB-9215A and USB-9215 both have built-in screw-terminal connectivity, so no additional accessories are required. The USB-9215A is also available with BNC connectors.

Common Applications

The USB-9215A and USB-9215 are ideal for a number of applications where small size and portability are essential, such as:
- Portable data logging – log voltage data quickly and easily
- Academic lab use – obtain academic discounts for quantities of five or more. Visit ni.com/academic for details.
- Environmental monitoring – monitor environmental conditions such as humidity or light
- Embedded OEM applications
- In-vehicle data acquisition

Information for OEM Customers

For information on special configurations and pricing, please visit ni.com/oem.

Ordering Information

NI USB-9215A[1]
  Screw Terminals 779434-01
  BNC Connectors 779435-01
NI USB-9215[2]
  Screw Terminals 778977-01
[1] Windows only
[2] Mac OS X and Linux only

BUY NOW!

For complete product specifications, pricing, and accessory information, call (800) 813 3693 (U.S. only) or go to ni.com/oem.

NATIONAL INSTRUMENTS

Figure A.3: NI USB-9125A specification sheet.
(http://www.ni.com/pdf/products/us/niusb9215a.pdf)
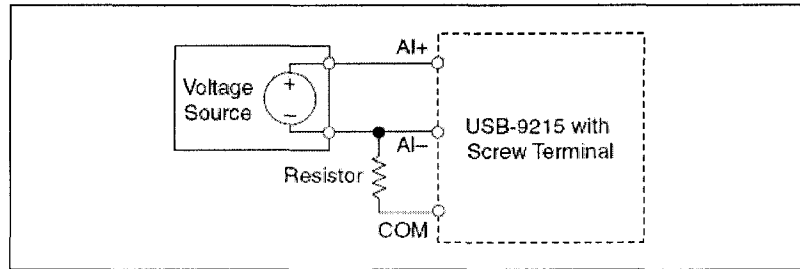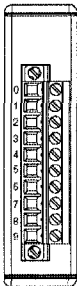
Figure 8. Connecting a Floating Differential Voltage Signal
(USB-9215 with Screw Terminal Shown)

Figure A.4: Connection diagram using the NI USB-9125A as a differential
signal input.
(http://www.ni.com/pdf/products/us/niusb9125a.pdf)

Table 1. Terminal Assignments

Module	Terminal	Signal
	0	AI0+
	1	AI0–
	2	AI1+
	3	AI1–
	4	AI2+
	5	AI2–
	6	AI3+
	7	AI3–
	8	No Connection
	9	Common (COM)

cRIO-9215 Operating Instructions   6   ni.com

Figure A.5: Terminal assignments for the NI USB-9125A.
(http://www.ni.com/pdf/products/us/niusb9215a.pdf)
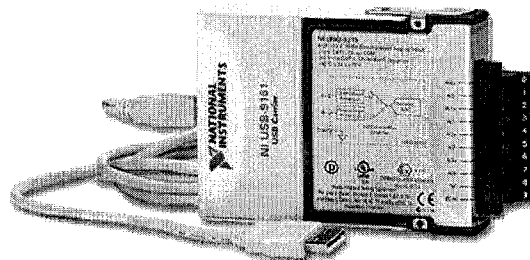
Figure A.6: National Instruments USB-9125A Data Acquisition Module.
(http://sine.ni.com/nips/cds/view/p/lang/en/nid/13881)

68

A/D Specifications

The following specifications are typical for the range 0 to 60 °C unless otherwise noted.

Number of channels	4 analog input channels.
ADC resolution	16 bits Type of ADC
Type of ADC	Successive approximation register (SAR)
Max sampling rate USB-9215A (USB 2.0)	100 kS/s (per channel)
Operating voltage range (AI+ to AI–)	±10.2 V Min, ±10.4 V Typical, ±10.6 V Max
Maximum working voltage (signal + CM)	Within ±10.2 V of common
Overvoltage protection	±30 V
Conversion time	One channel.....................................4.4 μs Two channels.................................6 μs Three channels...............................8 μs Four channels................................10 μs
Stability	Offset drift ....60 μV/ °C Gain drift ....10 ppm/ °C
CMRR (at 60 Hz)	–73 dB min
Input bandwidth (–3 dB)	420 kHz min
Input impedance	Resistance With screw terminal ......1 GΩ Capacitance....................................25 pF
Input bias current	10 nA
Input noise	RMS.......................................1.2 LSBrms Peak-to-peak.............................7 LSB
Crosstalk	–80 dB
Settling time (to 2 LSBs) With screw terminal	10 V step .... 10 μs 20 V step .... 15 μs
No missing codes	15 bits guaranteed
DNL	1.9 to 2 LSB max
INL	±6 LSB max
Power consumption from USB Suspend mode..............	500 mA, max. 2.5 mA, max
USB specifications USB-9215A	USB 2.0 full speed
Screw terminal wiring	12 to 24 AWG copper conductor wire
Torque for screw terminals	0.5 to 0.6 N · m (4.4 to 5.3 lb · in.)
Weight With screw terminal.	Approx. 250 g (8.8 oz)
Connect only voltages that are within limits.	Channel-to-COM.................................±30 V max
Designed to meet the requirements of the following standards of safety for electrical equipment for measurement and control.	IEC 61010-1, EN 61010-1 • UL 61010-1 • CAN/CSA-C22.2 No. 61010-1
Operating humidity (IEC 60068-2-56)	10 to 90% RH
Calibration interval	1 year

Table A.2: NI-USB09125A A/D technical performance specifications.

A.2   Software Description

The DAQ computer operates under the Windows[TM] operating system, while the

NI-USB-9125A A/D module was run under the NI DAQmx[TM] high-performance

multithreaded driver software. The data acquisition system was controlled using the

LabVIEW^{TM} programming environment with a graphical interface to program specific tasks. The graphical script files are called 'virtual instruments' with a .VI extension. They can be as involved or as simple as the programmer desires. The more complicated, the speed at which they operate greatly depends on the amount of computing power available to the user. The more tasks performed, the slower the host computer will run. The virtual instruments used for our analysis were kept simple but functional with sample rates from 20K to 40K samples/second/channel and displayed as separate channels. These sample rates were based on the Nyquist Frequency, where the sampling rate for a propagating signal must be sampled >2X its greatest frequency in order to reduce aliasing. In all cases of data collection, the data was samples greater than 4X the transmit pulse frequency. The hydrophone raw signal data was displayed and saved onto the hard drive as ASCII text files, (with an LVM or TXT extension). The acquired data files were post-processed using Matlab^{TM} scripts. During the evaluation, two versions of LabVIEW^{TM} were used, version 7.1 and 8.2.

APPENDIX B

LabVIEW™ VIRTUAL INSTRUMENTS

One type of virtual instruments (VI) used during the evaluation would capture raw

data indefinitely at specific intervals of time. The time duration was set in the block

diagram. The file was named: *1 minute Files Save All Data Sept 18.vi*. The front panel of

this virtual instrument is shown in Figure B.1. The block diagram is shown in Figure

B.2. This virtual instrument was used for the majority of data collection.
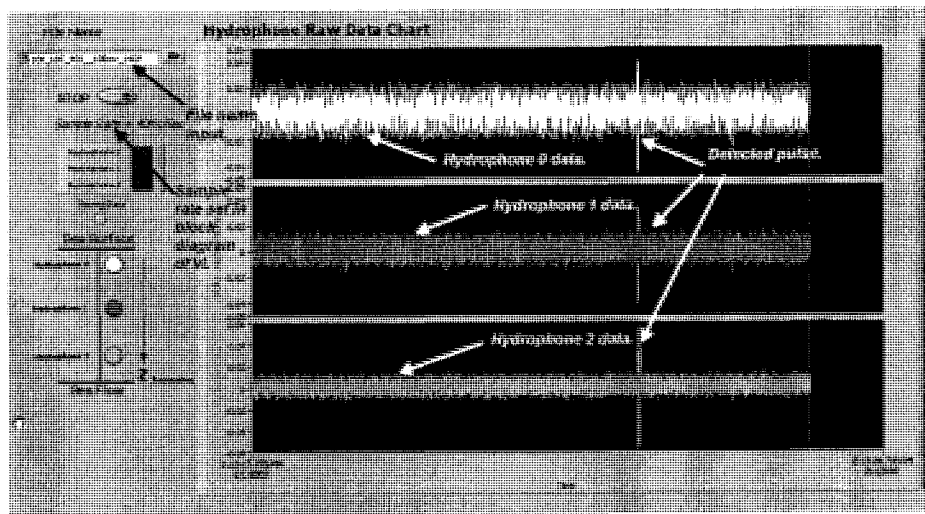
Figure B.1: Front panel of file: *1 minute Files Save All Data Sept 18.vi*.

The data file name is input in the dialog box in the upper right. The sampling frequency

(F_s) is displayed and set in the block diagram. The raw hydrophone data is displayed as

three separate plots. Each hydrophone is specified, with hydrophone 0 being the top plot,

hydrophone 1, the center plot and hydrophone 2 the bottom plot. This virtual instrument

was very reliable. The block diagram contains the subroutines that were generated using

the DAQ Assistant wizard. The DAQ Assistant controls the A/D, including the data

chart. The writing of the data files were controlled by the Write LabVIEW™

Measurement File subroutine. An indicator is placed onto the front panel to denote when

a data file is being created. Originally written in LabVIEW™ version 7.1, the data files

were written as ASCII text files and became very large. LabVIEW™ version 7.1, didn't

allow binary files to be created. A five minute data file containing data for the three

hydrophones could be upwards of 150 Mbytes. For this analysis, the collection time was

set at one minute intervals, allowing smaller data files. As can be seen from the block

diagram, this virtual instrument was simple and dependable for acquiring the acoustic

hydrophone data. This virtual instrument was portable for use in LabVIEW™ version

8.2.
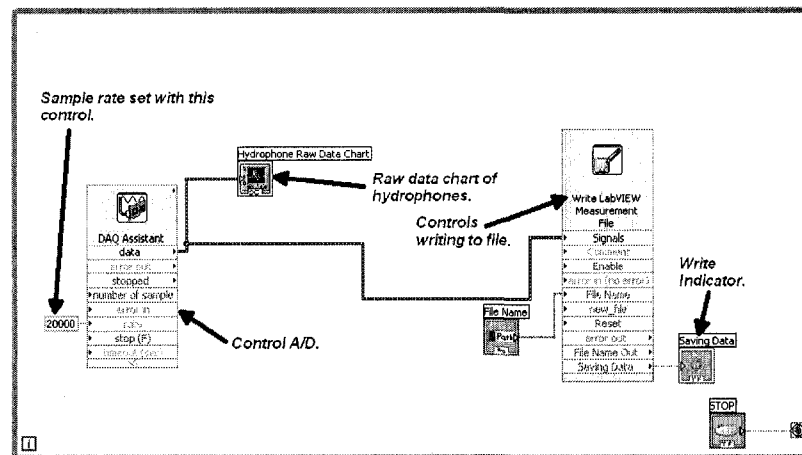
Figure B.2: Block diagram of file: *1 minute Files Save All Data Sept 18.vi.*

Another type of virtual instruments used during the evaluation would capture raw

data indefinitely, but would be triggered as a one shot, with file name:

2-1_Save_Data_40K_1min_10ms_.vi. When triggered, the data would be displayed, and

saved to an ASCII file, until another signal above the trigger level was received where the

process was repeated. The front panel of this virtual instrument is shown in Figure B.3 and the block diagram is shown in Figure B.4.
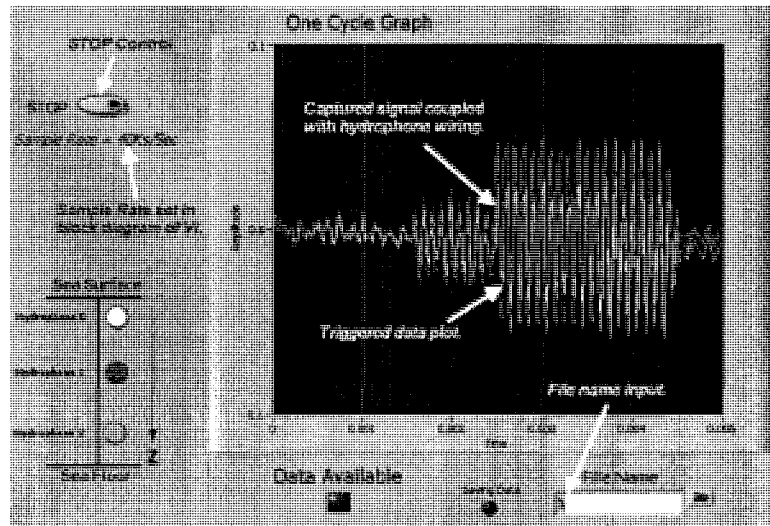
Figure B.3: Front panel of file: *2-1_Save_Data_40K_1min_10ms_.vi.*
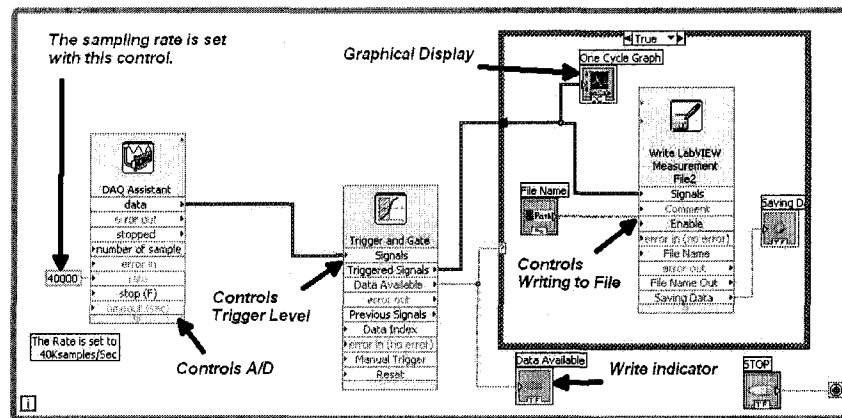
Figure B.4: Block diagram of file: *2-1_Save_Data_40K_1min_10ms_.vi.*

This virtual instrument allowed a file name to be specified. The sample rate was set in the block diagram using the DAQ Assistant. The Trigger and Gate subroutine set the trigger level. This virtual instrument was difficult to run consistently because noise was a problem throughout the evaluation. In Figure B.3 signal coupling can be seen, caused by cross-talk between the hydrophone wiring and the wiring to the source.

APPENDIX C

SAMPLE OF MATLAB CODE USED IN DATA ANALYSIS

C.1   High Pass Filter Analysis

This portion of Matlab™ script calculates the response of the high pass filters

used on the input channels of the NI-USB-9125A A/D. The selected resistor and

capacitor values were used in the calculations. The gain in voltage ratios and dB re 1V

are calculated and plotted.

```
%%%%%%%%%%%%%%%%%%%%%%%%%%%%%%%%%%%%%%%%%%%%%%
% Hydro Pre-Amp Frequency Response
% David Moceri 11-04-06

clear all;
close all;

%% 1st Order High Pass Filter  R = 100K and C = 47 uF %%%%%%%%%%%%%%%%%

R=100000;          % Resistor Value
C = 47e-6;         % Capacitor Value
f = 1 :1 : 8000;   % Frequency Range
w = 2*pi*f;        % Angular Frequency
n = (w*R*C);       % Numerator
d = sqrt(1+n.^2);  % Denominator
G = n./d;          % System Response
G_db = 20*log10(G);
figure(1)
semilogx(f,G)
xlabel('Frequency (Hz)')
ylabel('|Gain|')
title('Frequency Response of HPF C=47uF - R=100K')
grid on

figure(2)
semilogx(f,G_db)
xlabel('Frequency (Hz)')
ylabel('Gain - dB')
title('Frequency Response of HPF C=47uF - R=100K')
grid on
%%%%%%%%%%%%%%%%%%%%%%%%%%%%%%%%%%%%%%%%%%%%%%
```

C.2   Transform ASCII Data to Binary Data

This Matlab™ transforms the ASCII data into a binary file. This compacts the

data to allow faster data processing. The script loads the text file and converts it to a

three column array of binary data. Each column represents the data from a hydrophone

and given the names A (hydrophone 0), B (hydrophone 1), and C (hydrophone 2). The

file is saved with the same file name as was written in LabVIEW™. The file

'Data_07_10_06_0937_49.txt' is an example file name. Before the translation, the file

header is removed and saved.

```
%%%%%%%%%%%%%%%%%%%%%%%%%%%%%%%%%%%%%%%%%%%%
%   File Name:  Transform_All_Data.m
%   David Moceri  8-31-06
%   Translate ascii text file to mat file for data analysis (txt files or lvm files)
%   The mat file is a binary file.
%   The header must be removed from the data file and saved as its own data file.
%   This file reads all hydrophone data
%   Four (4) mat files are created.
%   1. MAT (H) file with all columns (qty 3)
%   2. MAT (A,B,C) Each column of hydrophone data has its own file.
%%%%%%%%%%%%%%%%%%%%%%%%%%%%%%%%%%%%%%%%%%%%

clear all;
close all;
clc;

% Load the data text file to the matrix H
H = load ('Data_07_10_06_0937_49.txt');

% Save data H to a .mat file
save Data_07_10_06_0937_49 H;

%%%%%%%%%%%%%%%%%%%%%%%%%%%%%%%%%%%%%%%%%%%%

A = H (:,1);        % data column of hydrophone 0
B = H (:,2);        % data column of hydrophone 1
C = H (:,3);        % data column of hydrophone 2

% Save data H channels to a .mat file called 'FILE-NAME.mat':
save Data_07_10_06_0937_49_A A;      % Hydrophone 1 data
save Data_07_10_06_0937_49_B B;      % Hydrophone 1 data
save Data_07_10_06_0937_49_C C;      % Hydrophone 2 data
%%%%%%%%%%%%%%%%%%%%%%%%%%%%%%%%%%%%%%%%%%%%
```

C.3   Process Acoustic Data

With the text data file converted to binary, processing could begin. A sample file,

'Data_1515_007.m' is used for the explanation. The analysis begins with loading the data

and declaring variables. The sensitivity or OCVR/FFVS/Mx of the hydrophones were

calculated during the hydrophone calibration.

```
%%%%%%%%%%%%%%%%%%%%%%%%%%%%%%%%%%%%%%%%%%%
% SPL Response of Hydrophones
% File Name: Data_1515_007.m
% Data File: Data_07_02_01_1515_007
% David Moceri 6-2-07
%%%%%%%%%% Variables %%%%%%%%%%%%%%%%%%%%%%
% Fs = 40000K Samples/Sec -- Sample rate set in LabVIEW™
% Vin = 140Vp-p  Voltage input to source
% Burst Rate = 1 pulse per 2 Seconds
% Burst Count = 20 Cycles
% Hydrophone Data
% A - Data column of hydrophone 1
% Af - Filtered data
% Arms - RMS value
% B - Data column of hydrophone 1
% Bf - Filtered data
% Brms - RMS value
% C - Data column of hydrophone 2
% Cf - Filtered data
% Crms - RMS value
%
clear all;
close all;
clc;
%
%%%% Load Data %%%%%%%%
load Data_07_02_01_1515_007_A;       % Load H0 data
load Data_07_02_01_1515_007_B;       % Load H1 data
load Data_07_02_01_1515_007_C;       % Load H2 data
t=length(A);          % length of number of elements in column of matrix H
Gain = 26;            % Pre-amp
MxA= 208              % Hydrophone 0 FFVS dB re 1V/uPa
MxB= 208              % Hydrophone 1 FFVS dB re 1V/uPa
MxC= 205              % Hydrophone 2 FFVS dB re 1V/uPa
Fs = 1/2.500000E-5;   % Sample Frequency from LabView Fs = 40KSamples/SEC
Vpp = 140;            % Voltage input to source
Vrms = Vpp/sqrt(2)    % Convert P-P to RMS
R = 1.5              % Range from source to hydrophones
TL = 20*log10(R)      % Calculate Spherical Spreading TL
SL = 112+20*log10(Vrms)    % Calculate SL from TVR data and V input
```

SPL = SL – TL   % Calculated theoretical SPL
%%

This section of Matlab™ code plots the acoustic RAW hydrophone data.

```
%%%% Plot Raw Data %%%%%%%%
figure(1)
subplot(2,2,1)        % Raw Hydrophone 0 Data
plot (A);
xlabel('Sample Number Fs = 40kSamples/Sec')
ylabel('Volts Input (V_P_P)')
title('Raw Data - 10K 20Cycles 140V_p_p')
grid on

subplot(2,2,2)        %Raw Hydrophone 1 Data
plot (B);
xlabel('Sample Number Fs = 40kSamples/Sec')
ylabel('Volts Input (V_P_P)')
title('Raw Data - 10K 20Cycles 140V_p_p')
grid on

subplot(2,2,3)        % Raw Hydrophone 2 Data
plot (C);
xlabel('Sample Number Fs = 40kSamples/Sec')
ylabel('Volts Input (V_P_P)')
title('Raw Data - 10K 20Cycles 140V_p_p')
grid on
```

This section of Matlab code uses a Chebyschev Type 2 filter centered at 10 kHz, with a

band width of 12 kHz to filter acoustic hydrophone data. The filtered data is then plotted.

```
Hd = BP_4000_16000_CHBYT2;        % Filter Characteristics 4000 to 16000 Hz –
                                  % Chebychev  Type 2
Af = filter(Hd,A); % Filtered Data
Bf = filter(Hd,B); % Filtered Data
Cf = filter(Hd,C); % Filtered Data

%%% Plot Filtered Data %%%

figure(2)
subplot(2,2,1)
plot (Af);
xlabel('Sample Number Fs = 40kS/Sec')
ylabel('Volts Input (V_P_P)')
title('Filtered Data - 10K 20Cycles 140V_p_p')
grid on
```

77

```
subplot(2,2,2)
plot (Bf);
xlabel('Sample Number Fs = 40kS/Sec')
ylabel('Volts Input (V_P_P)')
title('Filtered Data - 10K 20Cycles 140V_p_p')
grid on

subplot(2,2,3)
plot (Cf);
xlabel('Sample Number Fs = 40kS/Sec')
ylabel('Volts Input (V_P_P)')
title('Filtered Data - 10K 20Cycles 140V_p_p')
grid on
%%%%%%%%%%%%%%%%%%%%%%%%%%%%%%%%%%%%%%%%%%%%%%%%%%%%%%%%%%
```

This code plots multiple pulses. Each pulse location is specified in a zoom window. This allows the calculation of the SPL_{RMS}. The data points for the RAW and FILTERED data are plotted. Each pulse in the data file is analyzed using the same method.

```
%%%% Zoom Window %%%%%% Pulse 1
t1_ = 95;        % RAW data
t2_ = 185;       % RAW data
t1 = 100;        % FILTERED data
t2 = 185;        % FILTERED data

figure(3)
subplot(2,2,1)
AA_=A(t1_:t2_);
plot(AA_)
grid on
hold on
AA=Af(t1:t2);
plot(AA,'r')
xlabel('Sample Number Fs = 40kS/Sec')
ylabel('Volts_P_P')
title('Zoom of 10K 20 Cycles 140V_p_p')
grid on

subplot(2,2,2)
BB_=B(t1_:t2_);
plot(BB_)
grid on
hold on
BB=Bf(t1:t2);
plot(BB,'g')
```

```
xlabel('Sample Number Fs = 40kS/Sec')
ylabel('Volts_P_P')
title('Zoom of 10K 20 Cycles 140V_p_p')
grid on

subplot(2,2,3)
CC_=C(t1_:t2_);
plot(CC_)
grid on
hold on
CC=Cf(t1:t2);
plot(CC,'k')
xlabel('Sample Number Fs = 40kSamples/Sec')
ylabel('Volts_P_P')
title('Zoom of 10K 20 Cycles 140V_p_p')
grid on
```

This code solves for the FFT of the filtered data contained in the zoom window. For

multiple pulses, each pulse location is specified in a zoom window. The FFT is plotted

for each hydrophone. The SPL_{RMS} for the filtered data are calculated. Each pulse in the

data file is analyzed using the same method.

```
%%%%%%%%%%%%%%%%%%%%%%%%%%%%%%%%%%%%%%%%%%%%%

% % %%%%%% Calculate FFT of Filtered Zoom Window and Plot %%%%%%%
t3 = length(AA);              % Length of filtered zoom window H0
NFFT = 2^(nextpow2(t3));      % Use next highest power of 2 > or = to length to calculate
                              % fft.
FFTX = fft(AA,NFFT);          % Take fft padding with zeros so that length(FFTX) is
                              % equal
NumUniquePts = ceil((NFFT+1)/2);   % Calculate the number of unique points
FFTX = FFTX(1:NumUniquePts);       % FFT is symmetric, throw away second half
MX = abs(FFTX);      % Take the magnitude of fft of x
MX = MX/t1;          % Scale the fft so that it is not a function of the length of
MX = MX.^2;          % Take the square of the magnitude of fft of x which has been
                     % scaled properly.
MX = MX*2;           % Multiply by 2 to because you threw out the second half of
                     % FFTX above
MX(1) = MX(1)/2;     % DC Component should be unique.
if ~rem(NFFT,2)      % Nyquist component should also be unique.
MX(end) = MX(end)/2;    % Here NFFT is even; therefore, Nyquist point is included.
end
fA = (0:NumUniquePts-1)*Fs/NFFT; % This is an evenly spaced frequency vector with
                                 % NumUniquePts


%%%%%%%%%%%%%%%%%%%%%%%%%%%%%%%%%%%%%%%%%%%%%
```

```
t3 = length(BB);            % Length of filtered zoom window H1
NFFT = 2^(nextpow2(t3));    % Use next highest power of 2 > or = to length to calculate
                            % fft.
FFTX = fft(BB,NFFT);        % Take fft padding with zeros so that length(FFTX) is
                            % equal
NumUniquePts = ceil((NFFT+1)/2);   % Calculate the number of unique points
FFTX = FFTX(1:NumUniquePts);       % FFT is symmetric, throw away second half
MX = abs(FFTX);             % Take the magnitude of fft of x
MX = MX/t1;                 % Scale the fft so that it is not a function of the length of
MX = MX.^2;                 % Take the square of the magnitude of fft of x which has
                            % been  scaled properly.
MX = MX*2;                  % Multiply by 2 to because you threw out the second half
                            % of FFTX above
MX(1) = MX(1)/2;            % DC Component should be unique.
if ~rem(NFFT,2)             % Nyquist component should also be unique.
MX(end) = MX(end)/2;        % Here NFFT is even; therefore, Nyquist point is included.
end
fB = (0:NumUniquePts-1)*Fs/NFFT;  % This is an evenly spaced frequency vector with
                            % NumUniquePts


%%%%%%%%%%%%%%%%%%%%%%%%%%%%%%%%%%%%%%%%%%%%%%%%%%%


t3 = length(CC);            % Length of filtered zoom window H1
NFFT = 2^(nextpow2(t3));    % Use next highest power of 2 > or = to length to calculate
                            % fft.
FFTX = fft(CC,NFFT);        % Take fft padding with zeros so that length(FFTX) is
                            % equal
NumUniquePts = ceil((NFFT+1)/2);   % Calculate the number of unique points
FFTX = FFTX(1:NumUniquePts);       % FFT is symmetric, throw away second half
MX = abs(FFTX);             % Take the magnitude of fft of x
MX = MX/t1;                 % Scale the fft so that it is not a function of the length of
MX = MX.^2;                 % Take the square of the magnitude of fft of x which has been
                            % scaled properly.
MX = MX*2;                  % Multiply by 2 to because you threw out the second half
                            % of FFTX above
MX(1) = MX(1)/2;            % DC Component should be unique.
if ~rem(NFFT,2)             % Nyquist component should also be unique.
MX(end) = MX(end)/2;        % Here NFFT is even; therefore, Nyquist point is included.
end
fC = (0:NumUniquePts-1)*Fs/NFFT;  % This is an evenly spaced frequency vector with
                            % NumUniquePts


%%%%%%%%%%%%%%%%%%%%%%%%%%%%%%%%%%%%%%%%%%%%%%%%%%%


figure(4)
subplot(2,2,1) % FFT of H0
plot(fA,MX);
title('Power Spectrum 10K 20 Cycles 140V_p_p');
xlabel('Frequency (Hz)');
ylabel('Power (dB/Hz)');
grid on
```

```
subplot(2,2,2) % FFT of H1
plot(fB,MX);
title('Power Spectrum 10K 20 Cycles 140V_p_p');
xlabel('Frequency (Hz)');
ylabel('Power (dB/Hz)');
grid on

subplot(2,2,3) % FFT of H2
plot(fC,MX);
title('Power Spectrum 10K 20 Cycles 140V_p_p');
xlabel('Frequency (Hz)');
ylabel('Power (dB/Hz)');
grid on


%%%%%%%%   Calculate the RMS value of the filtered signals   %%%%%%%%%
Arms1 = norm(AA)/(sqrt(t2-t1))
Brms1 = norm(BB)/(sqrt(t2-t1))
Crms1 = norm(CC)/(sqrt(t2-t1))

%   Calculate SPL at the hydrophones based upon their sensitivity and RMS voltage
SPL_A1f= MxA - Gain + 20*log10(Arms1) % Calculate SPL
SPL_B1f= MxB - Gain + 20*log10(Brms1) % Calculate SPL
SPL_C1f= MxC - Gain + 20*log10(Crms1) % Calculate SPL

%%%   Calculate the difference in theoretical SPL to the calculated SPL   %%%
Delta_A1 = SPL_A1f - SPL
Delta_B1 = SPL_B1f - SPL
Delta_C1 = SPL_C1f – SPL
```

Sections of the Matlab[TM] code were modified to perform the analyses of acoustic data

using different ranges and source levels. This source code is a representation of the

algorithms used. The SPL of data 'zoom' windows were calculated by specifying the data

points. Knowing the TVR of any potential source and the input voltage to that source,

the SL was be found, thereby the sensitivity of the hydrophones were established,

knowing the range and the calculation TL.

APPENDIX D

HYDROPHONE SPECIFICATIONS AND ANALYSIS

D.1   Hydrophone Description

The AQ-2000 Hydrophone is designed for usage in "shallow or deep water exploration with stable operating performance over a wide range of water depths. They are manufactured on high volume and combine high performance with low cost." (http://www.benthos.com/) The mechanical dimensions and specifications are shown in Figures D.1 and D.2.

AQ-2000 HYDROPHONE

HYDROPHONES

The AQ-2000 hydrophone represents the latest innovative acoustic sensor technology developed by Benthos for shallow and deep water exploration.

The AQ-2000 is well suited for both towed streamer and ocean bottom cable (OBC) applications that require stable operating performance over a wide range of water depths.

The AQ-2000 has excellent acceleration canceling qualities and exceptionally wide frequency bandwidth. The AQ-2000 is ready for installation into standard array mounting configurations or integration into custom molded packages.

Figure D.1: Benthos AQ-2000 description.
(http://www.benthos.com)
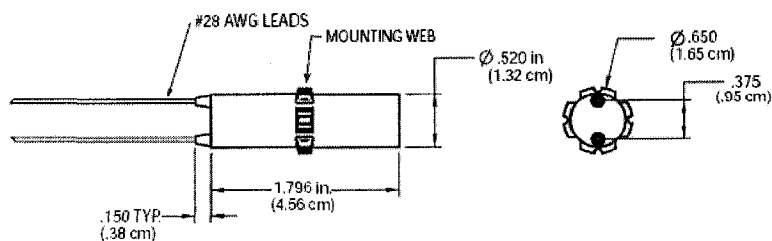
Figure D.2: Benthos AQ-2000 mechanical dimensions.
(http://www.benthos.com)

D.2 AQ-2000 Hydrophone Specifications:

Teledyne Benthos
49 Edgerton Drive • North Falmouth, Massachusetts 02556 USA
Telephone: +1 508 563–1000 • Fax: +1 508 563–6444 http://www.benthos.com/

The hydrophone specifications are shown in Table D.1. These values are stated for the uninstalled AQ-2000 hydrophone element. Figures D.3 and D.4 display the stated frequency performance of the transducer element. A specification to note is that the maximum *SPL* is 190 dB re 1 μPa.

Model	AQ-2000
Material	Flouroeleastomer, high strength epoxy, Hytrel® insulated leads
Weight in Air:	14 grams
Size:	4.56 cm long X 1.32 cm diameter
Displacement:	6.24 cc
Operating Temperature:	-10°C to 50°C
Storage Temperature:	-40°C to 60°C
Electrical Leads:	#28AWG (12.7 cm) red and black
Connector:	None
Polarity:	A positive increase in acoustic pressure generates a positive voltage on the red conductor
Capacitance:	4.5 nF ± 25% at 20°C and 1 kHz
Resistance	500 Mohm minimum across leads or to sea water at 20°C and 100% relative humidity, 50 VDC
Dissipation:	0.02 typical
Operating Range:	1 to 50000 Hz
Maximum SPL	190 dB re 1 μPa
Sensitivity @ 100 Hz Free-field Voltage:	-201 dB re 1V / μPa ± 1.5 dB
Sensitivity Change:	
vs. Frequency:	±.25 dB from 1 Hz to 1 kHz (±2.0 dB 1kHz to 10kHz)
vs. Depth:	<.5 dB to 1000 meters
vs. Temperature:	< .03 dB per 1° C change
Acceleration Sensitivity:	Output is < 1.5 mV/g due to acceleration in any of the three major axes at 20 Hz
Mechanical Resonance:	20 kHz (in water) typical
Max.	Operating Depth 2000 m
Destruct Depth:	>7,000 meters
Cost:	$50.00

Table D.1: Manufacturer specifications Benthos AQ-2000 hydrophones.
(http://www.benthos.com)
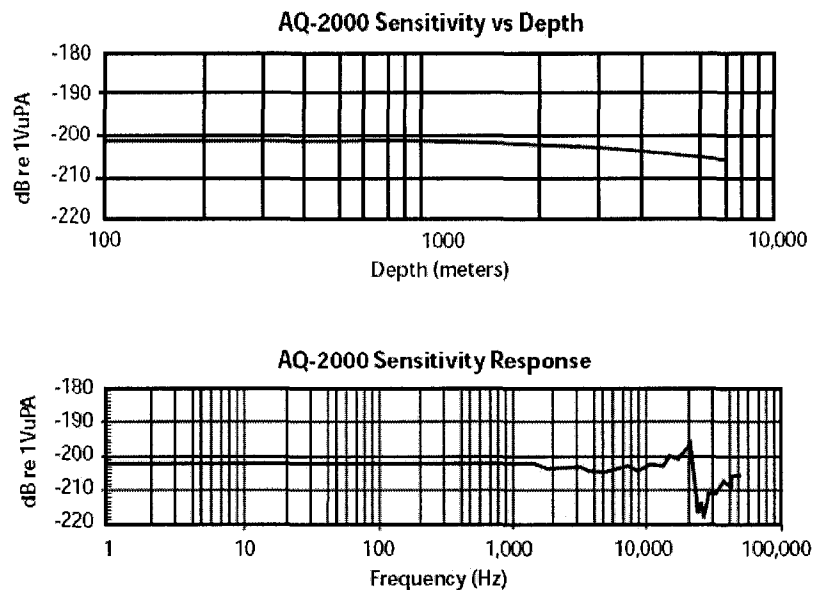
Figure D.3: Benthos AQ-2000 sensitivity versus depth and sensitivity response plots.
(http://www.benthos.com)
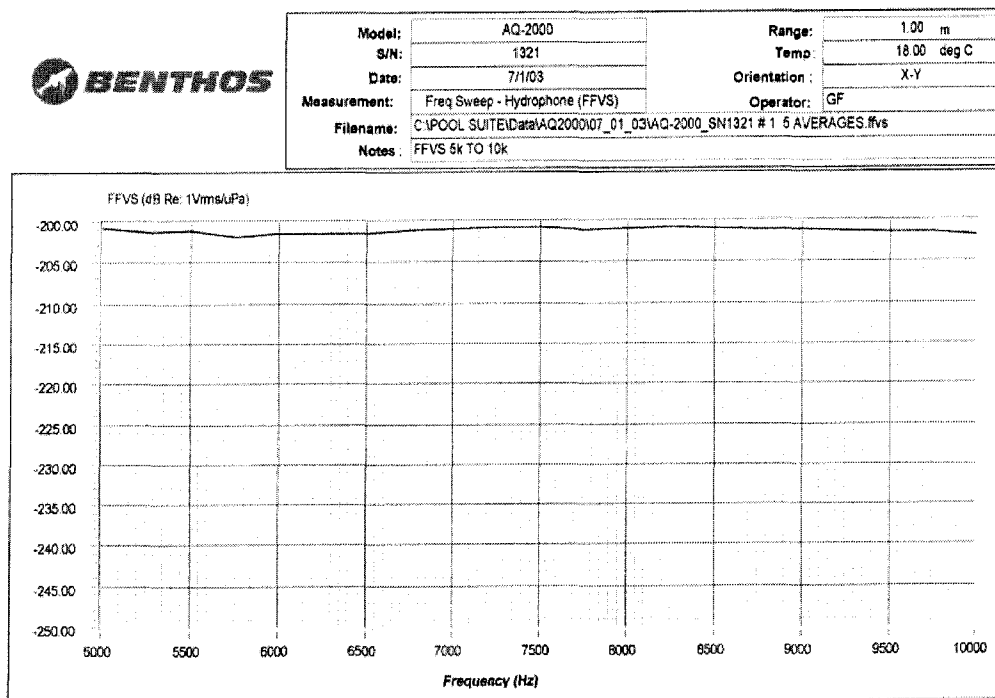
Figure D.4: Benthos AQ-2000 frequency sweep (*FFVS*).
(http://www.benthos.com)

D.3 Hydrophone Modes of Operation

Hydrophones operate in two modes, axial and radial. Axial mode operation is when the length (longest dimension) of the hydrophone is pointed at the source. Radial mode operation is when the longest length is perpendicular to the sound source as displayed below in Figure D.5.

Source
→

Axial

Radial
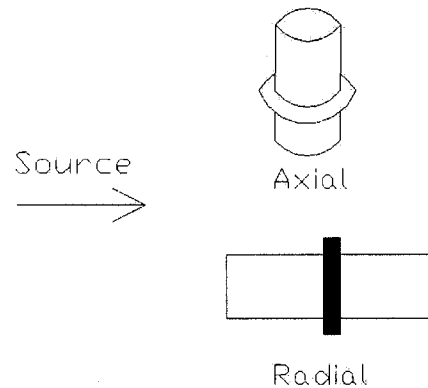
Figure D.5: Hydrophone mode orientation diagram.

As long as all physical dimensions of the hydrophone are small compared to the wavelength, the hydrophone is essentially omnidirectional. As the wavelength (λ) (or 1/2 λ) approaches the length, diameter or wall thickness of a hydrophone, the modes of vibration begin to affect directionality.

$$(\lambda = c / f) \qquad\qquad (D.1)$$

At 10kHz the wavelength is about 5-3/4 inches and a half wavelength is a bit less than 3 inches. This is approaching the length of the hydrophone. The radial pattern is omnidirectional as that dimension is still small compared to the length. The radial mode vibrates at one wavelength instead of 1/2 wavelength. Working in the 10kHz range it's best to orient the hydrophone in the radial direction in relation to the sound source. For a true omni-directional response at 10kHz, a better choice would be going to a smaller

hydrophone or use one with a spherical element. The directivity patterns are displayed in

Figures D.6 and D.7.

Model:	AQ-2000			Range:	1.00	m
S/N:	001			Temp:	18.00	deg C
Freq.:	5000.00	Hz		Orientation :	RADIAL	
Date:	8/2/06			Operator:	gf	
Directivity Type:	Select Measurement Type					
Filename:	C:\POOL SUITE\Data\AQ2000\AQ-2000_SN001-5_KHz.dir					
Notes :						
Limit:	160.50	# of Degrees Below Limit:	360.00	% Below Limit:	100.00	
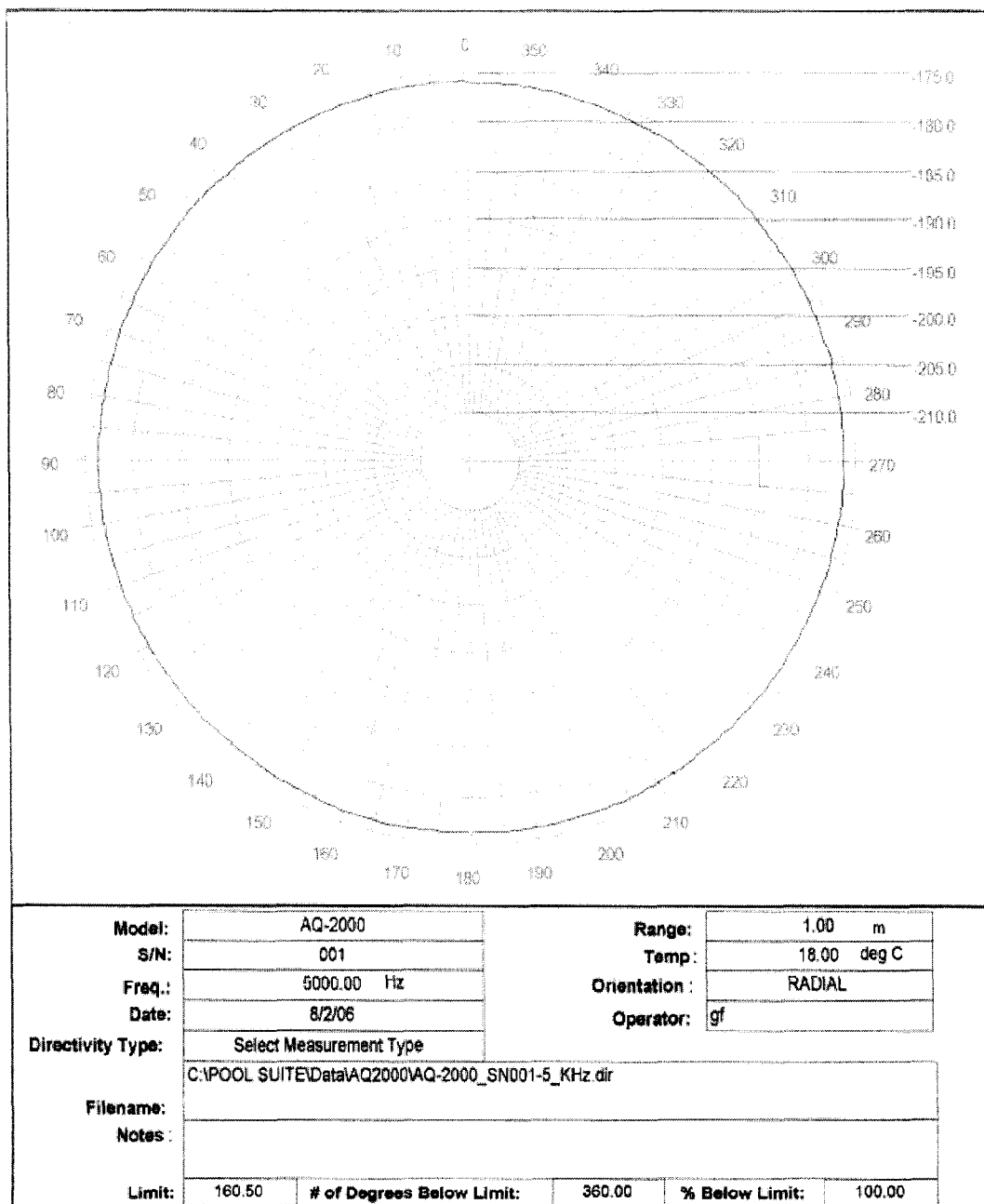
Figure D.6: Benthos AQ-2000 directionality at 5 kHz – radial mode.
(http://www.benthos.com)

Model:	AQ-2000	Range:	1.00	m
S/N:	001	Temp:	18.00	deg C
Freq.:	5000.00 Hz	Orientation :	AXIAL	
Date:	8/2/06	Operator:	gf	
Directivity Type:	Select Measurement Type			
Filename:	C:\POOL SUITE\Data\AQ2000\AQ-2000_SN001-5_KHz_VERTICAL.dir			
Notes :	26.6 dB PREAMP GAIN			
Limit:	160.50	# of Degrees Below Limit:	360.00	% Below Limit: 100.00
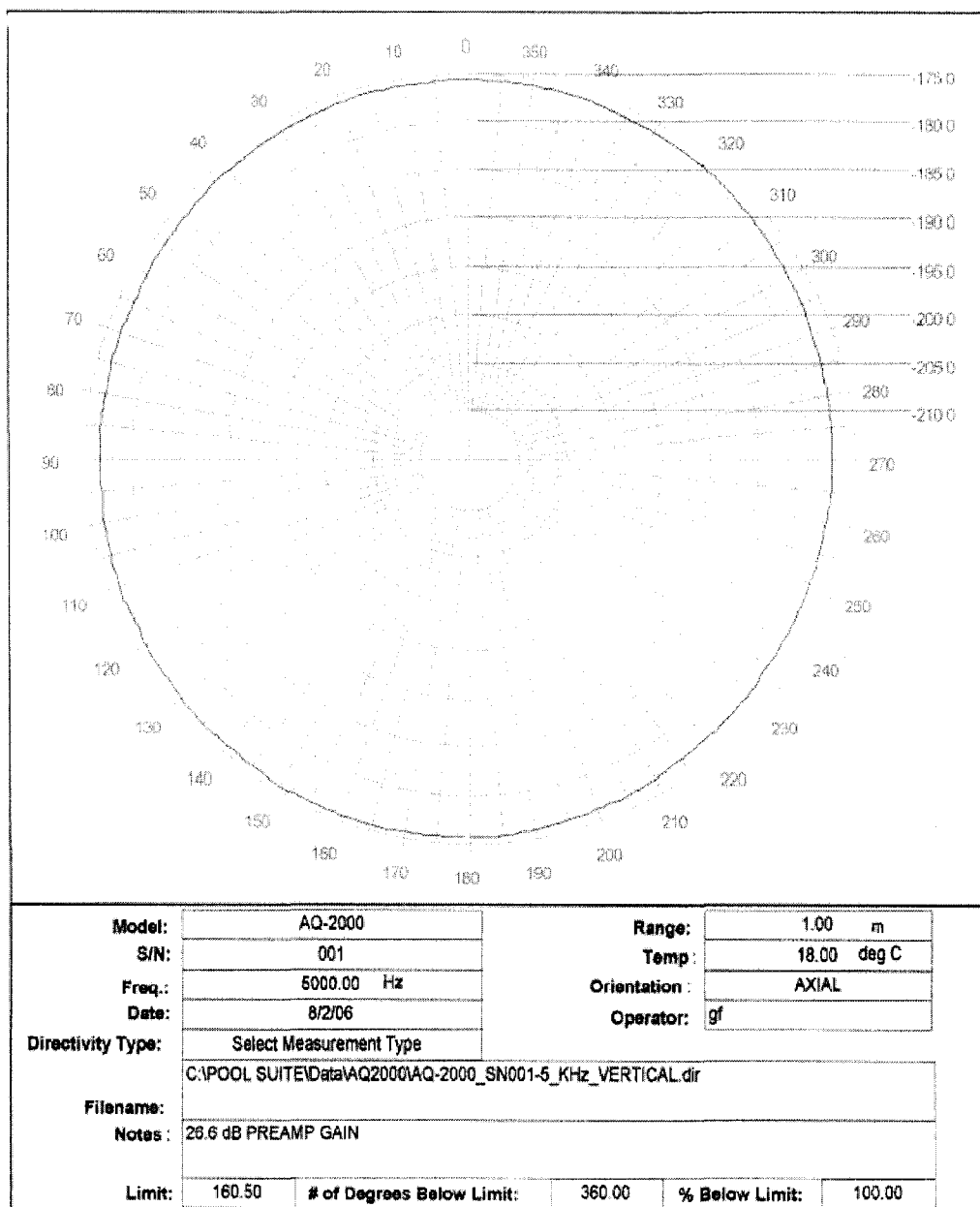
Figure D.7: Benthos AQ-2000 directionality at 5 kHz – axial mode.
(http://www.benthos.com)

D.4   Calculation of Frequency Response and Calculating the Q of the

Hydrophones

The frequency response for hydrophone 1 was experimentally determined and

plotted in Figure D.8. The bandwidth and Q were calculated. The analysis was

performed using an oscilloscope, a function generator and sense resistor. See Table D.2.

A CW sinusoid with a constant voltage of 1.0 VAC$_{P-P}$ was swept from 1Hz to 200kHz.

The voltage drop and phase shift were monitored across the sense resistor.
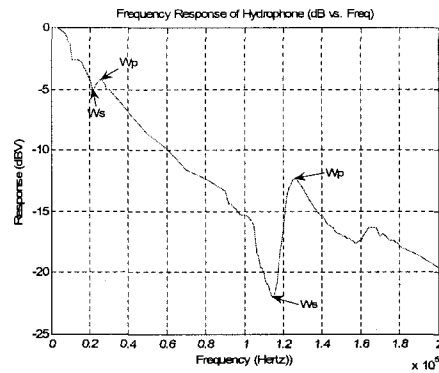
Figure D.8: Hydrophone frequency response from 1 Hz to 200 kHz.

Instrument	Model	Serial Number
Oscilloscope	Tektronix 2226	V/E 0972
Function Generator	Wavetek Model 22	Varian 169790E

Table D.2: Test equipment used for hydrophone frequency analysis.

To observe the frequency response and calculate resonance, a sense resistor (100 ohms, 5%, 1/4W, carbon) was placed in series with the hydrophone. The probes from the oscilloscope were connected to either side of the resistor. The output from the function generator was connected on one side of the sense resistor while the other side of the sense resistor was connected to the input of the unknown hydrophone impedance.

The measured voltage drop across the resistor, divided by the resistance value calculates the magnitude of the current. Measuring the phase shift on either side of the resistor allows the calculation of the phase angle between the voltage and the current.

- Knowing the input frequency, the period T (1/f) was calculated directly.
- The phase difference was observed directly from the oscilloscope.
- The phase angle was calculated using the following equation:

$$\Theta_{degrees} = (d1 \ / \ T) \ * \ 360 \ in \ degrees \qquad (D.2)$$

88

The bandwidth is defined as the frequency width of the frequencies –3 dB from the peak value. The important resonant frequency is the low value around 22kHz. The stated supplier specification was 20kHz in water. The bandwidth and Quality factor for hydrophone 1 was calculated, assuming a typical response for the three hydrophones. The resonance data is contained in table D.3. From Figure D.8, the bandwidth (W) equals 28kHz – 20kHz = 8kHz. The resonant frequency (Fc) equals 22kHz. Solving for the Mechanical Quality Factor (Q):

$$Q = Fc/W = 22 \ kHz \ / \ 8 \ kHz = 2.75 \qquad\qquad (D.3)$$

The value of the Q indicates the number of cycles required to excite the hydrophone. Using equation Q/π (Stansfield, 1991) and for 70% steady state = 0.875 cycles. Using equation Q/2 (Wallace et al, 1961) and for 80% steady state = 1.35 cycles. It would take between 1 and 2 cycles of a received signal for the hydrophone to reach steady state.

Transducer Frequency Transmit Response Data (in air)

f	Vin	Δt	ΔV	θ (deg)	θ (radians)	Vpp	I (amps)	Z
18000	5	-6.00E-06	1.68	-38.88	-0.68	3.32	0.00084	3952.381
19000	5	-6.00E-06	1.80	-41.04	-0.72	3.20	0.00090	3555.556
20000	5	-5.00E-06	1.88	-36.00	-0.63	3.12	0.00094	3319.149
21000	5	-3.00E-06	2.08	-22.68	-0.40	2.92	0.00104	2807.692
22000	5	-2.00E-06	2.24	-15.84	-0.28	2.76	0.00112	2464.286
23000	5	-2.00E-06	2.12	-16.56	-0.29	2.88	0.00106	2716.981
24000	5	-3.00E-06	2.00	-25.92	-0.45	3.00	0.00100	3000.000
25000	5	-3.00E-06	1.95	-27.00	-0.47	3.05	0.00097	3128.205
26000	5	-3.00E-06	1.96	-28.08	-0.49	3.04	0.00098	3102.041
115000	5	-1.00E-06	4.6	-41.4	-0.72	0.4	0.0023	173.913
116000	5	-1.00E-06	4.58	-41.76	-0.73	0.42	0.00229	183.406
117000	5	-5.00E-07	4.54	-21.06	-0.37	0.46	0.00227	202.643
118000	5	-4.00E-07	4.4	-16.992	-0.30	0.6	0.0022	272.727
119000	5	-2.00E-07	4.34	-8.568	-0.15	0.66	0.00217	304.147
120000	5	-5.00E-07	4.24	-21.6	-0.38	0.76	0.00212	358.491
121000	5	-4.00E-07	4.1	-17.424	-0.30	0.9	0.00205	439.024
122000	5	-5.00E-07	3.98	-21.96	-0.38	1.02	0.00199	512.563
123000	5	-7.00E-07	3.9	-30.996	-0.54	1.1	0.00195	564.103

Table D.3: Resonance data for typical AQ-2000 transducer. The resonant frequency at 22kHz is the resonance of concern.

D.5 Hydrophone Preamplifiers

Benthos AQ-201 Hydrophone Preamplifiers were selected. The complete manufacturers technical specifications are contained in Table D.4. As shown in Figure D.9, the AQ-201/202 preamplifiers are single ended devices. This affected common mode signal rejection during data collection. A better choice, allowing a differential input to the A/D would have been either the AQ-300 or AQ-302 preamplifiers. The gain of the AQ-202 is 26 dB, while the gain of the AQ-300 and AQ-302 preamplifiers is 20.8 dB. The gain is not affected by the supply voltage, but is set by the internal op-amp feedback resistor ratio. The current draw for the AQ-202 preamplifiers, as supplied by Benthos is contained in Table D.5 below. The AQ-202 preamplifier gain and output noise curves a contained in Figure D.10 and D.11.

Supply Voltage	Quiescent Current
9VDC	3.1 mA
12VDC	3.3 mA
18VDC	3.6 mA

Table D.4: Supply voltage and quiescent current.

Hydrophone Preamplifiers

These Preamplifiers have been specifically designed for small diameter arrays used to extreme depth ratings. High input impedance, low current, and high drive capability make them suitable for long cable lengths.

The AQ-201 and AQ-202 are single ended units with complimentary direct-coupled output drivers. The AQ-202 Model has higher current with lower noise.

The AQ-300 and AQ-302 have the same features as the AQ-201 with the exception of differential input and output circuits.

AQ-201

AQ-300

	AQ-201	AQ-202	AQ-300	AQ-302
Gain dB	28 dB	26 dB	20.8 dB	20.8 dB
Input Impedance	15 MΩ	15 MΩ	30 MΩ	30 MΩ
Current Quiescent mA 12VDC	<0.3 mA	<4.0 mA	<0.6 mA	<6 mA
Noise ref. input nv/√ Hz	<100 nv	<20 nv	<100 nv	<20 nv
High Pass -3 dB	1 Hz	1 Hz	.3 Hz	.3 Hz
Low Pass -3 dB	12 kHz	12 kHz	14 kHz	14 kHz
Depth in meters	1732	1732	1732	1732
Size in cm O.D./length	1.74/4.45	1.74/4.45	1.65/5.7	1.65/5.7
Weight in grams	17.4	17.4	17.1	17.1

Figure D.9: Benthos hydrophone preamplifier specification data sheet. (www.benthos.com)
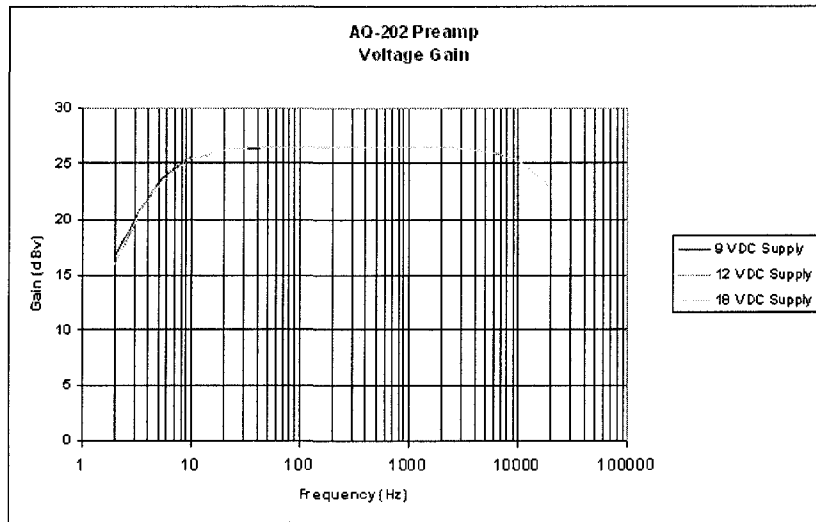
Figure D.10: Benthos AQ-201 preamplifier voltage gain curve.
(http://www.benthos.com)
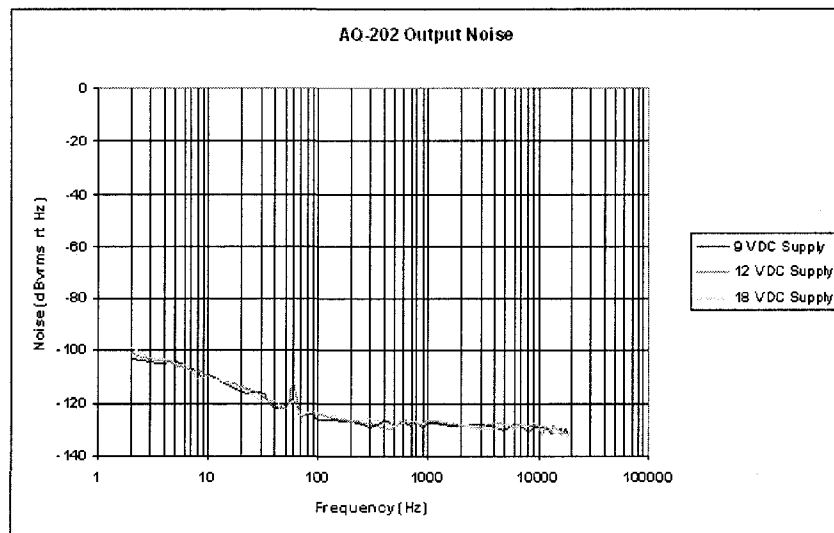
Figure D.11: Benthos AQ-202 preamplifier output noise curve.
(http://www.benthos.com)

D.6   Complete Hydrophone Assembly

The output signals of the hydrophone elements were fed directly into the

preamplifier inputs, forming the complete hydrophone assembly. The Benthos AQ-201

preamplifiers are DC coupled. The output signal rides on a DC level that is equal to

approximately ½ the supply voltage. To overcome this offset, a single pole high pass

filter was designed. This high pass filter acts as a DC block eliminating the DC offset. The DC blocking circuit (HPF) is discussed in section D.7. A major consideration was the packaging of the hydrophone assemblies. The individual pieces were assembled in a manner that would allow the hydrophones to be as sensitive as possible, allow the signals to amplified and be as robust as possible. During testing in the Jere Chase Ocean Engineering Laboratory, the signals were affected by a 60Hz signal. A consequence of the A/D inputs being single ended wired possibly the 115VAC monitor connected to the mainboard computer.

D.7   Design of a High Pass Filter (HPF) for the Pre-Amp Assembly

A single pole (first order) HPF / DC block was installed into the input channels of the NI-USB-9125A A/D module, which eliminated any DC offset. The circuit is shown schematically in Figure D.12. The circuit analysis is described in Figure D.13 and the filter frequency response is shown in Figure D.14.
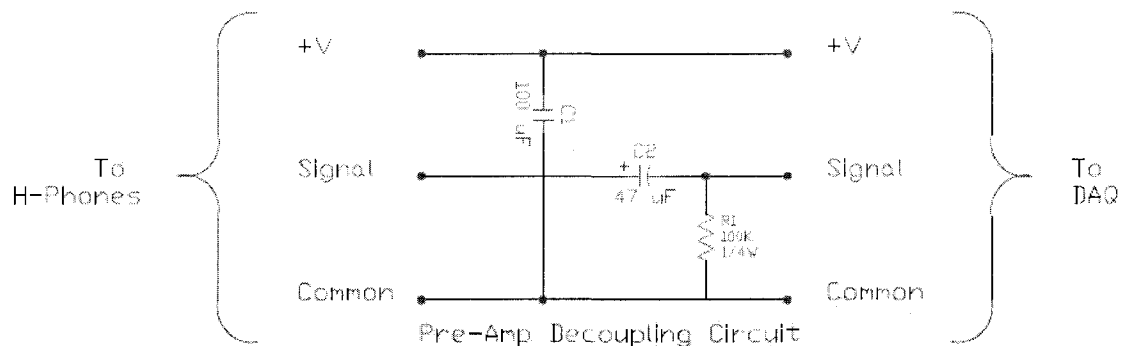
Figure D.12: Preamplifier DC de-coupling circuit.

First Order High Pass Filter
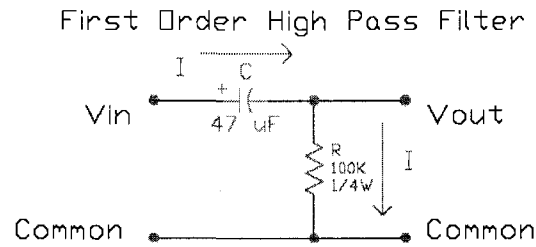
Circuit Analysis

$Vin = ZinI = \left(R + 1/jwC\right)I$

$Vout = ZoutI = RI$

Transfer Function $H(w)$

$$H(w) = \frac{(jw/w_o)}{1 + jw/w_o} \qquad w_o = 1/RC$$

$$H(w) = \frac{Vout}{Vin} = \frac{jwRC}{1 + jwRC}$$

$$|H(w)| = \frac{wRC}{1 + (RC)^2 w^2}$$

$$\angle H(w) = \arctan\left(\frac{w_o}{w}\right)$$

Figure D.13: Preamplifier high-pass / DC de-coupling circuit analysis.

The theoretical response has been experimentally calculated and validated. The circuit removes the DC offset and the 3dB point is less than 1Hz. Being a single order high pass filter, this value of the break point was chosen so gain at the expected low frequencies was as close to unity as possible. Table D.5 contains calculations of the 3 dB break frequency using other resistor and capacitor values.
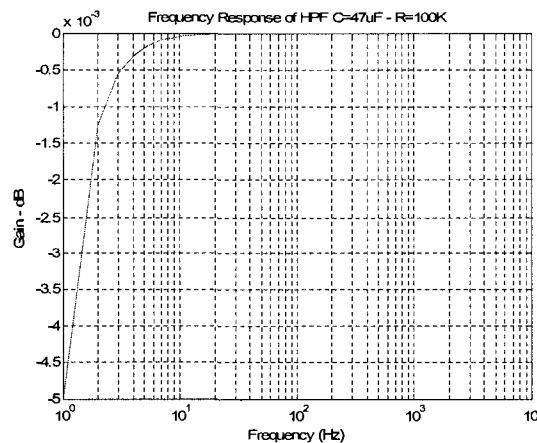
Figure D.14: Preamplifier de-coupling circuit frequency response.

R	C	RC	F_{-3dB}
100K	22 uF	2.2 Sec	0.0723 Hz
100K	47 uF	4.7 Sec	0.0339 Hz
1M	10 uF	10 Sec	0.0159 Hz
100K	.01 uF	1 mSec	159 Hz

Table D.5: 3 dB point for different component values in HPF.

APPENDIX E

LUBELL ACOUSTIC PROJECTOR / PEAVY AMPLIFIER SPECIFICATIONS

AND ANALYSIS

E.1   Introduction

This appendix contains the manufacturer specification and data sheets for the

amplifier and source. The amplifier frequency response was analyzed on the bench under

different load conditions to validate output voltages. A relationship between output

voltage to input voltage using the front panel gain level knob on the amplifier was

established, see section E.6. Additional improvements and changes to the packaging and

mounting are described.

E.2   Lubell LL9162 Underwater Acoustic Transducer

The Lubell LL9162 Underwater Acoustic Transducer is "designed for general

purpose military and scientific applications and may also be used as an underwater

loudspeaker when high power is required". (Lubbell Labs 2006) The LL9162 has a

useful frequency range of 240Hz-20kHz, a minimum impedance of 10 ohms, and with 50

V_{RMS} applied a source level of 186 dB re $1\mu Pa$ at 900Hz and 190 dB re $1\mu Pa$ at 10.6kHz.

This input voltage is supplied by a Peavy IPA300T 300 watt power amplifier. The

LL9162 and IPA300T amp were delivered as a matched unit. The LL9162 operates at

depths between 6' to 50' and is constructed from PVC and stainless steel. For operation, a

power resistor is used in series with the output of the Peavey amplifier. For electrical

safety, the amplifier's AC power cord should connect to a GFCI outlet. (Lubbell Labs 2006). Table E.1 summarizes technical specifications and Figure E.2 is a pictorial of the Lubell source. In Figure E.3 the SL_{MAX} (f) for the source is plotted.

- Frequency Response: 250Hz - 20kHz
- Output Level: 186dB/uPa/m @ 900Hz, 190dB/uPa/m @ 10.6kHz (50 Vrms applied)
- Maximum Voltage: 50 Vrms (70 Vrms for LL9162T)
- Maximum Current: 3A @ 100% D.C. (5A for LL9162T)
- Impedance: 16 ohms nominal - use only with series resistor per instructions
- Directivity: Omnidirectional up to 2kHz, slight scalloping at higher frequencies
- Minimum/Maximum Depth: 6' (1.83 meters) to 50' (15.24 meters)
- Installed Bulkhead Connector: Impulse IERD2F-BC single pin right angle
- Included Cable: Underwater pluggable IE2M-7/16 on 75' SJOW cable
- Included Power Resistor: Milwaukee 18-136-7.5R w/brkt
- Weight: 15 lbs (less cable)
- Dimensions: 8.75"D x 10.75"W x 10.75"H
- Certification: CE
- Warranty: 2 year limited
- Price: $1922
- Recommended Amplifier: IPA300T-120V or IPA300T-240V
- Documents: Owners manual, impedance plot, SPL plot

Table E.1: Lubell LL9162 specification summary.
(http://www.lubell.com)
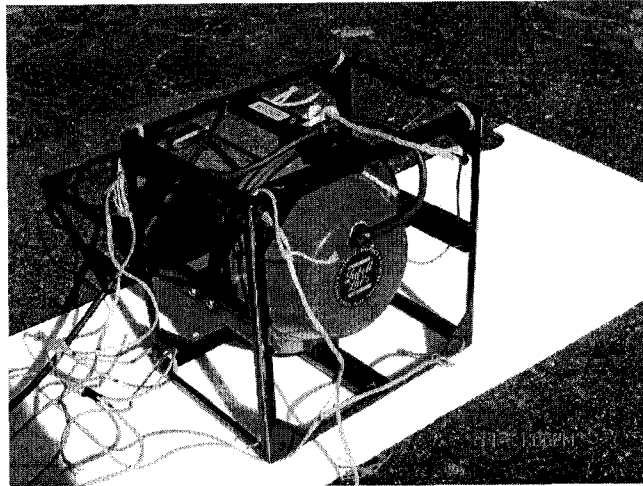
Figure E.1: Close up of Lubell source.

Figure E.2: SL versus frequency of the source and amplifier.
(http://www.lubell.com)

To calculate the *SL* use Equation E.1. The *TVR* (*f*) was available from the supplier.

Figure E.3 plots the *SL* data vs. frequency for the Lubell source and the Peavey amplifier.

$$SL = TVR \ (freq) + 20 \ log(V_{in\_RMS}) \ \ dB \ re \ 1 \ uPa \qquad (E.1)$$

Figure E.3: TVR and SL frequency response plots from supplier specification sheet.

97

Table E.2 summarizes the *TVR* (dB re 1μPa / volt) and *SPL* (dB re 1μPA) for the Lubell

source. The data were collected at a depth of 28 ft, distance of 9.8 ft, drive voltage of

50Vrms nominal and a water temperature of 44.4° F. Reference Figure E.2.

Freq (Hz)	Vin (RMS)	TVR dB re 1μPa / volt	SPL dB re 1 1μPa
150	49.75	110.82	144.76
200	49.99	117.88	151.85
250	49.57	120.71	154.61
300	49.42	123.55	157.43
400	49.15	130.59	164.42
500	49.97	136.22	170.2
600	50.55	140.54	174.62
700	50.4	145.04	179.09
800	50.05	149.57	183.56
900	49.96	151.39	185.36
1000	49.98	151.36	185.34
1100	50.41	149.9	185.34
1200	50.41	148.6	182.65
1300	50.2	147.63	181.64
1400	50.3	146.59	180.62
1500	50.25	146.2	180.22
1600	50.64	145.65	179.74
1700	50.33	145.34	179.38
1800	50.15	145.31	179.31
1900	49.96	144.96	178.93
2000	50.05	144.78	178.77
2500	49.75	145.51	179.44
2600	49.65	145.83	179.75
2700	49.51	145.98	179.88
2800	49.37	146.02	179.89
2900	49.31	145.8	179.66
3000	49.27	145.3	179.15
3500	49.63	144.14	178.05
4000	49.27	144.88	178.73
4500	49.7	148.85	182.78
5000	49.68	151.54	185.46
6000	49.42	140.45	174.32
7000	49.59	149.14	183.05
8000	49.7	149.09	183.02
9000	49.5	152.46	186.35
10000	49.87	155.41	189.36
12000	49.75	150.33	184.27
14000	49.57	148.64	182.54
16000	49.44	151.75	185.64
18000	49.17	145.52	179.36

Table E.2: Lubell LL9162 TVR / SL data. (http://www.lubell.com)

E.3 Peavey IPA300T 300 Watt Power Amplifier Specifications

The IPA300T is a high quality commercial grade mono amplifier with screw terminal line input and transformer isolated screw terminal outputs. The IPA300T meets all safety and power requirements for use with the Lubell Labs LL9162 underwater speaker. The LEVEL knob on the front panel sets the output voltage. The internal circuitry of the amplifier limits the maximum voltage, indicated by the SPS™ LED being lit. The front panel is displayed in Figure E.4 and the specifications are contained in Table E.3.
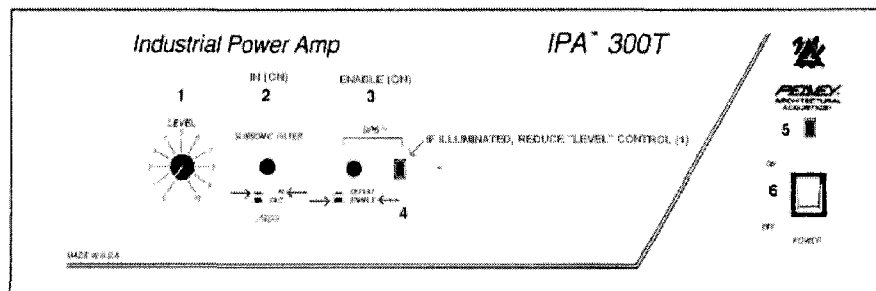
Figure E.4: Peavey IPA300T 300 watt power amplifier front panel.
(http://aa.peavey.com/poweramps/ipa300t.cfm)

- Frequency Response: 40Hz-20kHz +0/-1 dB
- Input Sensitivity: 100mV/20 k ohms, 1V/20 k Ohms (switchable)
- Power Output: 300 watts RMS @ 0.1% THD
- Output Impedance: 4 ohm direct, 8 ohm/25V/70V transformer isolated
- Patented SPS speaker protection circuitry
- Mounting: Rack mount (3RU) or shelf mount
- Finish: Gray powder coat
- Certifications: UL, CE
- Warranty: 3 yr + 2 yr limited
- Operating Voltages: IPA300T-120V, or IPA300T-240V
- Dimensions: 19"W x 5.25"H x 13.125"D
- Shipping Weight: 37 lbs
- List Price: $896
- Documents: Data sheet, manual

Table E.3: Peavey IPA300T 300 watt power amplifier specifications.
(http://aa.peavey.com/poweramps/ipa300t.cfm)

E.4 Amplifier and Source Wiring

A setup block was fabricated to accommodate a bracket to hold the manufacturer supplied 7.5 ohm resistor, inline fuse and terminal block. A CPC (circular plastic) connector was added to the setup block, allowing a quick disconnect for the Lubell projector to the amp. The Lubell source was wired to the terminal block. Figure E.5 is a pictorial of the setup block. The mechanical design is displayed in Figure E.6.
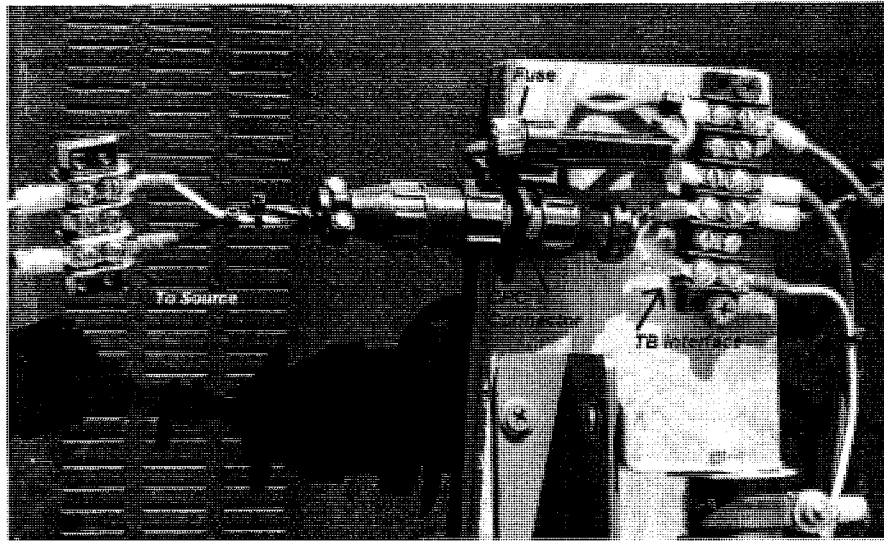
Figure E.5: Overhead view of Peavey amplifier.
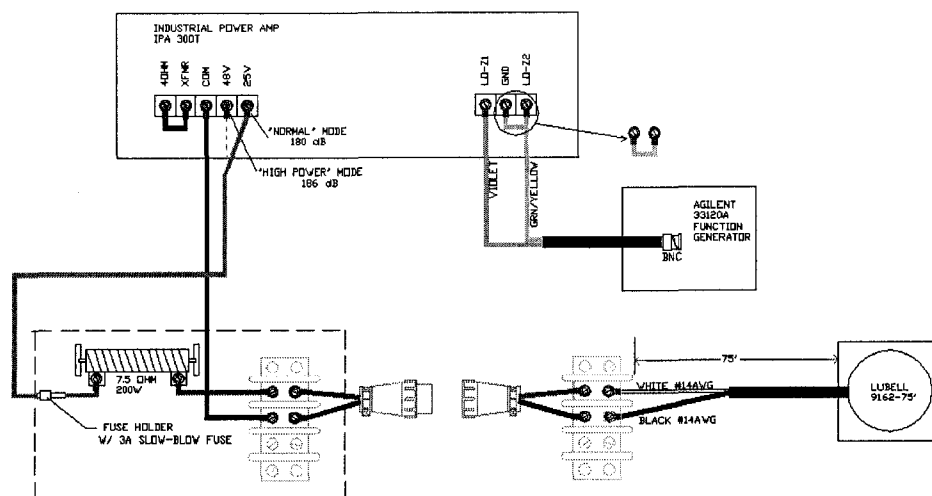
Figure E.6: Mechanical Layout.

E.5   Frequency Response Calculation

The amplifier was tested for flatness across the operating frequency band using

two load impedances, (10 and 15 ohms), and observed for different values of Vin and

Level knob settings. Data was taken across the frequencies from 1kHz to 22kHz, keeping

Vin constant (2Vp-p) and the Level knob set to 5. Across the band from 1kHz to

8000kHz the response was flat. For the frequency band of concern, from 200Hz to

8000Hz, the maximum deviation was < 0.1 dB. The data is plotted in Figure E.7.
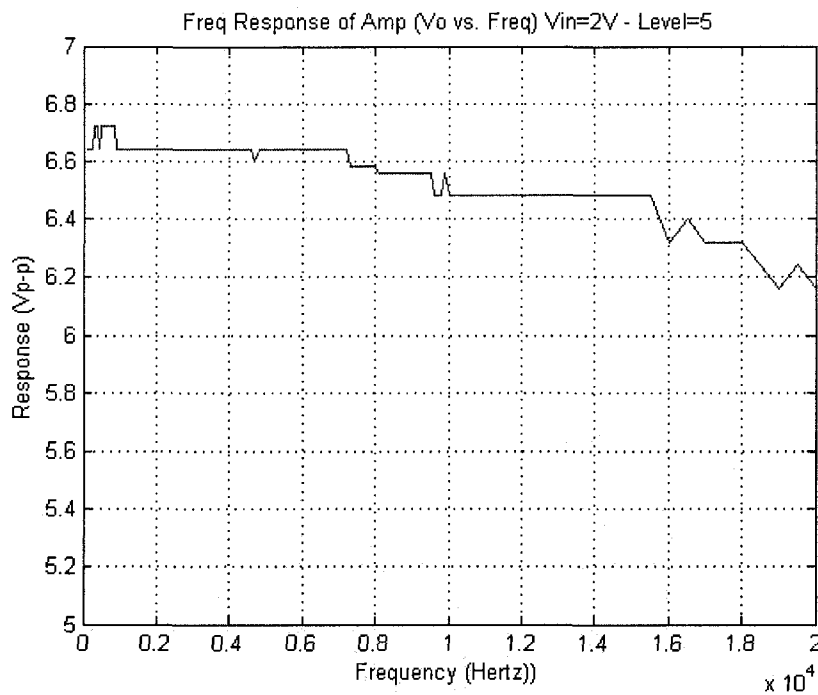
Figure E.7: Frequency response (Vin_{p-p} = 2 volts vs. frequency).

E.6   Amplifier Gain vs. Level Knob Setting

Keeping the input voltage and frequency constant, the Level knob on the Peavey IPA300T amplifier was adjusted from 0 to 10 and the output voltage across a load impedance of 15 ohms was recorded. Typical values are plotted in Figure E.8. The output is a maximum of 51 Vp-p with a load impedance of 15 ohms. The maximum output voltage is load dependant. The data is contained in Table E.4. Using table E.2, the presented data concludes that the maximum voltage into the load is achieved with the SPS switch enabled, and the SPS LED on front panel of the Peavey IPA300T amplifier lights. If the Level knob is set above a set level as shown in E.8, the output voltage is at a maximum for all input voltages.

Figure E.8: Vout across 15 ohm load at 1kHz versus Level knob setting on the Peavey amplifier. The maximum Vout depends on the load impedance.

Constant Frequency z   F = 1kH
3V <Vin <20V into   15 ohms
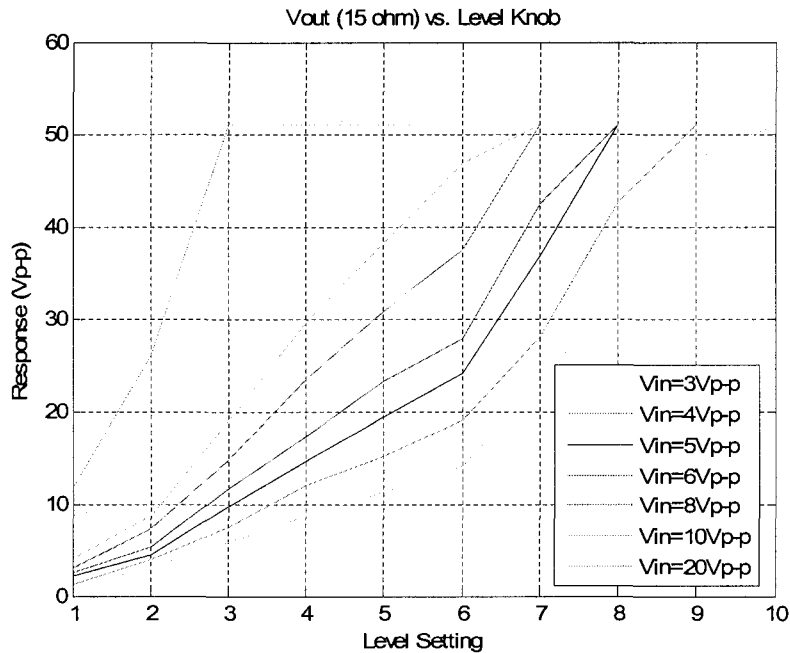Level from 0-10

1kHz	Vout	Vin	1kHz	Vout	Vin	1kHz	Vout	Vin
1	1.4	3	1	1.4	4	1	2.2	5
2	3	3	2	3.9	4	2	4.4	5
3	5.8	3	3	7.4	4	3	9.8	5
4	8.6	3	4	12	4	4	14.6	5
5	11.4	3	5	15.2	4	5	19.4	5
6	14.2	3	6	19	4	6	24.2	5
7	23	3	7	28	4	7	36.8	5
8	33	3	8	42.6	4	8	51	5
9	47.2	3	9	51	4	9	51	5
10	51	3	10	51	4	10	51	5

1kHz	Vout	Vin	1kHz	Vout	Vin	1kHz	Vout	Vin	1kHz	Vout	Vin
1	2.6	6	1	3	8	1	4.2	10	1	11.8	20
2	5.4	6	2	7.2	8	2	8.6	10	2	26	20
3	11.6	6	3	14.8	8	3	19	10	3	51	20
4	17.2	6	4	23.4	8	4	29.6	10	4	51	20
5	23.2	6	5	30.8	8	5	38.2	10	5	51	20
6	27.8	6	6	37.4	8	6	46.8	10	6	51	20
7	42.4	6	7	51	8	7	51	10	7	51	20
8	51	6	8	51	8	8	51	10	8	51	20
9	51	6	9	51	8	9	51	10	9	51	20
10	51	6	10	51	8	10	51	10	10	51	20

Table E.4: Vout versus Level knob setting.

E.7: Summary

❏ A CPC connector was added to the amplifier output to facilitate quick disconnect.

❏ The frequency response of the Peavey amplifier is within 1 dB from 240Hz to 22kHz. For output frequencies below 240Hz, the output tends to be unstable.

❏ The output voltage of the amplifier is dependant on the load impedance. Per the literature, the impedance from the amp to the source are matched in order to obtain the most efficient of power to the source.

❏ On the Peavey amplifier, with the SPS switch enabled and the SPS LED on, the maximum output voltage, typically 51 V_{P-P} would be produced, reference Table E.4 and Figure E.8. Any Vin > 5Vp-p, and the Level knob set to 8 or above, would achieve these results.

103

APPENDIX F

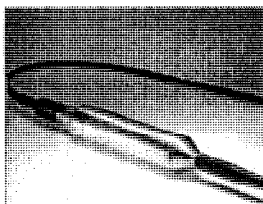## RESON HYDROPHONE TC 4014 SPECIFICATION DATA
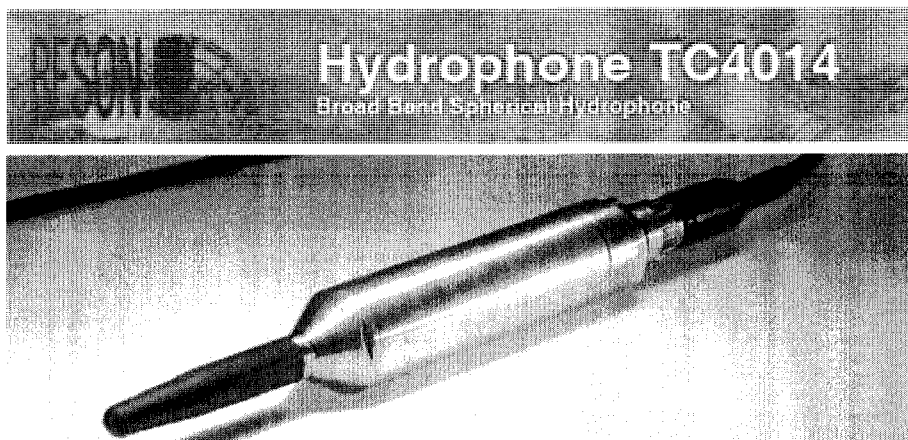
TC4014

- Wide usable frequency range
- Omnidirectional in all planes
- Built-in low noise preamplifier
- Long term stability
- Individually calibrated

The TC4014 broad band spherical hydrophone offers a very wide usable frequency range with excellent omnidirectional characteristics in all planes. The overall receiving characteristics makes the TC4014 an ideal transducer for making absolute underwater sound measurements up to 480kHz. The wide frequency range also makes the TC4014 perfect for calibration purposes, particularly in higher frequencies.
The TC4014 incorporates a low-noise 26dB preamplifier providing signal conditioning for transmission over long underwater cables.

The TC4014 features an insert calibration facility, which allows for a reliable test of the hydrophone. The TC4014 is available with integrated SUBCON 8GH MGP connector. Ask for TC4039.
The sensor element is permanently encapsulated in Special formulated NBR to ensure long term reliability. The rubber has been specially compounded to ensure acoustic impedance close to that of water. The hydrophone and connector housing are made of corrosion resistant aluminum-bronze.

TECHNICAL SPECIFICATIONS

|	
Usable Frequency range:	15Hz to 480kHz
Linear Frequency range:	30Hz to 100kHz ±2dB 25Hz to 250kHz ±3dB
Receiving Sensitivity:	-186dB ±3dB re 1V/µPa
Horizontal directivity:	Omnidirectional ±2dB at 100kHz
Vertical directivity:	270° ±2dB at 100kHz
Operating depth:	900meter
Survival depth:	1200meter
Operating temperature range:	-2°C to +55°C
Storage temperature range:	-40°C to +80°C
Weight in (air):	850g without cable
Max. output voltage:	≥2.8Vrms (at 12VDC)
Preamplifier gain:	26dB
Supply voltage:	12 to 24VDC
High pass filter:	15Hz -3dB
Calibration path attenuation:	at 10kHz 14dB
Current consumption:	<28mA at 12VDC <34 mA at 24VDC
Max. output effect:	50mW

www.reson.com

Figure F.1: Reson TC4014 hydrophone technical specifications.
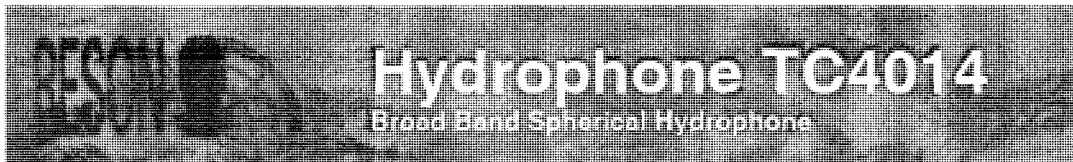
Documentation:

Receiving sensitivity:	Individually calibration curves:	Sensitivity at ref.: frequencies:
At 5 kHz to 500 kHz		250 Hz
Horizontal directivity:	Vertical directivity:	
At 100, 200, 300 kHz	At 100, 200, 300 kHz	

Horizontal directivity pattern
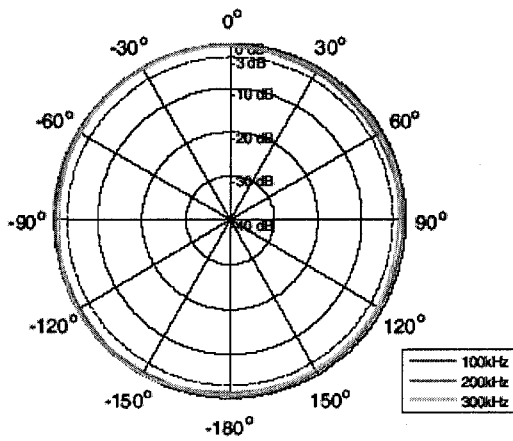
Receiving Sensitivity [dB re 1V/µPa @ 1m]
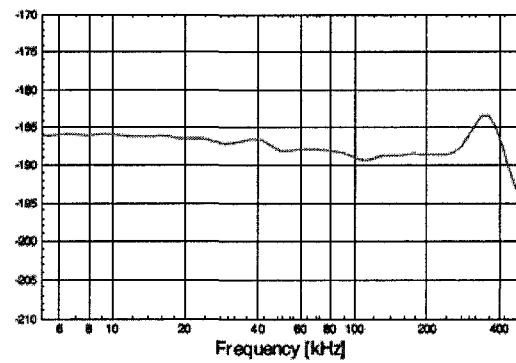
Vertical directivity pattern

Typical equivalent noise pressure curve

Figure F.2: Reson TC4014 hydrophone graphical specifications.

105

APPENDIX G

ITC 1042 TRANSDUCER SPECIFICATIONS

Figure G.1: Generic ITC-1042 omni-directional transducer specifications.
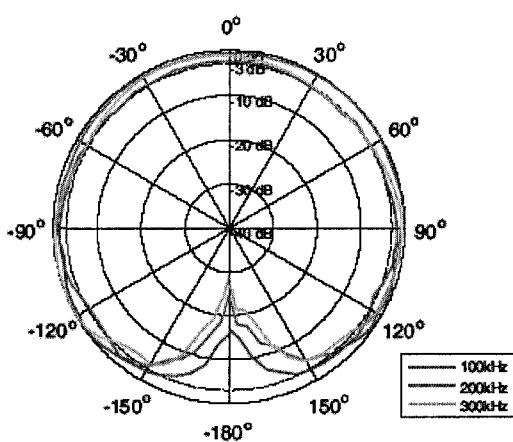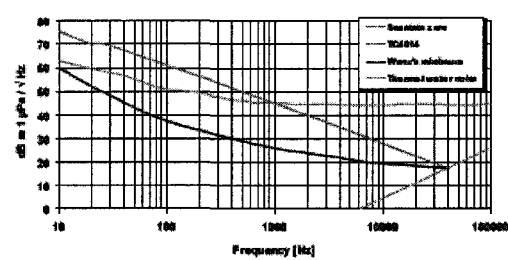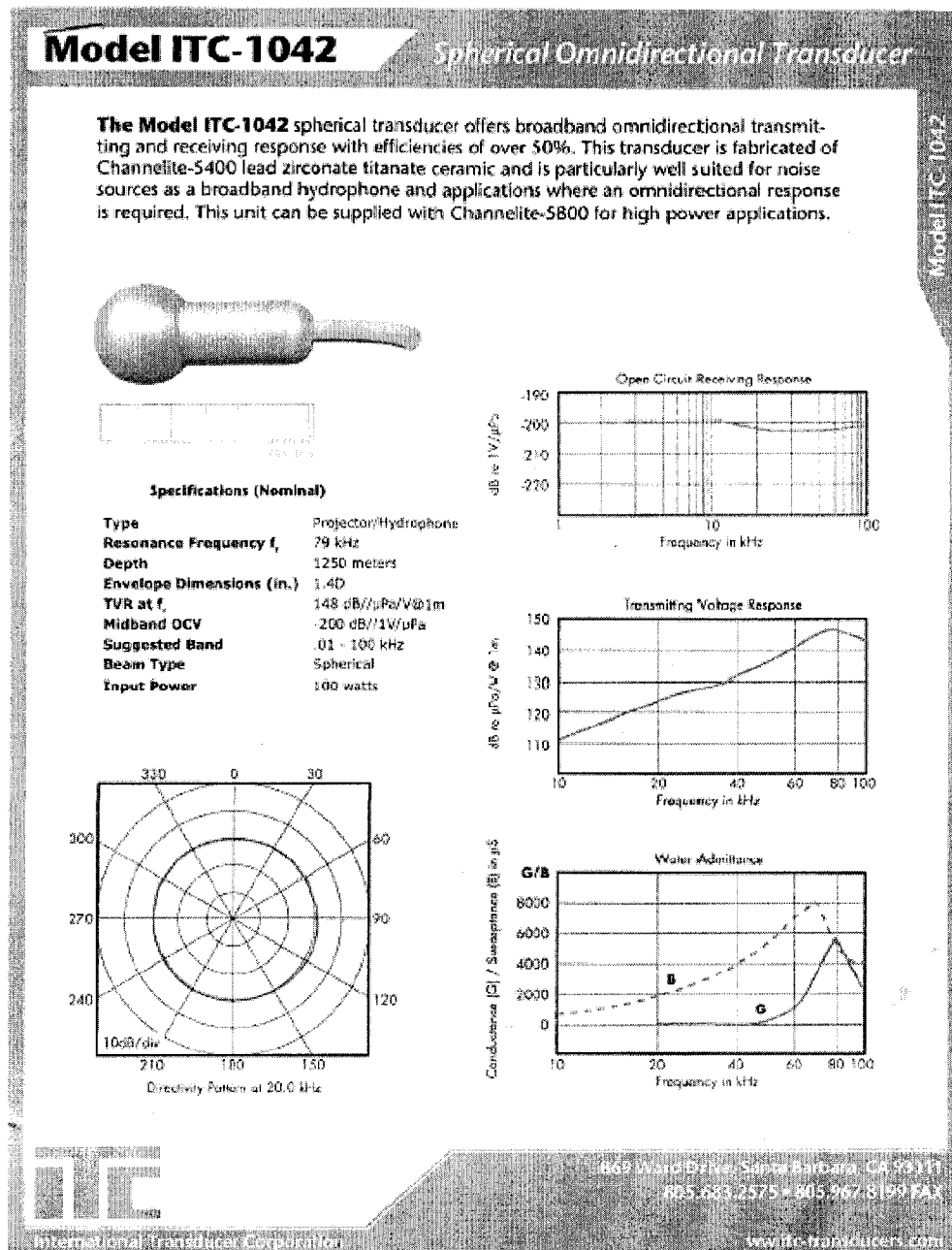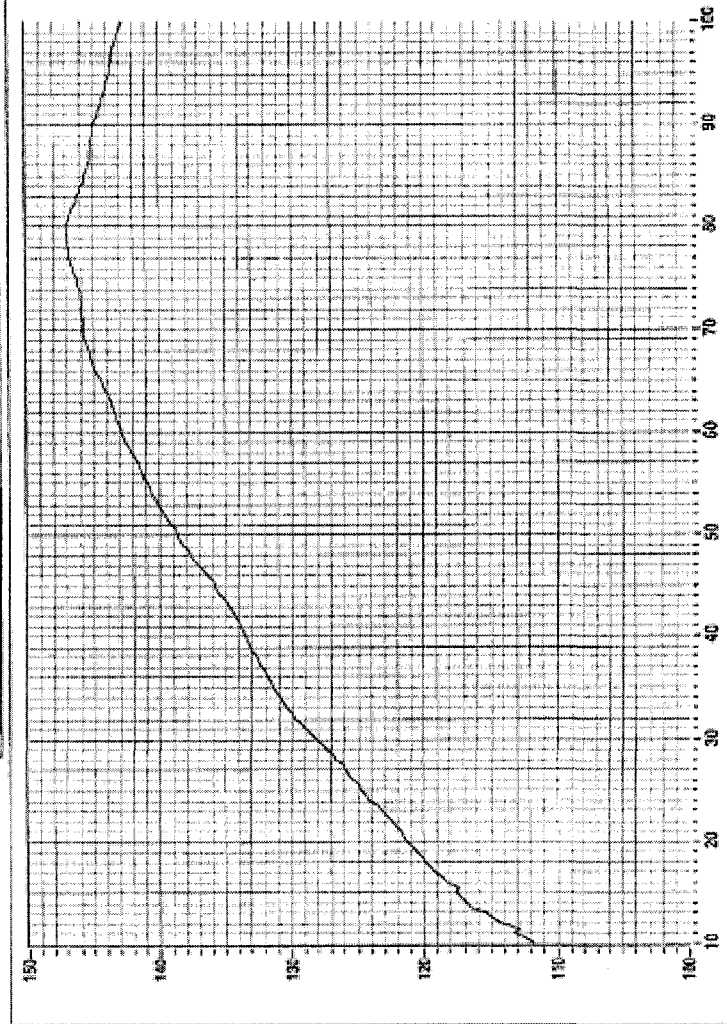
Figure G.2: ITC – 1042 S/N 1337 TVR specifications.

APPENDIX H

POTENTIAL ANTI-ALISING FILTER DATA SHEET

FREQUENCY DEVICES`, INC.

D74 & DP74 Series

**1.0 Hz to 100 kHz
Fixed Frequency**

**16 Pin DIP
4-Pole Filters**

Description

The D74 and DP74 Series of low-power, fixed-frequency, linear active filters are high performance, 4-pole filters in a compact package. These Butterworth and Bessel low-pass and Butterworth high-pass filters (D74 only) combine linear active filter design with the space savings of a 16-pin dual in-line package (DIP). Each model comes factory tuned to a user-specified corner frequency between 1 Hz and 100 kHz (DP74, 1 Hz to 5kHz). These fully self-contained units require no external components or adjustments and operate with dynamic input voltage range from non-critical ±5V to ±18V power supplies.

Features/Benefits:

- Low cost solution for low frequency signal conditioning
- Compact DIP design minimizes board space requirements
- Plug-in ready-to-use, reducing engineering design and manufacturing time
- Factory tuned, no external clocks or adjustments needed saving time and labor of other discrete assembly solutions
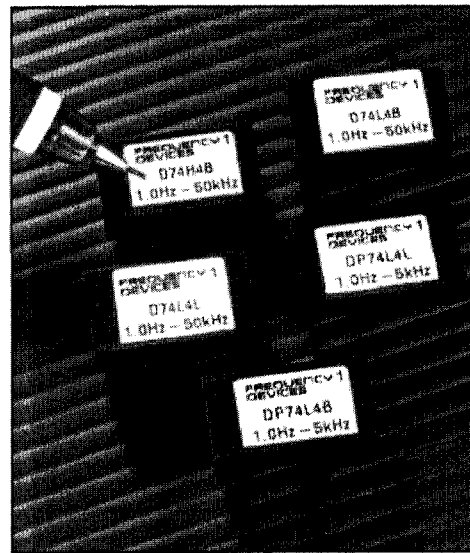- Low harmonic distortion and wide signal-to-noise ratio to 12 bit resolution

Applications

- Anti-alias filtering
- Vibration & shock analysis
- Automatic test equipment
- Aerospace, navigation and sonar
- Communication systems
- Medical electronics
- Sound and vibration testing
- Noise elimination
- Process control

Available Low-Pass Models:

D74L4B	4-pole Butterworth	2
DP74L4B	4-pole Butterworth (Low Power)	2
D74L4L	4-pole Bessel	2
DP74L4L	4-pole Bessel (Low Power)	2

Available High-Pass Models:

D74H4B	4-pole Butterworth	2

General Specifications:

Pin-out/package data & ordering information 3

Figure H.1: Data sheet for Frequency Devices D74 and DP74 fixed frequency filter modules.

Fixed Frequency

4-Pole
Low-Pass and High-Pass Filters

Model	D74L4B & DP74L4B	D74L4L & DP74L4L	Model	D74H4B
Product Specifications	Low-Pass	Low-Pass		High-Pass
Transfer Function	4-Pole, Butterworth	4-Pole, Bessel	Transfer Function	4-Pole, Butterworth
Size	0.88" x 0.46" x 0.375"	0.88" x 0.46" x 0.375"	Size	0.88" x 0.46" x 0.375"
Range f_c D74 DP74	1 Hz to 100 kHz 1 Hz to 5 kHz	1 Hz to 100 kHz 1 Hz to 5 kHz	Range f_c	1 Hz to 100 kHz
Theoretical Transfer Characteristics	Appendix A Page 7	Appendix A Page 2	Theoretical Transfer Characteristics	Appendix A Page 27
Passband Ripple (theoretical)	0.0 dB	0.0 dB	Passband Ripple (theoretical)	0.0 dB
DC Voltage Gain (non-inverting)	0 ± 0.1 dB typ.	0 ± 0.1 dB typ.	Voltage Gain (non-inverting)	0 ± 0.1 dB to 100 kHz
Stopband Attenuation Rate	24 dB/octave	24 dB/octave	Stopband Attenuation Rate	24 dB/octave
			Power Bandwidth	120 kHz
			Small Signal Bandwidth	(-6 dB) 1 MHz
Cutoff Frequency Stability Amplitude Phase	f_c ± 2% max. ± 0.03% /°C -3 dB -180°	f_c ± 2% max. ± 0.03% /°C -3 dB -121°	Cutoff Frequency Stability Amplitude Phase	f_c ± 2% max. ± 0.03% /°C -3 dB -180°
Filter Attenuation (theoretical)	0.67 dB 0.80 f_c 3.01 dB 1.00 f_c 60.0 dB 5.62 f_c 80.0 dB 10.0 f_c	1.86 dB 0.80 f_c 3.01 dB 1.00 f_c 60.0 dB 8.48 f_c 80.0 dB 15.12 f_c	Filter Attenuation (theoretical)	80 dB 0.10 f_c 60 dB 0.18 f_c 3.01 dB 1.00 f_c 0.00 dB 4.00 f_c
Total Harmonic Distortion @ 1 kHz D74 DP74	<-70 dB <-70 dB	<-70 dB <-70 dB	Total Harmonic Distortion @ 1 kHz D74	<-70 dB
Wide Band Noise (5 Hz - 2 MHz)	200 µVrms typ.	200 µVrms typ.	Wide Band Noise (5 Hz - 2 MHz)	400 µVrms typ.
Narrow Band Noise (20 Hz - 100 kHz)	50 µVrms typ.	50 µVrms typ.	Narrow Band Noise (20 Hz - 100 kHz)	100 µVrms typ.
Filter Mounting Assembly	FMA-01A	FMA-01A	Filter Mounting Assembly	FMA-01A

Figure H.2: Data sheet for Frequency Devices D74 and DP74 low-pass and high pass filters.

109

D74 & DP74 Series

Specification
(25°C and Vs ±15 Vdc)

Pin-Out and Package Data
Ordering Information

Analog Input Characteristics[1]

Impedance	10 kΩ min.
Voltage Range	± 10 Vpeak
Max. Safe Voltage	±Vs

Analog Output Characteristics

Impedance	1 Ω
Linear Operating Range	±10 V

Maximum Current[2]

D74	±10 mA
DP74	±5 mA

Offset Voltage

f_c < 100 Hz	f_c ≥100 Hz
0 – 50°C	0 – 70°C
10 mV max.	10 mV max.
3 mV typ.	3 mV typ.

Offset Temp. Coeff.   20 µV / °C

Power Supply (±V)

Rated Voltage	± 15 Vdc
Operating Range	±5 to ±18 Vdc
Maximum Safe Voltage	±18 Vdc

Quiescent Current **D74**
5 mA max.
3 mA typ.

Quiescent Current **DP74**
1.5 mA max.
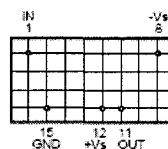600 µA typ.

Temperature

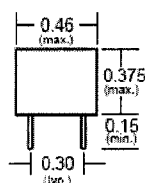|	
Operating	0 to + 70 °C
Storage	- 25 to + 85 °C

Notes:
1. Input and output signal voltage referenced to supply common.
2. Output is short circuit protected to common. DO NOT CONNECT TO ±Vs.

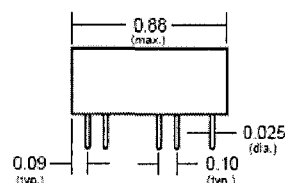All dimensions are in inches
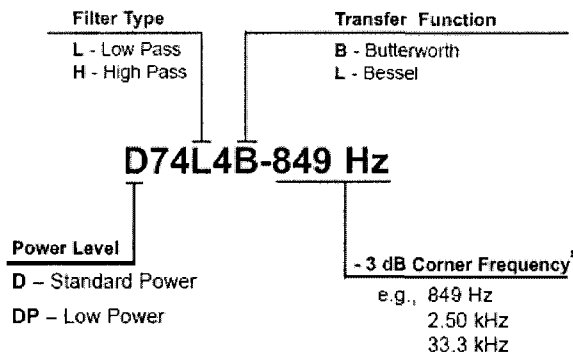All case dimensions ±0.01"
Grid Dimensions 0.1" x 0.1"

IN 1   -Vs 8
15 GND   12 +Vs   11 OUT

BOTTOM VIEW

0.46 (max.)
0.375 (max.)
0.15 (min.)
0.30 (typ.)

FRONT VIEW

0.86 (max.)
0.025 (dia.)
0.09 (typ.)   0.10 (typ.)

SIDE VIEW

Filter Mounting Assembly-See FMA-01A

Ordering Information

Filter Type	Transfer Function
L - Low Pass	**B** - Butterworth
H - High Pass	**L** - Bessel

D74L4B-849 Hz

Power Level

D – Standard Power

DP – Low Power

- 3 dB Corner Frequency[3]
e.g., 849 Hz
2.50 kHz
33.3 kHz

3. How to Specify Corner Frequency:
Corner frequencies are specified by attaching a three digit frequency designator to the basic model number. Corner frequencies can range from 1 Hz to 100 kHz.

3

Figure H.3: Data sheet for Frequency Devices D74 and DP74 pin out and package data.

FREQUENCY DEVICES¨, INC.

Low-Pass

4-Pole
Bessel

Theoretical Transfer Characteristics

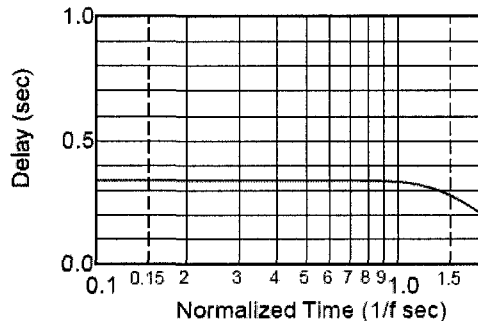| f/fc (Hz)	Amp (dB)	Phase (deg)	Delay[1] (sec)
0.00	0.00	0.00	.336
0.10	-0.028	-12.1	.336
0.20	-0.111	-24.2	.336
0.30	-0.251	-36.3	.336
0.40	-0.448	-48.4	.336
0.50	-0.705	-60.6	.336
0.60	-1.02	-72.7	.336
0.70	-1.41	-84.8	.336
0.80	-1.86	-96.8	.335
0.85	-2.11	-103	.334
0.90	-2.40	-109	.333
0.95	-2.69	-115	.332
1.00	-3.01	-121	.330
1.10	-3.71	-133	.325
1.20	-4.51	-144	.318
1.30	-5.39	-156	.308
1.40	-6.37	-166	.295
1.50	-7.42	-177	.280
1.60	-8.54	-187	.263
1.70	-9.71	-195	.246
1.80	-10.9	-204	.228
1.90	-12.2	-212	.211
2.00	-13.4	-219	.194
2.25	-16.5	-235	.158
2.50	-19.5	-248	.129
2.75	-22.4	-259	.107
3.00	-25.1	-267	.089
3.25	-27.6	-275	.076
3.50	-30.0	-281	.065
4.00	-34.4	-291	.049
5.00	-41.9	-305	.031
6.00	-48.1	-315	.021
7.00	-53.4	-321	.016
8.00	-58.0	-326	.012
9.00	-62.0	-330	.009
10.0	-65.7	-333	.008

1. **Normalized Group Delay:**
   The above delay data is normalized to a corner frequency of 1.0Hz. The actual delay is the normalized delay divided by the actual corner frequency (fc).

$$\text{Actual Delay} = \frac{\text{Normalized Delay}}{\text{Actual Corner Frequency (fc) in Hz}}$$

Frequency Response

Normalized Frequency(f/fc)

Delay (Normalized)

Normalized Time (1/f sec)

Step Response

Normalized Time (1/f sec)

2

Figure H.4: Data sheet for Frequency Devices D74 and DP74 4 pole Bessel low-pass frequency response.

FREQUENCY DEVICES™, INC.

Low-Pass

4-Pole
Butterworth

Theoretical Transfer Characteristics

f/fc (Hz)	Amp (dB)	Phase (deg)	Delay[1] (sec)
0.00	0.00	0.00	.416
0.10	0.00	-15.0	.418
0.20	0.00	-30.1	.423
0.30	-0.00	-45.5	.433
0.40	-0.003	-61.4	.449
0.50	-0.017	-78.0	.474
0.60	-0.072	-95.7	.511
0.70	-0.243	-115	.558
0.80	-0.674	-136	.604
0.85	-1.047	-147	.619
0.90	-1.555	-158	.622
0.95	-2.21	-169	.612
1.00	-3.01	-180	.588
1.10	-4.97	-200	.513
1.20	-7.24	-217	.427
1.30	-9.62	-231	.350
1.40	-12.0	-242	.289
1.50	-14.3	-252	.241
1.60	-16.4	-260	.204
1.70	-18.5	-266	.175
1.80	-20.5	-272	.152
1.90	-22.3	-277	.134
2.00	-24.1	-282	.119
2.25	-28.2	-291	.091
2.50	-31.8	-299	.072
2.75	-35.1	-304	.059
3.00	-38.2	-309	.049
3.25	-41.0	-313	.041
3.50	-43.5	-317	.035
4.00	-48.2	-322	.027
5.00	-55.9	-330	.017
6.00	-62.3	-335	.012
7.00	-67.6	-339	.009
8.00	-72.2	-341	.007
9.00	-76.3	-343	.005
10.0	-80.0	-345	.004

1.Normalized Group Delay:
The above delay data is normalized to a corner frequency
of 1.0Hz.The actual delay is the normalized delay divided
by the actual corner frequency (fc).

$$\text{Actual Delay} = \frac{\text{Normalized Delay}}{\text{Actual Corner Frequency (fc) in Hz}}$$

Frequency Response

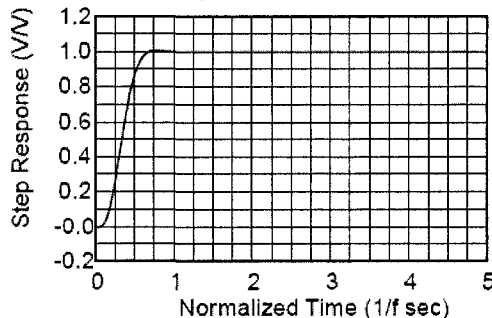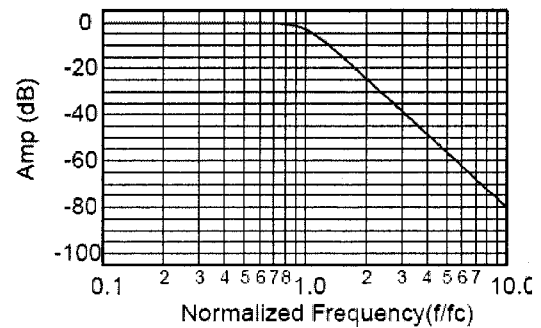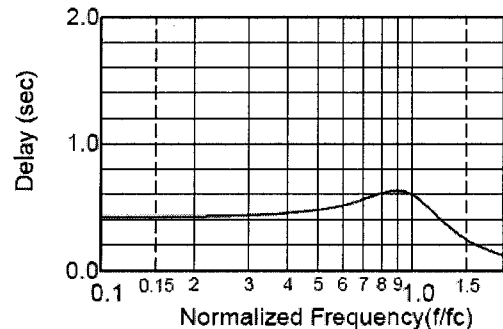### Delay (Normalized)

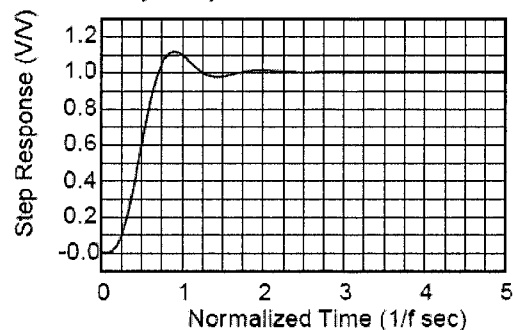
Step Response

7

Figure H.5: Data sheet for Frequency Devices D74 and DP74 4 pole Butterworth
low-pass frequency response.

FREQUENCY DEVICES°, INC.

For Fixed Frequency Filters

Single Channel
Filter Mounting Assembly

Description

The FMA-01S, Filter Mounting Assembly eliminates the need to breadboard or hand-wire filter modules into individual test set-ups.
FMA-01S's are factory assembled 3" x 5" printed-circuit boards with socket pins for filter insertion, various electronic components, and screw terminal connections for power and signal input/output. The FMA-01S operates with any of the D61, D64, D66, D68, D70, D72, D74, D76 or D78 Series filter modules.
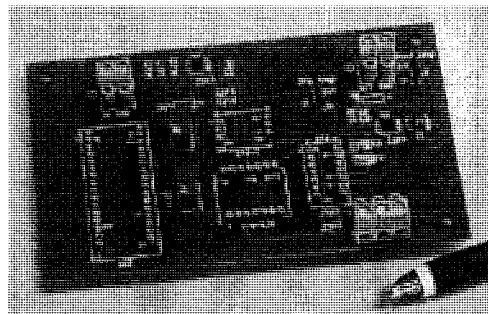
Features/Benefits

- No more building of breadboards.
- Utilized as a single channel bench-top test set or rack mounted via mounting holes for instrumentation applications.
- Accepts a broad range of filter modules allowing for selected cut-off frequencies and transfer functions specific to each application.
- Provide quick and easy connection between circuit card and wired electrical circuits.
- All external connections are easily made with a screwdriver, reducing engineering design, set-up and test time.

Applications

- Aerospace, navigation, sonar applications
- ATE, research and development
- Automotive and transportation
- Communication systems and electronics
- Data acquisition systems
- Industrial process control
- Medical electronics equip. and research
- Sound and vibration testing
- Noise elimination
- Signal reconstruction

Low-Pass Filters Available

D61	4-pole	0.05 Hz to 1.00 Hz
D64	4-pole	1.00 Hz to 100.0 kHz
D66	6-pole	1.00 Hz to 100.0 kHz
D68	8-pole	1.00 Hz to 100.0 kHz
D70	4, 6, 8-pole	100 Hz to 50.0 kHz
D72	2-pole	1.00 Hz to 100 kHz
D74	4-pole	1.00 Hz to 100 kHz
D76	6-pole	1.00 Hz to 100 kHz
D78	8-pole	1.00 Hz to 100 kHz
D100	4 & 8-pole	100 Hz to 100 kHz

High-Pass Filters Available

D61	4-pole	0.05 Hz to 1.00 Hz
D64	4-pole	1.00 Hz to 100.0 kHz
D66	6-pole	1.00 Hz to 100.0 kHz
D68	8-pole	1.00 Hz to 100.0 kHz
D70	4, 6, 8-pole	100 Hz to 50.0 kHz
D72	2-pole	1.00 Hz to 100 kHz
D74	4-pole	1.00 Hz to 100 kHz
D76	6-pole	1.00 Hz to 100 kHz
D78	8-pole	1.00 Hz to 100 kHz
D101	8-pole	1.0 kHz to 500 kHz

Band-Pass Filters Available

D64BP	2-pole pair	1.00 Hz to 100.0 kHz
D68BP	4-pole pair	1.00 Hz to 100.0 kHz
D100	2-pole pair	100 Hz to 100.0 kHz

Band-Reject (Notch) Filters Available

D68BR	4-pole pair	1.00 Hz to 100.0 kHz

Special notes

- Provision for bypass of I/O buffers.
- Provision for gain adjustment of I/O buffers.
- Enhanced output current to drive cables.

1

Figure H.6: Data sheet for Frequency Devices FMA-01S single channel filter mounting assembly.

APPENDIX I

DATA COLLECTION DATES

Date	Location	Issues	Usable Files
9-7-06	Wave Tank	• No Real Approach • Practice Only • Analyzed Data • DC Offset on H-phones	NO USABLE FILES
9-25-06	Tank	• DC offset gone • Continuous Capture • Large Files	???
10-5-06	Gulf Challenger	• Hydrophones Cut	NONE – Taken too far for usable data. TL. Data_1555 Data_1605 Data_1615 Data_1623
11-30-06	Tank	• Used Lubell Source • No scientific approach • Other hydrophone in tank	NO USABLE FILES
1-25-07 Ths	Tank	• Used Lubell Source • No scientific approach • Other hydrophone in tank	NO USABLE FILES
1-29-07 Mon	Tank	• Calibration with Reson. • DAQ hydrophones didn't work. • Spent day with Reson data	SOME DATA – GOOD for calibration
2-1-07 Ths	Tank	• Finish calibration	DATA for Calibration
2-13-07 Tues	Tank	• Source and wrap in water • Data taken with OE690 class – no time for DAQ data.	NONE – Noise Issues
2-16-07 Friday	Tank	• Only Reson Data • Data taken with OE690 class – no time for DAQ numbers.	NONE – Noise Issues
2-19-07 Mon	Tank	• Lubell Source • 4 meters with wrap • no data, too much attenuation for DAQ • Original Wrap	NONE – Noise Issues
2-21-07 Wed	Tank	• Only Reson Data	NONE – Noise Issues
2-22-07 Ths	Tank	• Gunderboom wrap • Only Reson worked • NO DAQ Data • S/N ratio too low.	NONE – Noise Issues
10-6-07 Sat	YF Dock	• Hydrophone response changed • Data from 500 Hz to 8000 Hz	PLENTY

Table I.1: Data collection dates and metadata.